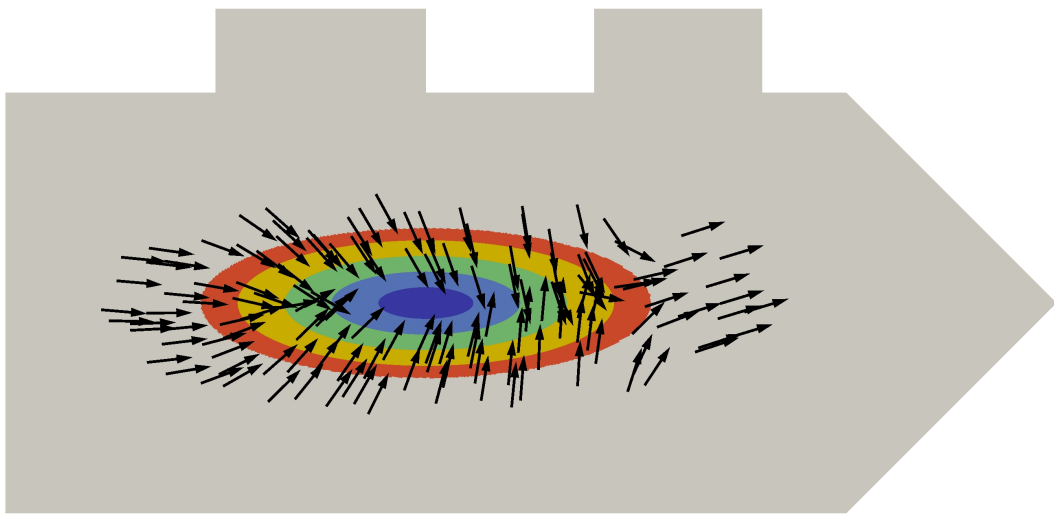


Shape Optimization for Interface Problems using unfitted Finite Elements

Masterarbeit im Studiengang Mathematik

Institut für Numerische und Angewandte Mathematik
Georg-August Universität Göttingen



von:

Hans-Georg Raumer

Betreuer:

Jr.-Prof. Dr. Christoph Lehrenfeld

Zweitgutachter:

Prof. Dr. Gert Lube

28.03.2018

Eigenständigkeitserklärung

Hiermit versichere ich, dass ich die vorliegende Arbeit selbstständig verfasst und keine anderen als die angegebenen Quellen und Hilfsmittel benutzt habe.

Göttingen, den 28.03.2018

Acknowledgements

I would like to sincerely thank Jr.-Prof. Dr. Christoph Lehrenfeld for his great support during the supervision of this thesis. Thanks for many hours of discussions and sharing your expertise with me.

Many thanks also to Prof. Dr. Gert Lube, the second assessor of this thesis, who held most of my lectures and seminars in numerical mathematics for teaching me many aspects of numerics of partial differential equations.

Last but not least, I want to thank Fabian Heimann and Henry von Wahl for valuable hints on the implementation with NGSolve and the layout of this thesis.

Contents

1	Introduction	5
2	Theory of Shape Optimization	9
2.1	Basic Definitions and Theorems	9
2.2	Shape Functions with PDE Constraints	14
2.3	Optimization Aspects	15
3	Shape Optimization for two Model Problems	19
3.1	Stationary Heat Transport Problem	19
3.2	One-phase Poisson Problem	31
4	Level Set Representation of the Geometry	33
4.1	Continuous Level Set Functions	33
4.2	FE Discretization of the Level Set Function and the Level Set Transport .	34
5	FE Approximation of the One-phase Problem	40
5.1	Fictitious Domain Method	40
5.2	Approximation of the Descent Direction	43
6	FE Approximation of the Optimal Interface Problem	48
6.1	The unfitted Finite Element Method (XFEM and CutFEM)	48
6.2	Shape Optimization Procedure for an Interface Problem	51
6.2.1	An unfitted Nitsche Method for the State and Adjoint State	51
6.2.2	Construction of a Descent Direction	55
6.2.3	Optimization Algorithm	59
7	Numerical Results	61
7.1	Comparison of Volume and Boundary Expression	61
7.2	Approximation Spaces for the Descent Direction	64
7.3	Full Geometry Optimization	68
7.4	Velocity Extension	73
7.5	Geometry and Residual Error	75
8	Conclusion and Outlook	78
8.1	Summary	78
8.2	Open Problems	78
A	Auxiliary Proofs	82

Chapter 1

Introduction

Optimization of geometries is a task that is highly interesting from a practical point of view and is very commonly used in many fields of engineering and physics. To give the reader an impression on how diverse those applications can be, we will list a few examples.

Acoustics: One is often interested in the reduction of noise stemming from machines or motors. For example road traffic, aircrafts or machine noise in large factory halls. Usually this leads to a coupled problem of acoustic-structure-interaction. A nice overview on possible numerical strategies and techniques for such problems is presented in [Mar02]. The interesting application of optimizing noise barriers is considered in [Duh06]. It is also possible to optimize the structure of walls and ceilings in concert halls with respect to acoustical effects. The *Grand Hall* of the *Elbphilharmonie Hamburg* represents a famous case where such techniques were successfully used [Kor18].

Elasticity: In architecture or engineering it is often desirable to minimize the amount of material (for instance concrete or steel) under the constraint that the component of interest (for instance a beam) is still able to resist a specific amount of stress. An introduction to those topics is presented for example in [Her12] and [BS95]. The structure of a truss that is obtained by geometry optimization is shown in Figure 1.1.



Figure 1.1: Optimized truss structure (image taken from [BS13, p. 2]).

Imaging technology: Structures consisting of different materials frequently appear in medical applications. Electrical impedance tomography (EIT) is a medical imaging technique that is able to reconstruct the interfaces between those materials [Bor02], [CIN99]. The process of reconstruction leads to a shape optimization problem which is mathematically analyzed in [Cal06], [ADK07] and [LS13]. The underlying interface problems

are also closely related to those we will consider in this thesis.

There are many approaches and techniques to solve geometry optimization problems. What they have in common is that a function depending on the geometry (*shape function*) has to be minimized (or maximized). It is investigated how the shape function behaves under variations of the geometry. This procedure is also known as *sensitivity analysis* in the literature. There exist different possibilities to perform such a variation of the geometry and each possibility is linked to a branch of geometry optimization. We will mention three important branches here.

Variation of parameters (parametric optimization): For this class of problems there exists a finite set of parameters that describes the geometry (for example control points of Bézier curves). The sensitivity analysis leads to a finite dimensional optimization problem. This structure allows the application of many well understood finite dimensional optimization algorithms. A drawback of this approach is that it is very restrictive, since only geometries that can be parametrized by the chosen model are considered.

Variation of topology (topology optimization): We can also investigate how the shape function behaves under topology changes (for example insertion of infinitesimal holes). This approach allows much more freedom for the admissible geometries. A mathematical foundation for topology optimization is given by [NS12].

Variation of boundaries (shape optimization): The idea to consider small perturbations of the boundary goes back to J. Hadamard (1908) [Had08] and his research on elastic plates. Since then a rigorous theory for many aspects of the optimization process was developed, see for instance [SZ92], [DZ11]. The approach of shape optimization was chosen for this thesis because the large quantity of mathematical theory makes it possible to establish a solid theoretical framework for everything that is done afterwards.

Generic Gradient Method

In order to solve our shape optimization problem, we will develop a gradient-type optimization method in this thesis. To set up a gradient method, several sub problems have to be solved. We will motivate those sub problems by means of a generic optimization problem on a (infinite dimensional) Banach space \mathcal{X} . Each problem in the generic setting has a counterpart in the shape optimization setting. To conclude this introduction and provide an overview of this thesis, we will list all sub problems of the generic gradient method together with their correspondent in shape optimization and references to the associated chapters/sections.

Banach space gradient method
Shape optimization method**Minimization problem**

Find a minimum of $F : \mathcal{X} \rightarrow \mathbb{R}$, where \mathcal{X} is a Banach space.

Find a minimum of $J : \mathcal{A} \rightarrow \mathbb{R}$, where \mathcal{A} is a set of shapes.

The structure of J and \mathcal{A} is discussed in Section 2.1 and 2.2.

Differentiability

Definition of the Fréchet derivative DF as a linear mapping $DF : \mathcal{X} \rightarrow \mathcal{L}(\mathcal{X}, \mathbb{R})$.

Definition of the shape derivative $dJ(\Omega)[\vartheta]$ at $\Omega \in \mathcal{A}$ in direction of $\vartheta \in \mathbf{X}$.

The differentiability theory will be presented in Section 2.1, the velocity space \mathbf{X} is discussed in Section 2.3. In Chapter 3, dJ is explicitly computed for a model problem.

Find a descent direction

For $x^0 \in \mathcal{X}$ given, find $y \in \mathcal{X}$ s.t.
 $DF(x^0)[y] < 0$.

For $\Omega^0 \in \mathcal{A}$ given, find $\vartheta \in \mathbf{X}$ s.t.
 $dJ(\Omega^0)[\vartheta] < 0$.

The definition of a descent direction and further characterizations are presented in Section 2.3.

Discretization of spaces and derivatives

Approximate \mathcal{X} by a finite dimensional subspace \mathcal{X}_h and replace the derivative by an approximation $D_h F : \mathcal{X}_h \rightarrow \mathcal{L}(\mathcal{X}_h, \mathbb{R})$.

Discretize shapes $\Omega \rightarrow \Omega_h$, velocities $\mathbf{X} \rightarrow \mathbf{X}_h$ and the shape derivative $dJ \rightarrow d_h J$.

The representation and discretization of shapes by means of level set functions is discussed in Chapter 4. The discretization of velocities and the shape derivative by means of (unfitted) Finite Element spaces is presented in Chapters 5, 6.

Find a discrete descent direction

For $x_h^0 \in \mathcal{X}_h$ given, find $y_h \in \mathcal{X}_h$ s.t.
 $D_h F(x_h^0)[y_h] < 0$.

For Ω_h^0 given, find $\beta_h \in \mathbf{X}_h$ s.t.
 $dJ_h(\Omega_h^0)[\beta_h] < 0$.

Discrete descent directions are discussed in Section 5.2 and 6.2.2.

Optimization step

Choose a stepsize $t \in \mathbb{R}$ and update $x_h^0 \rightarrow x_h^0 + ty_h = x_h'$. We obtain
 $F(x_h') < F(x_h^0)$.

Choose a stepsize $t \in \mathbb{R}$ and update $\Omega_h^0 \rightarrow \Omega_h^0 + t\beta_h$.

The geometry update by means of a level set transport is discussed in Chapter 4. An optimization algorithm is presented in Section 6.2.3. Numerical experiments are presented in Chapter 7.

Overview

In the second chapter we will present the mathematical background from the theory of shape optimization which results in the definition of a derivative with respect to the domain, the so called *shape derivative* or *Eulerian semi-derivative*. The presented framework is taken from the standard literature in shape optimization. Chapter 3 introduces two scalar PDE constrained shape optimization problems, namely a one-phase and a two-phase/interface problem. Whereas the one-phase problem is a standard problem from the literature, the interface problem is not. Therefore a rigorous proof of the existence of the shape derivative is presented. Chapter 4 discusses the implicit geometry representation by means of a level set function and presents the appropriate numerical treatment by suitable continuous and discontinuous Finite Element spaces. For the entire thesis we will only consider lowest order (piecewise linear) Finite Elements. In Chapter 5 and 6 we establish the numerical framework to solve shape optimization problems of one-phase and two-phase type by means of the Finite Element method. We choose unfitted Finite Element discretizations i.e. meshes that are not aligned with the boundary or the interface. Two aspects of the numerical shape optimization procedure are discussed in detail. First, we will compare two different discrete representations of the shape derivative (*volume expression* and *boundary expression*) and conclude why the volume expression is superior in a Finite Element context. Second, we will present the construction of a specific descent direction with beneficial properties for the level set transport. A proof of approximation properties of this descent direction will be included. The final result of Chapter 6 will be a shape optimization algorithm for the two-phase model problem. Chapter 7 presents various numerical examples that illustrate different aspects of the optimization process.

Chapter 2

Theory of Shape Optimization

In this chapter the theoretical framework from the field of shape optimization will be provided. It should be emphasized that it presents only a very small part of the whole theory. We will restrict ourselves to those statements which are essential to set up and understand the numerical methods in the following chapters. This means that we will present one possibility to derive a "derivative with respect to the domain" without giving any existence or uniqueness theorems of optimal solutions. More aspects are out of scope for this thesis because the main focus will be on the numerical methods and the derivation of a meaningful optimization algorithm. For a deeper investigation of many aspects of shape optimization we refer to [DZ11], [SZ92] and [Stu15], where also many of the definitions and proofs in the subsequent chapter are taken from.

2.1 Basic Definitions and Theorems

First we introduce the notion of a shape function.

2.1. DEFINITION [*shape function*] [DZ11, p. 170]

Let $\emptyset \neq \Omega_0 \subset \mathbb{R}^d$ be a set and $\mathcal{A} \subset \mathcal{P}(\Omega_0) = \{\Omega \mid \Omega \subset \Omega_0\}$. Then a function

$$J : \mathcal{A} \rightarrow \mathbb{R} \quad \Omega \rightarrow J(\Omega)$$

is called *shape function*.

The superset Ω_0 is often called *holdall* and any set $\Omega \in \mathcal{A}$ *admissible set*. For a given shape function a shape optimization problem can be formulated in the most general way as:

$$\begin{aligned} &\text{find } \Omega \in \mathcal{A} \text{ such that} \\ &J(\Omega) = \min_{\Omega' \in \mathcal{A}} J(\Omega'). \end{aligned} \tag{2.1}$$

To obtain statements on existence and/or uniqueness of optimal solutions there is no straight forward approach. To apply well known theory on optimal solutions we would need a Banach space structure on \mathcal{A} which is in general not given. By restrictions on the set \mathcal{A} at least weaker structures can be achieved. One of the most common approaches (which will also be considered here) is to define \mathcal{A} by the image of a reference domain under a family of mappings i.e. $\mathcal{A} = \{T(\Omega_{ref}) \mid T \in \mathfrak{T}\}$. For a suitable choice of \mathfrak{T} a group

structure (*Micheletti group*) together with a metric (*Courant metric*) can be observed. A deeper analysis provides also existence statements for many problems (cf. [DZ11]). In this thesis we will restrict ourselves to a definition of a directional derivative with respect to the domain. This derivative can be further used to set up a gradient type optimization algorithm.

Remark: From now on we will always consider bounded holdall domains $\Omega_0 \subset \mathbb{R}^d$ with a piecewise C^1 boundary.

We will choose T as a perturbation of the identity, which is closely related to the more general *velocity method* [SZ92].

2.2. DEFINITION [*perturbation of identity*]

Let $\vartheta \in C_c^\infty(\Omega_0; \mathbb{R}^d)$ the associated perturbation of identity is defined as

$$T_t : \mathbb{R}^d \rightarrow \mathbb{R}^d \quad x \mapsto x + t\vartheta(x) \quad (2.2)$$

where ϑ is extended to \mathbb{R}^d by zero.

Remark: Of course T_t depends on the vector field ϑ . To be correct one should write T_t^ϑ . We will keep this in mind but will omit the upper index.

We chose the representation of T_t as a perturbation of the identity because it offers a direct intuition, how the transformations act on a domain. The *velocity method* considers transformations Φ_t that are defined as the flow mapping of a corresponding ordinary differential equation. As many proofs in the literature consider this approach, we will show that our choice of T_t fits also into that setting. The next theorem states that T_t is invertible for small t . Taking advantage of that fact we can define a time dependent vector field $\hat{\vartheta}(t, x) := \vartheta \circ T_t^{-1}(x)$ which is related to T_t by an ordinary differential equation.

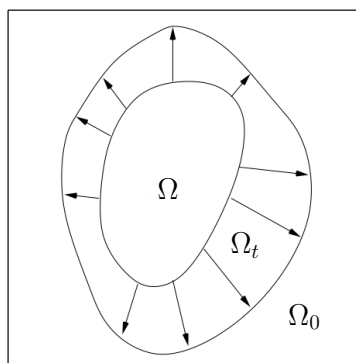


Figure 2.1: Initial domain, perturbed domain and holdall domain (image taken from [Stu15] and modified)

2.3. THEOREM [characterization of T_t] [DZ11, p. 180 ff.]

Let $T(t, x) := T_t(x)$, then $\exists \tau > 0$ s.t.

(i) The mapping T has the following properties:

$$\begin{aligned} \forall x \in \mathbb{R}^d, T(\cdot, x) &\in C^1([0, \tau]; \mathbb{R}^d) \text{ and } \exists c > 0 \text{ s.t.} \\ \forall x, y \in \mathbb{R}^d, \|T(\cdot, x) - T(\cdot, y)\|_{C^1([0, \tau]; \mathbb{R}^d)} &\leq c|x - y| \\ \forall t \in [0, \tau], x \mapsto T_t(x) = T(t, x) &\text{ is invertible} \\ \forall x \in \mathbb{R}^d, T^{-1}(\cdot, x) &\in C([0, \tau]; \mathbb{R}^d) \text{ and } \exists c > 0 \text{ s.t.} \\ \forall x, y \in \mathbb{R}^d, \|T^{-1}(\cdot, x) - T^{-1}(\cdot, y)\|_{C([0, \tau]; \mathbb{R}^d)} &\leq c|x - y| \end{aligned}$$

(ii) $\hat{\vartheta} = \vartheta \circ T_t^{-1}$ is well defined on $[0, \tau] \times \mathbb{R}^d$ and uniformly Lipschitzian i.e.

$$\begin{aligned} \forall x \in \mathbb{R}^d, \hat{\vartheta}(\cdot, x) &\in C([0, \tau]; \mathbb{R}^d) \\ \exists c > 0, \forall x, y \in \mathbb{R}^d, \|\hat{\vartheta}(\cdot, x) - \hat{\vartheta}(\cdot, y)\|_{C([0, \tau]; \mathbb{R}^d)} &\leq c|x - y|. \end{aligned}$$

(iii) T_t can be characterized as the flow of an ODE

$$\begin{aligned} \forall x \in \mathbb{R}^d, t \in [0, \tau], \gamma(t) &:= T_t(x) = T(t, x) \\ \frac{d}{dt}\gamma(t) &= \hat{\vartheta}(t, \gamma(t)), \quad \gamma(0) = x. \end{aligned}$$

(iv) $t \mapsto DT_t$ and $t \mapsto (DT_t)^{-1}$ belong to $C([0, \tau]; C(\overline{\Omega_0}, \mathbb{R}^{d \times d}))$

(v) For $t < \tau$, $T_t : \overline{\Omega_0} \rightarrow \overline{\Omega_0}$ is an homeomorphism with $T_t(\partial\Omega_0) = \partial\Omega_0$

Proof. As $\vartheta \in C_c^\infty(\Omega_0; \mathbb{R}^d)$, it is in particular uniformly Lipschitzian. Thus we can apply Theorem 4.2 in [DZ11, p. 184] which yields (i) and (ii). Since (i) and (ii) are fulfilled, we can apply Theorem 4.1 [DZ11, p. 181] to obtain statement (iii). For the statement (iv) we refer to Theorem 2.16 in [SZ92, p. 51]. The continuity and the continuity of the inverse of T_t has been already proven by the previous steps. We still need that T_t maps $\overline{\Omega_0}$ onto $\overline{\Omega_0}$. This follows also from Theorem 2.16 in [SZ92, p. 51] if the following property of $\hat{\vartheta}$ holds

$$x \in \partial\Omega_0 \implies \hat{\vartheta}(t, x) \cdot n(x) = 0 \tag{2.3}$$

where $n(x)$ denotes the outer unit normal on $\partial\Omega_0$. For the singular points of $\partial\Omega_0$ where the unit normal is not defined, we set $n(x) = 0$. We will show that (2.3) is valid to conclude the proof. Let $x \in \partial\Omega_0$ where $n(x)$ is well defined, then

$$T_t(x) = x + t\vartheta(x) = x,$$

since ϑ has compact support in Ω_0 . Thus on $\partial\Omega_0$ we obtain

$$x = T_t(x) = T_t^{-1}(x) .$$

Inserting this identity into $\hat{\vartheta}(t, \cdot)$ yields

$$\hat{\vartheta}(t, x) \cdot n(x) = \vartheta(T_t^{-1}(x)) \cdot n(x) = \vartheta(x) \cdot n(x) = 0 .$$

□

We will point out the main consequences of the last theorem. For an initial domain $\Omega \subset \Omega_0$, we can define the perturbed domain (see Figure 2.1 for a sketch)

$$\Omega_t := T_t(\Omega). \tag{2.4}$$

For t sufficiently small (depending on ϑ) the following statements are valid due to Theorem 2.3

- $T_t(\Omega_0) = \Omega_0$ (invariance of the holdall domain).
- $\Omega_t \subset \Omega_0$ (preservation of inclusion).
- $\partial\Omega \in C^1 \Rightarrow \partial\Omega_t \in C^1$ (preservation of smooth boundaries).
- $\partial\Omega \in C^{0,1} \Rightarrow \partial\Omega_t \in C^{0,1}$ (preservation of Lipschitz boundaries).

Statements (ii) and (iii) show that our choice of T_t can be regarded as a special case of the *velocity method*. This is very useful, since most of the results from the literature consider transformations defined as a flow mapping. All these results are now directly valid for T_t . Many statements of Theorem 2.3 are also later needed to derive differentiability properties of quantities related to T_t .

Usually we will consider subsets with smooth or Lipschitz boundaries as admissible sets i.e. $\mathcal{A} = \{\Omega \subset \Omega_0 : \partial\Omega \in C^1\}$ or $\mathcal{A} = \{\Omega \subset \Omega_0 : \partial\Omega \in C^{0,1}\}$. As mentioned, the characterization theorem (Theorem 2.3) ensures that for sufficiently small t also Ω_t is an admissible set, i.e. $\Omega_t \in \mathcal{A}$. This is all we need to come up with a definition of a derivative with respect to the domain, the so-called *Eulerian semi-derivative* or *shape derivative*.

2.4. DEFINITION [*Eulerian semi-derivative/ shape derivative*]

Let $\Omega \subset \Omega_0$, then the Eulerian semi-derivative of J at Ω in direction of ϑ is defined as the limit (if it exists)

$$dJ(\Omega)[\vartheta] = \lim_{t \rightarrow 0} \frac{J(\Omega_t) - J(\Omega)}{t} . \quad (2.5)$$

(i) If the limit exists $\forall \vartheta \in C_c^\infty(\Omega_0, \mathbb{R}^d)$ and $\exists k \geq 0$ such that the mapping

$$\vartheta \mapsto dJ(\Omega)[\vartheta] =: G(\vartheta)$$

is linear and continuous with respect to the $C^k(\Omega_0, \mathbb{R})$ -norm we call J shape differentiable at Ω and $G(\cdot)$ its shape derivative.

(ii) The smallest integer $k \geq 0$ for which G is continuous with respect to the $C^k(\Omega_0, \mathbb{R})$ norm is called the order of G .

Under further assumptions on the smoothness of the boundary of Ω , the shape derivative can be represented as a functional that acts only on the boundary. This property was first detected by J. Hadamard (1908) [Had08] for the special case of C^∞ boundaries. The statement for C^{k+1} boundaries was first proven by J.-P. Zolésio in 1979 [Zol79] and can be summarized in the famous *structure theorem*. For more details we refer to [DZ11, Remark 3.2, p. 481].

2.5. THEOREM [*structure theorem*] [DZ11, p. 479 ff.]

Let $\Omega \subset \Omega_0$ with compact boundary $\partial\Omega$ and let G be of order $k \geq 0$. If $\partial\Omega \in C^{k+1}$, then the outward unit normal n of $\partial\Omega$ is well defined and $\exists g \in C^k(\partial\Omega)'$ such that $\forall \vartheta \in C_c^k(\Omega_0, \mathbb{R}^d)$ holds

$$dJ(\Omega)[\vartheta] = \langle g, \vartheta|_{\partial\Omega} \cdot n \rangle_{C^k(\partial\Omega)} . \quad (2.6)$$

If further $g \in L^1(\partial\Omega)$

$$dJ(\Omega)[\vartheta] = \int_{\partial\Omega} g(\vartheta \cdot n) . \quad (2.7)$$

Proof. See [DZ11, Theorem 3.6, p. 479] and [DZ11, Corollary 1, p. 480]. \square

A direct consequence of the structure theorem which is of great importance for the numerical treatment of shape optimization problems is stated in the next Corollary.

2.6. COROLLARY [*normal components*]

Let the assumptions of Theorem 2.5 be valid and $\vartheta_1, \vartheta_2 \in C_c^k(\Omega_0, \mathbb{R}^d)$ then

$$\vartheta_1 \cdot n = \vartheta_2 \cdot n \quad \Rightarrow \quad dJ(\Omega)[\vartheta_1] = dJ(\Omega)[\vartheta_2]$$

Proof. If the assumptions are valid, the shape derivative depends only on the normal components of the vector fields ϑ_1, ϑ_2

$$dJ(\Omega)[\vartheta_1] = \langle g, \vartheta_1|_{\partial\Omega} \cdot n \rangle_{C^k(\partial\Omega)} = \langle g, \vartheta_2|_{\partial\Omega} \cdot n \rangle_{C^k(\partial\Omega)} = dJ(\Omega)[\vartheta_2] .$$

□

2.2 Shape Functions with PDE Constraints

In this thesis we will only deal with a special class of shape functions, namely PDE constrained shape functions. We will clarify this term by the next definition.

2.7. DEFINITION [PDE constrained shape function]

Let $V(\Omega)$ be a Hilbert space of functions defined $\forall \Omega \in \mathcal{A}$. We consider a bilinear form

$$a(\Omega, \cdot, \cdot) : V(\Omega) \times V(\Omega) \rightarrow \mathbb{R}$$

and a linear form

$$f(\Omega, \cdot) : V(\Omega) \rightarrow \mathbb{R} .$$

Further let the following variational formulation be uniquely solvable $\forall \Omega \in \mathcal{A}$:

$$\begin{aligned} \text{find } u(\Omega) \in V(\Omega) \text{ such that } \forall v \in V(\Omega) \\ a(\Omega, u(\Omega), v) = f(\Omega, v) . \end{aligned} \quad (2.8)$$

Then the solution $u = u(\Omega)$ of (2.8) is called state and a shape function which depends implicitly on the state i.e.

$$J(\Omega) = J(\Omega, u(\Omega))$$

is called PDE constrained shape function.

The approach of our choice to derive the Eulerian semi-derivative of such an J is linked to differentiability properties of the state u . Since $\Omega_t \in \mathcal{A}$ for small t and by construction of the state equation, there exists a unique $u_t \in V(\Omega_t)$ such that

$$a(\Omega_t, u_t, v_t) = f(\Omega_t, v_t) \quad \forall v_t \in V(\Omega_t) . \quad (2.9)$$

And we can define

$$u^t := u_t \circ T_t .$$

Although u^t is defined on Ω it is not guaranteed that $u^t \in V(\Omega)$. This leads to an important property of the spaces $V(\Omega)$ which has to be valid and will be stated as an assumption here:

$$\tilde{u} \in V(\Omega_t) \Leftrightarrow \tilde{u} \circ T_t \in V(\Omega) . \quad (\text{A})$$

Remark: Later we will choose $V(\Omega) = H^1(\Omega)$ or $V(\Omega) = H_0^1(\Omega)$, which both fulfill assumption (A) (see Lemma 3.1).

The crucial point for the existence of the Eulerian semi-derivative is the existence of the so-called *material derivative*.

2.8. DEFINITION [material derivative]

Let assumption (A) be valid, then \dot{u} is defined as the weak/strong limit

$$\dot{u} = \lim_{t \searrow 0} \frac{u^t - u}{t} ,$$

if it exists.

The whole derivation using the material derivative approach including a rigorous existence proof of the Eulerian semi-derivative will be done in the next chapter for two model problems.

2.3 Optimization Aspects

For the moment we will assume existence of the Eulerian semi-derivative and shape differentiability of $J(\Omega)$ i.e $\exists k \geq 0$ such that

$$dJ(\Omega)[\cdot] : C_c^\infty(\Omega_0, \mathbb{R}^d) \rightarrow \mathbb{R} \quad \vartheta \mapsto dJ(\Omega)[\vartheta]$$

is linear and bounded with respect to the $C_c^k(\Omega_0, \mathbb{R}^d)$ norm. We state further an assumption on the extension of $dJ(\Omega)$:

$$dJ(\Omega) \text{ is a linear and bounded functional on } \mathbf{X} := [H_0^1(\Omega_0)]^d . \quad (\mathbb{B})$$

If we can find a smooth vector field $\vartheta \in C_c^\infty(\Omega_0, \mathbb{R}^d)$ that fulfills

$$dJ(\Omega)[\vartheta] < 0 ,$$

we can as well find $\tau > 0$ such that $\forall t < \tau$ holds:

$$\frac{J(\Omega_t) - J(\Omega)}{t} < 0 \quad \Rightarrow \quad J(\Omega_t) < J(\Omega) .$$

So we reduced the value of our shape function. This motivates the following definition.

2.9. DEFINITION [*descent direction*]

Let assumption (\mathbb{B}) be valid, then a vector field $\beta \in \mathbf{X}$ is called descent direction of $J(\Omega)$ if

$$dJ(\Omega)[\beta] < 0 \quad .$$

If even holds that

$$\beta \in \arg \min_{\|\vartheta\|_{\mathbf{X}}=1} dJ(\Omega)[\vartheta] \quad , \quad (2.10)$$

we call β a steepest descent.

Considering the inner product on $\mathbf{X} = [H_0^1(\Omega_0)]^d$

$$b(\beta, \psi) = \int_{\Omega_0} \nabla \beta : \nabla \psi + \beta \cdot \psi$$

and the structure theorem 2.5, we get some characterizations of a steepest descent.

2.10. LEMMA [*characterizations of a steepest descent*]

Let β' be the Riesz representative of $-dJ(\Omega)$ i.e

$$b(\beta', \psi) = -dJ(\Omega)[\psi] \quad \forall \psi \in \mathbf{X} \quad .$$

Let further the assumptions of the structure theorem 2.5 be valid with $g \in L^2(\partial\Omega)$, then the following expressions define a steepest descent

- (i) $\beta_1 := (\|\beta'\|_{\mathbf{X}})^{-1} \beta'$
- (ii) any $\beta_2 \in \mathbf{X}$ with $\|\beta_2\|_{\mathbf{X}} = 1$ and $\beta_2 \cdot n = \beta_1 \cdot n$ on $\partial\Omega$
- (iii) $\beta_3 := (\|\tilde{\beta}\|_{\mathbf{X}})^{-1} \tilde{\beta}$ with $\tilde{\beta} \in \mathbf{X}$ such that $\tilde{\beta} \cdot n = -g$ on $\partial\Omega$

Proof. (i) Let $\psi \in \mathbf{X}$ be arbitrary with $\|\psi\|_{\mathbf{X}} = 1$, then we compute

$$\begin{aligned} dJ(\Omega)[\beta_1] - dJ(\Omega)[\psi] &= (\|\beta'\|_{\mathbf{X}})^{-1} dJ(\Omega)[\beta'] + b(\beta', \psi) \\ &= -(\|\beta'\|_{\mathbf{X}})^{-1} b(\beta', \beta') + b(\beta', \psi) \\ &\leq -\|\beta'\|_{\mathbf{X}} + \|\beta'\|_{\mathbf{X}} \|\psi\|_{\mathbf{X}} \\ &= 0 \quad . \end{aligned}$$

Where we used Cauchy Schwarz in the third line. Thus β_1 is a minimizer and normalized by construction.

- (ii) The normal components of β_1 and β_2 coincide, thus we can apply Corollary 2.6 which yields

$$\min_{\|\vartheta\|_{\mathbf{X}}=1} dJ(\Omega)[\vartheta] = dJ(\Omega)[\beta_1] = dJ(\Omega)[\beta_2]$$

(iii) Let $\psi \in \mathbf{X}$ be arbitrary with $\|\psi\|_{\mathbf{X}} = 1$ and C_{tr} the constant from the trace theorem, then the structure theorem yields

$$\begin{aligned} dJ(\Omega)[\beta_3] - dJ(\Omega)[\psi] &= -(\|\tilde{\beta}\|_{\mathbf{X}})^{-1} \int_{\partial\Omega} g^2 - \int_{\partial\Omega} g(\psi \cdot n) \\ &\leq -(\|\tilde{\beta}\|_{\mathbf{X}})^{-1} \|g\|_{L^2(\partial\Omega)}^2 + \|g\|_{L^2(\partial\Omega)} \|\psi \cdot n\|_{L^2(\partial\Omega)} \\ &\leq -(\|\tilde{\beta}\|_{\mathbf{X}})^{-1} \|\tilde{\beta}\|_{\mathbf{X}}^2 C_{tr}^2 + C_{tr}^2 \|\tilde{\beta}\|_{\mathbf{X}} \\ &= 0 . \end{aligned}$$

□

Remark: Note that if we omit the scaling for β_1 and β_3 , we still obtain a descent direction. The lemma shows that a steepest descent is anything else but unique. This gives us some freedom in the choice of the descent direction in the optimization method and we can choose a velocity field which is best suited for the numerical treatment of the optimization problem.

For the Riesz representative β' and the steepest descent β_1 from the previous lemma, an additional regularity result is valid.

2.11. LEMMA [regularity of β_1] cf. [BEH⁺17]

Let the assumptions of Lemma 2.10 be valid and $\partial\Omega \in C^1$ then

$$\beta_1 \in \left[H_0^1(\Omega_0) \right]^d \cap \left[H^2(\Omega_0 \setminus \Omega) \right]^d \cap \left[H^2(\Omega) \right]^d$$

Proof. For the Riesz representative of $-dJ(\Omega)$ holds

$$b(\beta', \psi) = -dJ(\Omega)[\psi] \quad \forall \psi \in \mathbf{X} .$$

By the structure theorem this can be rewritten as

$$b(\beta', \psi) = - \int_{\partial\Omega} g(\psi \cdot n) \quad \forall \psi \in \mathbf{X} .$$

This is the weak formulation of the vector valued interface problem

$$\begin{aligned} -\Delta\beta' + \beta' &= \vec{0} && \text{in } \Omega_1 \text{ and } \Omega_2 \\ [[\beta']] &= \vec{0} && \text{on } \Gamma \\ [[\nabla\beta' \cdot n]] &= g \cdot n && \text{on } \Gamma \\ \beta &= \vec{0} && \text{on } \partial\Omega_0, \end{aligned}$$

with the subdomains $\Omega_1 := \Omega$, $\Omega_2 := \Omega_0 \setminus \Omega$ and the interface $\Gamma := \partial\Omega$. The jump operator $[[\cdot]]$ on the interface is defined by

$$[[v]] = v|_{\Omega_1} - v|_{\Omega_2} .$$

The regularity of solutions of such elliptic interface problems is a standard result from the literature and states

$$\|\beta'\|_{[H_0^1(\Omega_0)]^d} + \|\beta'\|_{[H^2(\Omega_1)]^d} + \|\beta'\|_{[H^2(\Omega_2)]^d} \leq C \|g\|_{H^{1/2}(\Gamma)} .$$

A proof for $d = 2$ can be found in [CZ98, Theorem 2.1]. Since the regularity result holds for β' , the descent direction β_1 has the same regularity. \square

Chapter 3

Shape Optimization for two Model Problems

In this section the theory from the previous chapter will be applied on two scalar model problems. The first problem is a two-phase problem and physically motivated. A rigorous proof of the existence of the corresponding shape derivative will be presented. Similarly to the statement of the structure theorem, under additional regularity assumptions, the shape derivative can be reformulated as a functional that acts only on the interface. The second problem is well known in the literature and will be used later to highlight some aspects of the numerical analysis. Volume and boundary expression of the corresponding shape derivative will be quoted from the literature for this case.

3.1 Stationary Heat Transport Problem

We consider a bounded domain $\Omega \subset \mathbb{R}^2$ which can be decomposed into two subdomains Ω_1 and Ω_2 . The subdomains are separated by the interface $\Gamma := \overline{\Omega}_1 \cap \overline{\Omega}_2$. Further we assume that Ω_1 is fully surrounded by Ω_2 which implies $\Gamma \cap \partial\Omega = \emptyset$. The full domain Ω can be regarded as a room which is heated by a heat source located inside Ω_1 . Some parts of the wall can be fully isolated whereas the remaining parts allow some heat flux. We are interested in minimizing the deviation of the temperature distribution from a reference temperature distribution. So let $u = u(x, y)$ denote the temperature in Ω and $\bar{u} \in C^1(\Omega)$ is some reference temperature distribution. Then we seek to minimize the shape function

$$J(\Omega) = \int_{\Omega} (u - \bar{u})^2 \rightarrow \min . \quad (3.1)$$

Where u solves the following interface problem:

$$-\operatorname{div}(\alpha \nabla u) = f \quad \text{in } \Omega, \quad (3.2)$$

$$[[u]] = 0 \quad \text{on } \Gamma, \quad (3.3)$$

$$[[-\alpha \nabla u \cdot n_{\Gamma}]] = 0 \quad \text{on } \Gamma, \quad (3.4)$$

$$\nabla u \cdot n + \gamma u = 0 \quad \text{on } \partial\Omega , \quad (3.5)$$

where n_Γ denotes the outer unit normal of $\Gamma = \partial\Omega_1$ and the interface jump of a function v is defined by

$$[[v(x)]] := \lim_{h \searrow 0} v(x - hn_\Gamma) - v(x + hn_\Gamma) .$$

Remark: In the context of shape optimization u is often referred to as the *state* and equations (3.2)-(3.5) as the *state equation*. We will adopt this notion.

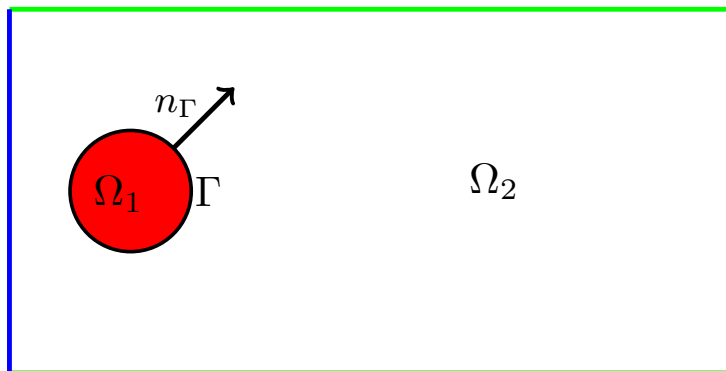


Figure 3.1: Sketch of the geometrical setting.

The diffusion coefficient α is assumed to be discontinuous over the interface and domain wise constant,

$$\alpha = \begin{cases} \alpha_1 \in \mathbb{R} & \text{in } \Omega_1, \\ \alpha_2 \in \mathbb{R} & \text{in } \Omega_2 . \end{cases}$$

The heat source f is only active inside Ω_1

$$f = \begin{cases} f_1 > 0 & \text{in } \Omega_1, \\ 0 & \text{in } \Omega_2 . \end{cases}$$

For ease of presentation we fix $f_1 \in \mathbb{R}$ but the derivation of the shape derivative can be easily extended to the case $f_1 \in H^1(\Omega)$. Conditions (3.3) and (3.4) enforce continuity of the temperature and the heat flux over the interface. Let further the boundary be decomposed into two parts $\partial\Omega = \partial\Omega_R \cup \partial\Omega_N$ with $meas(\partial\Omega_R)_{d-1} > 0$. The heat transfer coefficient γ is also piecewise defined:

$$\gamma = \begin{cases} \gamma_0 > 0 & \text{on } \partial\Omega_R, \\ 0 & \text{on } \partial\Omega_N. \end{cases}$$

The physical meaningful notion of the Robin boundary condition would be

$$-\alpha \nabla u \cdot n = \gamma(u - u_{ref}) \tag{3.6}$$

with a reference temperature u_{ref} . Equation (3.6) shows that the heat flux is proportional to the temperature difference between u and u_{ref} . For simplicity we set u_{ref} to zero in our case. According to this comment, the piecewise defined heat transfer coefficient γ and condition (3.5) model an isolated part of the wall ($\partial\Omega_N$) and another part that allows heat flux ($\partial\Omega_R$).

In our example only the interface Γ will be moved whereas the outer boundary $\partial\Omega$ stays fixed, hence Ω is a natural choice for the holdall domain. Starting with Ω_i $i \in \{1, 2\}$ as a reference domain we can take any $\vartheta \in C_c^\infty(\Omega, \mathbb{R}^2)$ and apply the corresponding perturbation T_t from the previous chapter. This defines the perturbed subdomains $\Omega_{i,t} := T_t(\Omega_i)$ and the perturbed interface $\Gamma_t := T_t(\Gamma)$ with outer unit normal n_{Γ_t} . Similarly we get

$$\alpha_t = \begin{cases} \alpha_1 & \text{in } \Omega_{1,t}, \\ \alpha_2 & \text{in } \Omega_{2,t} \end{cases}$$

and

$$f_t = \begin{cases} f_1 > 0 & \text{in } \Omega_{1,t}, \\ 0 & \text{in } \Omega_{2,t}. \end{cases}$$

Please note that by construction $f = f_t \circ T_t$ and $\alpha = \alpha_t \circ T_t$. Since T_t keeps the outer boundary $\partial\Omega$ fixed, nothing has to be changed there. Canonically this defines the perturbed state equation i.e. we seek u_t (*perturbed state*) that solves:

$$-\operatorname{div}(\alpha \nabla u_t) = f_t \quad \text{in } \Omega \quad (3.7)$$

$$[[u_t]] = 0 \quad \text{on } \Gamma_t \quad (3.8)$$

$$[-\alpha_t \nabla u_t \cdot n_{\Gamma_t}] = 0 \quad \text{on } \Gamma_t \quad (3.9)$$

$$\nabla u_t \cdot n + \gamma u = 0 \quad \text{on } \partial\Omega \quad (3.10)$$

The state equation and the perturbed state equation can be reformulated as a variational problem which reads as:

$$\begin{aligned} & \text{find } u \in H^1(\Omega) \text{ such that } \forall v \in H^1(\Omega) \\ & \sum_{i=1}^2 \alpha_i \int_{\Omega_i} \nabla u \cdot \nabla v + \oint_{\partial\Omega_R} \gamma_0 u v = \int_{\Omega} f v \end{aligned} \quad (3.11)$$

and similarly

$$\begin{aligned} & \text{find } u_t \in H^1(\Omega) \text{ such that } \forall \tilde{v} \in H^1(\Omega) \\ & \sum_{i=1}^2 \alpha_i \int_{\Omega_{i,t}} \nabla u_t \cdot \nabla \tilde{v} + \oint_{\partial\Omega_R} \gamma_0 u_t \tilde{v} = \int_{\Omega} f_t \tilde{v}. \end{aligned} \quad (3.12)$$

Please note that the outer boundary $\partial\Omega$ stays invariant under transformation.

The first important observation is that via the transformation T_t we get an isomorphism on $H^1(\Omega)$. We will state this as a lemma.

3.1. LEMMA [H^1 isomorphism property]

For the spaces $H^1(\Omega)$ and $H_0^1(\Omega)$ the isomorphism assumption (A) is valid i.e.

$$\begin{aligned}\tilde{v} \in H^1(\Omega) &\Leftrightarrow \tilde{v} \circ T_t \in H^1(\Omega) \\ \tilde{w} \in H_0^1(\Omega) &\Leftrightarrow \tilde{w} \circ T_t \in H_0^1(\Omega)\end{aligned}$$

Proof. The proof can be found in [Zie12, p. 52, Theorem 2.2.2]. \square

Following the notation from the previous chapter we define $u^t = u_t \circ T_t$. Now we can insert $u_t = u^t \circ T_t^{-1}$ into (3.12) and application of the transformation theorem on the volume integrals yields

$$\begin{aligned}\int_{\Omega_{i,t}} \nabla u_t \cdot \nabla \tilde{v} &= \int_{\Omega_{i,t}} \nabla (u^t \circ T_t^{-1}) \cdot \nabla ((\tilde{v} \circ T_t) \circ T_t^{-1}) \\ &= \int_{\Omega_{i,t}} (DT_t^{-T} \nabla u^t) \circ T_t^{-1} \cdot (DT_t^{-T} \nabla (\tilde{v} \circ T_t)) \circ T_t^{-1} \\ &= \int_{\Omega_i} \det(DT_t) (DT_t^{-1} DT_t^{-T} \nabla u^t) \cdot \nabla (\tilde{v} \circ T_t)\end{aligned}$$

and

$$\int_{\Omega} f_t \tilde{v} = \int_{\Omega} \det(DT_t) f(\tilde{v} \circ T_t) .$$

To simplify notation we define further auxilliary quantities on $\Omega_0 = \Omega$

$$\xi(t) := \det(DT_t), \quad (3.13)$$

$$A(t) := \xi(t)(DT_t)^{-1}(DT_t)^{-T}, \quad (3.14)$$

$$B(t) := (DT_t)^{-T}, \quad (3.15)$$

$$C(t) := DT_t. \quad (3.16)$$

Remark: Of course all these quantities depend also on the space variable x but we will omit this in the notation for the sake of convenience. When the transformation theorem is applied, we should take the absolute value of the determinant $\xi(t)$. However, we will see that $\xi(t)$ is positive for small t , therefore we omit the absolute value.

Making use of the previous Lemma and the fact that $u^t = u_t$ on $\partial\Omega$, we can now rewrite (3.12) as a variational problem on the reference subdomains.

$$\begin{aligned}\text{find } u^t \in H^1(\Omega) \text{ such that } \forall v \in H^1(\Omega) \\ \sum_{i=1}^2 \alpha_i \int_{\Omega_i} (A(t) \nabla u^t) \cdot \nabla v + \oint_{\partial\Omega_R} \gamma_0 u^t v = \int_{\Omega} \xi(t) f v .\end{aligned} \quad (3.17)$$

To obtain existence of the material derivative we would like to differentiate under the integral in (3.17). To come up with such a statement we need some more properties of the auxiliary quantites (3.13)-(3.16), stated by the next two lemmas.

3.2. LEMMA [positivity and ellipticity]

$\exists \tau > 0, \eta_1, \eta_2 > 0$ such that $\forall t \in [0, \tau], \zeta \in \mathbb{R}^d$

$$(i) \quad \xi(t) > 0 \quad \forall x \in \overline{\Omega_0}$$

$$(ii) \quad \eta_1 |\zeta|^2 \leq A(t)\zeta \cdot \zeta \leq \eta_2 |\zeta|^2$$

Proof. From Theorem 2.3 we obtain directly that $\xi(\cdot) \in C([0, \tau]; C(\overline{\Omega_0}))$ and $A(\cdot) \in C([0, \tau]; C(\overline{\Omega_0}, \mathbb{R}^{d \times d}))$ with $\xi(0) = 1$ and $A(0) = I$. Thus we can apply Proposition 2.12 in [Stu15, p. 16] which yields the claim. \square

3.3. LEMMA [differentiability properties]

For the auxiliary quantities (3.13)-(3.16) the following limit properties hold:

$$(i) \quad \lim_{t \searrow 0} \frac{1}{t} (\xi(t) - 1) = \operatorname{div}(\vartheta) =: \xi'(0) \quad \text{in } C(\overline{\Omega_0}, \mathbb{R})$$

$$(ii) \quad \lim_{t \searrow 0} \frac{1}{t} (C(t) - Id) = D\vartheta =: C'(0) \quad \text{in } C(\overline{\Omega_0}, \mathbb{R}^{d \times d})$$

$$(iii) \quad \lim_{t \searrow 0} \frac{1}{t} (B(t) - Id) = -D\vartheta^T =: B'(0) \quad \text{in } C(\overline{\Omega_0}, \mathbb{R}^{d \times d})$$

$$(iv) \quad \lim_{t \searrow 0} \frac{1}{t} (A(t) - I) = \operatorname{div}(\vartheta)I - (D\vartheta + D\vartheta^T) =: A'(0) \quad \text{in } C(\overline{\Omega_0}, \mathbb{R}^{d \times d})$$

Proof. By the characterization theorem (Theorem 2.3) we can identify T_t with a flow mapping and the corresponding speed $\hat{\vartheta}$ is well defined. Lemma 2.31 in [SZ92, p. 64] then states exactly (i).

For the second statement we directly compute for t sufficiently small

$$\lim_{t \searrow 0} \frac{1}{t} (D(T_t) - D(T_0)) = \lim_{t \searrow 0} \frac{1}{t} (tD\vartheta) = D\vartheta$$

which yields the claim.

For statement (iii) we mimic the proof in [Stu15, p. 17]. For two Banach spaces X, Y the mapping $\operatorname{inv} : A \mapsto A^{-1}$ with $A \in \mathcal{L}(X, Y)$ and $A^{-1} \in \mathcal{L}(Y, X)$ is continuously differentiable with Fréchet derivative $\operatorname{inv}'(A)(B) = -A^{-1}BA^{-1}$ (see [AE01, p. 222]). By the chain rule we obtain

$$\frac{d}{dt} (\operatorname{inv}(C(t)))|_{t=0} = \operatorname{inv}'(C(0))(C'(0)) = -I^{-1}D\vartheta I^{-1} = -D\vartheta.$$

Finally we can interchange the limit and the transposed which yields the claim.

Statement (iv) follows directly by the product rule. \square

Remark: For the previous proofs we used the notation Ω_0 for the holdall domain. Since for our two-phase problem holds $\Omega_0 = \Omega$, we will replace Ω_0 by Ω in the further notation.

The next theorem ensures now that we can differentiate under the integral in (3.17) and that the material derivative exists in a strong sense.

3.4. THEOREM [*existence of the material derivative*]

The sequence $w^t = \frac{1}{t}(u^t - u)$ converges strongly in $H^1(\Omega)$ as $t \searrow 0$ and the limit \dot{u} is characterized as the unique solution of the variational problem

$$\begin{aligned} & \text{find } \dot{u} \in H^1(\Omega) \text{ such that } \forall v \in H^1(\Omega) \\ & \sum_{i=1}^2 \alpha_i \int_{\Omega_i} \nabla \dot{u} \cdot \nabla v + \oint_{\partial\Omega_R} \gamma_0 \dot{u} v = - \sum_{i=1}^2 \alpha_i \int_{\Omega_i} (A'(0) \nabla u) \cdot \nabla v + \int_{\Omega} \xi'(0) f v . \end{aligned} \quad (3.18)$$

Proof. We consider the following triple norm $\|v\|^2 := \sum_{i=1}^2 \alpha_i \int_{\Omega_i} \nabla v \cdot \nabla v + \oint_{\partial\Omega_R} \gamma_0 v^2$ which is equivalent to the H^1 norm. By the uniform ellipticity of $A(t)$ we have

$$\min\{\eta_1, 1\} \|u^t\|^2 \leq \sum_{i=1}^2 \alpha_i \int_{\Omega_i} (A(t) \nabla u^t) \cdot \nabla u^t + \oint_{\partial\Omega_R} \gamma_0 (u^t)^2,$$

with the ellipticity constant η_1 as in Lemma 3.2. According to Lemma 3.3, $\exists \tau > 0$ such that $\xi(t) > 0$ for $t < \tau$. Thus, we can use the variational problem to bound the right hand side for $t < \tau$

$$\sum_{i=1}^2 \alpha_i \int_{\Omega_i} (A(t) \nabla u^t) \cdot \nabla u^t + \oint_{\partial\Omega_R} \gamma_0 (u^t)^2 = \int_{\Omega} \xi(t) f u^t \leq C \|\xi\|_{C([0,\tau])} \|f\|_{L^2(\Omega)} \|u^t\| ,$$

hence $\|u^t\|$ is uniformly bounded. Using the definition of the triple norm and the variational problems (3.11) and (3.17), we can further estimate

$$\begin{aligned} \|u^t - u\|^2 &= \sum_{i=1}^2 \alpha_i \int_{\Omega_i} \nabla (u^t - u) \cdot \nabla (u^t - u) + \oint_{\partial\Omega_R} \gamma_0 (u^t - u)^2 \\ &= \sum_{i=1}^2 \alpha_i \int_{\Omega_i} ((I - A(t)) \nabla u^t) \cdot \nabla (u^t - u) \\ &\quad + \sum_{i=1}^2 \alpha_i \int_{\Omega_i} (A(t) \nabla u^t) \cdot \nabla (u^t - u) + \oint_{\partial\Omega_R} \gamma_0 u^t (u^t - u) \\ &\quad - \left(\sum_{i=1}^2 \alpha_i \int_{\Omega_i} \nabla u \cdot \nabla (u^t - u) - \oint_{\partial\Omega_R} \gamma_0 u (u^t - u) \right) \\ &= \sum_{i=1}^2 \alpha_i \int_{\Omega_i} ((I - A(t)) \nabla u^t) \cdot \nabla (u^t - u) \\ &\quad + \int_{\Omega} (\xi(t) - 1) f (u^t - u) \\ &\leq C \left(\|I - A(t)\|_{C(\bar{\Omega}, \mathbb{R}^{d \times d})} \|u^t\| + \|\xi(t) - 1\|_{C(\bar{\Omega}, \mathbb{R})} \right) \|u^t - u\| . \end{aligned}$$

We can divide by $\|u^t - u\|$ and recall the properties of $A(t)$ and $\xi(t)$ from Lemma 3.3 as well as the boundedness of $\|u^t\|_{H^1(\Omega)}$. Hence, the remaining right hand side tends to zero as $t \searrow 0$ and thus $u^t \rightarrow u$ in the triple norm (H^1 norm). Dividing by t^2 in every step in the last computation we arrive at

$$\begin{aligned} \|w^t\|^2 &\leq \frac{C}{t} \left(\sum_{i=1}^2 \alpha_i \int_{\Omega_i} ((I - A(t))\nabla u^t) \cdot \nabla w^t \right) \\ &\quad + \frac{C}{t} \left(\int_{\Omega} (\xi(t) - 1) f w^t \right) \\ &\leq C \left\| \frac{1}{t} (I - A(t)) \right\|_{C(\bar{\Omega}, \mathbb{R}^{d \times d})} \|u^t\| \|w^t\| \\ &\quad + C \left\| \frac{1}{t} (\xi(t) - 1) \right\|_{C(\bar{\Omega})} \|f\|_{L^2(\Omega)} \|w^t\|. \end{aligned}$$

Dividing by $\|w^t\|$ leaves only bounded terms on the right hand side. The boundedness for u^t has been shown and the boundedness of the difference quotients is stated in Lemma 3.3. Since $\|w^t\|$ is uniformly bounded, we can extract a weak convergent subsequence w^{t_k} with weak limit w . For $v \in H^1(\Omega)$ arbitrary but fixed we have following equality

$$\begin{aligned} \sum_{i=1}^2 \alpha_i \int_{\Omega_i} \nabla w^{t_k} \cdot \nabla v + \oint_{\partial\Omega_0} \gamma_0 w^{t_k} v &= \sum_{i=1}^2 \alpha_i \int_{\Omega_i} \left(\frac{1}{t_k} (I - A(t_k)) \nabla u^{t_k} \right) \cdot \nabla v \\ &\quad + \int_{\Omega} \left(\frac{1}{t_k} (\xi(t_k) - 1) \right) f v. \end{aligned}$$

Now we can pass to the limit $t_k \searrow 0$ on both sides and arrive at

$$\sum_{i=1}^2 \alpha_i \int_{\Omega_i} \nabla w \cdot \nabla v + \oint_{\partial\Omega_0} \gamma_0 w v = \sum_{i=1}^2 \alpha_i \int_{\Omega_i} (-A'(0)\nabla u) \cdot \nabla v + \int_{\Omega} \xi'(0) f v. \quad (3.19)$$

Since $v \in H^1(\Omega)$ was chosen arbitrary, w is also characterized as the unique solution of the elliptic problem (3.19). This characterization implies that any subsequence of w^t contains another subsequence which weakly converges towards w . Taking advantage of the fact that a bounded sequence in \mathbb{R} is either convergent or has at least two accumulation points, we get additionally that also the full sequence w^t converges weakly towards w and it remains to show strong convergence. By the two upper equalities we get

$$\begin{aligned} \lim_{t \searrow 0} (\|w^t\|) &= \lim_{t \searrow 0} \left(\sum_{i=1}^2 \alpha_i \int_{\Omega_i} \nabla w^t \cdot \nabla w^t + \oint_{\partial\Omega_R} \gamma_0 (w^t)^2 \right) \\ &= \lim_{t \searrow 0} \left(\sum_{i=1}^2 \alpha_i \int_{\Omega_i} \left(\frac{1}{t} (I - A(t)) \nabla u^t \right) \cdot \nabla w^t + \int_{\Omega} \left(\frac{1}{t} (\xi(t) - 1) \right) f w^t \right) \\ &= \sum_{i=1}^2 \alpha_i \int_{\Omega_i} (-A'(0)\nabla u) \cdot \nabla w + \int_{\Omega} (\xi'(0)) f w \\ &= \sum_{i=1}^2 \alpha_i \int_{\Omega_i} \nabla w \cdot \nabla w + \oint_{\partial\Omega_R} \gamma_0 w w = \|w\|. \end{aligned}$$

Thus we have shown so far that w^t weakly converges towards w and $\|w^t\| \rightarrow \|w\|$. A well known result from functional analysis states that in uniformly convex Banach spaces (especially Hilbert spaces), weak convergence and convergence of norms imply strong convergence (cf. [Bre10, Proposition 3.32, p.78]). Thus we have shown strong convergence $w^t \rightarrow w$ and rename $w = \dot{u}$. \square

Also the shape function J can be rewritten as an integral over the reference domain:

$$J(\Omega_t) := \int_{\Omega_t} (u_t - \bar{u})^2 = \int_{\Omega} \xi(t)(u^t - \bar{u} \circ T_t)^2. \quad (3.20)$$

According to the last Theorem, we are allowed to differentiate under the integral in (3.20), which yields a first expression of the Eulerian semi-derivative

$$\begin{aligned} dJ(\Omega)[\vartheta] &= \int_{\Omega} \xi'(0)(u - \bar{u})^2 - 2 \int_{\Omega} (\nabla \bar{u} \cdot \vartheta)(u - \bar{u}) + 2 \int_{\Omega} \dot{u}(u - \bar{u}) \\ &= \int_{\Omega} \operatorname{div}(\vartheta)(u - \bar{u})^2 - 2 \int_{\Omega} (\nabla \bar{u} \cdot \vartheta)(u - \bar{u}) + 2 \int_{\Omega} \dot{u}(u - \bar{u}). \end{aligned} \quad (3.21)$$

This is still unsatisfactory, since we have an implicit dependency on ϑ via \dot{u} . That means to evaluate $dJ(\Omega)$ at ϑ , we would have to solve the elliptic problem (3.18) first, which is a different one for every ϑ . To eliminate the material derivative we define an auxiliary problem, the adjoint problem.

3.5. DEFINITION [adjoint problem]

Let u be the unique solution of (3.11), then the unique solution of the elliptic problem

$$\begin{aligned} &\text{find } u^* \in H^1(\Omega) \text{ such that } \forall v \in H^1(\Omega) \\ &\sum_{i=1}^2 \alpha_i \int_{\Omega_i} \nabla u^* \cdot \nabla v + \oint_{\partial\Omega_R} \gamma_0 u^* v = \int_{\Omega} 2(u - \bar{u})v \end{aligned} \quad (3.22)$$

is called the adjoint state.

Now we are able to eliminate the material derivative in (3.21) by a substitution trick.

3.6. LEMMA [volume expression]

Let u, u^* be the solutions of (3.11) and (3.22), then the Eulerian semi-derivative of $J(\Omega)$ can be represented as

$$\begin{aligned} dJ(\Omega)[\vartheta] &= \int_{\Omega} \operatorname{div}(\vartheta) \left((u - \bar{u})^2 + f u^* \right) - \int_{\Omega} 2(\nabla \bar{u} \cdot \vartheta)(u - \bar{u}) \\ &\quad - \sum_{i=1}^2 \alpha_i \int_{\Omega_i} \operatorname{div}(\vartheta) \nabla u \cdot \nabla u^* + \sum_{i=1}^2 \alpha_i \int_{\Omega_i} \left((D\vartheta + D\vartheta^T) \nabla u \right) \cdot \nabla u^* \end{aligned} \quad (3.23)$$

Proof. We test the adjoint problem with the material derivative \dot{u} and use the variational formulations (3.22) and (3.18) which yields

$$\begin{aligned} \int_{\Omega} 2(u - \bar{u})\dot{u} &= \sum_{i=1}^2 \alpha_i \int_{\Omega_i} \nabla u^* \cdot \nabla \dot{u} + \oint_{\partial\Omega_R} \gamma_0 u^* \dot{u} \\ &= - \sum_{i=1}^2 \alpha_i \int_{\Omega_i} (A'(0)\nabla u) \cdot \nabla u^* + \int_{\Omega} \xi'(0) f u^* . \end{aligned}$$

Inserting the above identity into (3.21) and using the further identities

$$\begin{aligned} A'(0) &= \operatorname{div}(\vartheta)I - D\vartheta + D\vartheta^T \\ \xi'(0) &= \operatorname{div}(\vartheta) \end{aligned}$$

yields the claim. \square

In spirit of the *structure theorem* we would finally like to find a formulation of $dJ(\Omega)[\cdot]$ that consists only of interface integrals. The next lemma shows that such an expression exists under additional regularity assumptions.

3.7. LEMMA [*interface expression*]

Let $u, u^* \in H^2(\Omega_1) \cap H^2(\Omega_2)$ and the interface $\partial\Omega_1 = \Gamma \in C^1$, then (3.23) can be equivalently represented by

$$dJ(\Omega)[\vartheta] = \oint_{\Gamma} (f_1 u^* + 2 \llbracket \alpha(\nabla u \cdot n_{\Gamma})(\nabla u^* \cdot n_{\Gamma}) \rrbracket - \llbracket \alpha \nabla u \cdot \nabla u^* \rrbracket) \vartheta \cdot n_{\Gamma} . \quad (3.24)$$

Proof. We follow some ideas from [Ber10] and [LS13].

At first we observe that on the subdomains Ω_i , $i \in \{1, 2\}$ holds

$$\operatorname{div}(\vartheta(u - \bar{u})^2) = \operatorname{div}(\vartheta)(u - \bar{u})^2 + 2(u - \bar{u})\vartheta \cdot \nabla u - 2(u - \bar{u})\vartheta \cdot \nabla \bar{u} .$$

Using the above identity and Gauss's theorem yields for expression (3.21)

$$\begin{aligned} dJ(\Omega)[\vartheta] &= \int_{\Omega} \operatorname{div}(\vartheta)(u - \bar{u})^2 - 2 \int_{\Omega} (\nabla \bar{u} \cdot \vartheta)(u - \bar{u}) + 2 \int_{\Omega} \dot{u}(u - \bar{u}) \\ &= \sum_{i=1}^2 \int_{\Omega_i} \operatorname{div}(\vartheta)(u - \bar{u})^2 + 2 \int_{\Omega} (u - \bar{u}) (\dot{u} - \nabla u \cdot \vartheta) \\ &= \oint_{\Gamma} \llbracket (u - \bar{u})^2 \rrbracket \vartheta \cdot n_{\Gamma} + 2 \int_{\Omega} (u - \bar{u}) (\dot{u} - \nabla u \cdot \vartheta) \\ &= 2 \int_{\Omega} (u - \bar{u}) (\dot{u} - \nabla u \cdot \vartheta) . \end{aligned} \quad (3.25)$$

The interface integral vanishes due to $\bar{u} \in C^1(\Omega)$ and the continuity condition (3.3). We will also rewrite the right hand side of the variational formulation for the material

derivative (3.18) summand by summand. Similarly as before we obtain by Gauss's theorem

$$S_1 := \sum_{i=1}^2 \int_{\Omega_i} \operatorname{div}(\vartheta) f v = \sum_{i=1}^2 \int_{\Omega_i} \operatorname{div}(\vartheta f v) - \int_{\Omega} f \nabla v \cdot \vartheta = \oint_{\Gamma} \llbracket f v \rrbracket \vartheta \cdot n_{\Gamma} - \int_{\Omega} f \nabla v \cdot \vartheta . \quad (3.26)$$

To modify also the second summand we need the following identity for $u, v \in H^1(\Omega) \cap H^2(\Omega_i)$ with $i \in \{1, 2\}$ (see [Ber10, p. 14])

$$\vartheta \cdot \nabla(\nabla u \cdot \nabla v) + \left((D\vartheta + D\vartheta^T) \nabla u \right) \cdot \nabla v = \nabla(\vartheta \cdot \nabla u) \cdot \nabla v + \nabla(\vartheta \cdot \nabla v) \cdot \nabla u . \quad (3.27)$$

A proof can be found in the Appendix (Proposition A.1). By (3.27) and integration by parts on the subdomains we obtain for $v \in H^1(\Omega) \cap H^2(\Omega_i)$

$$\begin{aligned} S_2 &:= - \sum_{i=1}^2 \alpha_i \int_{\Omega_i} \operatorname{div}(\vartheta) \nabla u \cdot \nabla v + \sum_{i=1}^2 \alpha_i \int_{\Omega_i} \left((D\vartheta + D\vartheta^T) \nabla u \right) \cdot \nabla v \\ &= \sum_{i=1}^2 \alpha_i \int_{\Omega_i} \vartheta \cdot \nabla(\nabla u \cdot \nabla v) - \oint_{\Gamma} \llbracket \alpha \nabla u \cdot \nabla v \rrbracket \vartheta \cdot n_{\Gamma} + \sum_{i=1}^2 \alpha_i \int_{\Omega_i} \left((D\vartheta + D\vartheta^T) \nabla u \right) \cdot \nabla v \\ &\stackrel{(3.27)}{=} \sum_{i=1}^2 \alpha_i \int_{\Omega_i} (\nabla(\vartheta \cdot \nabla u) \cdot \nabla v + \nabla(\vartheta \cdot \nabla v) \cdot \nabla u) - \oint_{\Gamma} \llbracket \alpha \nabla u \cdot \nabla v \rrbracket \vartheta \cdot n_{\Gamma} \\ &= \sum_{i=1}^2 \alpha_i \int_{\Omega_i} (-\Delta v (\vartheta \cdot \nabla u) - \Delta u (\vartheta \cdot \nabla v)) \\ &\quad + \oint_{\Gamma} (\llbracket (\alpha \vartheta \cdot \nabla u) (\nabla v \cdot n_{\Gamma}) \rrbracket + \llbracket (\alpha \vartheta \cdot \nabla v) (\nabla u \cdot n_{\Gamma}) \rrbracket) - \oint_{\Gamma} \llbracket \alpha \nabla u \cdot \nabla v \rrbracket \vartheta \cdot n_{\Gamma} . \end{aligned} \quad (3.28)$$

Due to the regularity assumption we can set $v = u^*$ and together with (3.26)/(3.28) that yields

$$\begin{aligned} &\sum_{i=1}^2 \alpha_i \int_{\Omega_i} \nabla u \cdot \nabla u^* + \oint_{\partial\Omega_R} \gamma_0 \dot{u} u^* = S_1 + S_2 \\ &= \sum_{i=1}^2 \alpha_i \int_{\Omega_i} -\Delta u^* (\vartheta \cdot \nabla u) - \int_{\Omega} (\Delta u + f) \nabla u^* \cdot \vartheta + \oint_{\Gamma} \llbracket f v \rrbracket \vartheta \cdot n_{\Gamma} \\ &\quad + \oint_{\Gamma} (\llbracket (\alpha \vartheta \cdot \nabla u) (\nabla u^* \cdot n_{\Gamma}) \rrbracket + \llbracket (\alpha \vartheta \cdot \nabla u^*) (\nabla u \cdot n_{\Gamma}) \rrbracket) - \oint_{\Gamma} \llbracket \alpha \nabla u \cdot \nabla u^* \rrbracket \vartheta \cdot n_{\Gamma} . \end{aligned} \quad (3.29)$$

By assumption u is a strong solution of (3.2) and thus the second volume integral vanishes. Similarly to the proof for the volume expression, we can eliminate the material derivative in (3.25)

$$\begin{aligned}
dJ(\Omega)[\vartheta] &= 2 \int_{\Omega} (u - \bar{u}) (\dot{u} - \nabla u \cdot \vartheta) \\
&\stackrel{(3.22)}{=} \sum_{i=1}^2 \alpha_i \int_{\Omega_i} \nabla \dot{u} \cdot \nabla u^* + \oint_{\partial\Omega_R} \gamma_0 \dot{u} u^* - \int_{\Omega} 2(u - \bar{u}) \nabla u \cdot \nabla \vartheta \\
&\stackrel{(3.29)}{=} \sum_{i=1}^2 \alpha_i \int_{\Omega_i} -(\Delta u^* + 2(u - \bar{u})) \vartheta \cdot \nabla u + \oint_{\Gamma} \llbracket f u^* \rrbracket \vartheta \cdot n_{\Gamma} \\
&\quad + \oint_{\Gamma} (\llbracket (\alpha \vartheta \cdot \nabla u) (\nabla u^* \cdot n_{\Gamma}) \rrbracket + \llbracket (\alpha \vartheta \cdot \nabla u^*) (\nabla u \cdot n_{\Gamma}) \rrbracket) - \oint_{\Gamma} \llbracket \alpha \nabla u \cdot \nabla u^* \rrbracket \vartheta \cdot n_{\Gamma} \\
&= \oint_{\Gamma} \llbracket f u^* \rrbracket \vartheta \cdot n_{\Gamma} + \oint_{\Gamma} (\underbrace{\llbracket (\alpha \vartheta \cdot \nabla u) (\nabla u^* \cdot n_{\Gamma}) \rrbracket}_{J_1} + \underbrace{\llbracket (\alpha \vartheta \cdot \nabla u^*) (\nabla u \cdot n_{\Gamma}) \rrbracket}_{J_2}) \\
&\quad - \oint_{\Gamma} \llbracket \alpha \nabla u \cdot \nabla u^* \rrbracket \vartheta \cdot n_{\Gamma} .
\end{aligned}$$

The volume integral vanishes because u^* is a strong solution to (3.22). We found an expression of the shape derivative that consists only of interface integrals but it has not the desired form yet. Since $\llbracket u \rrbracket = \llbracket u^* \rrbracket = 0$ on Γ , the tangential gradient $\nabla_{\Gamma} u = \nabla u|_{\Gamma} - n_{\Gamma} n_{\Gamma}^T \nabla u|_{\Gamma}$ is single valued on the interface (in the L^2 sense) i.e.

$$\llbracket \nabla_{\Gamma} u \rrbracket = 0 \quad \text{in } L^2(\Gamma) \quad (3.30)$$

$$\llbracket \nabla_{\Gamma} u^* \rrbracket = 0 \quad \text{in } L^2(\Gamma) . \quad (3.31)$$

A proof of this statement can be found in the Appendix (Proposition A.2). This is also the point where we need the smoothness assumption $\Gamma \in C^1$. Taking advantage of the continuity of ϑ , we can rewrite the jump terms J_1, J_2 and (3.30) implies

$$\begin{aligned}
J_1 &= \llbracket (\alpha \vartheta \cdot \nabla u) (\nabla u^* \cdot n_{\Gamma}) \rrbracket = \llbracket (\alpha \vartheta \cdot ((\nabla u \cdot n_{\Gamma}) n_{\Gamma} + \nabla_{\Gamma} u)) (\nabla u^* \cdot n_{\Gamma}) \rrbracket \\
&= \llbracket \alpha (\nabla u \cdot n_{\Gamma}) (\nabla u^* \cdot n_{\Gamma}) \rrbracket \vartheta \cdot n_{\Gamma} + \llbracket \alpha \nabla_{\Gamma} u \cdot n_{\Gamma} \rrbracket \vartheta \cdot \nabla_{\Gamma} u \\
&= \llbracket \alpha (\nabla u \cdot n_{\Gamma}) (\nabla u^* \cdot n_{\Gamma}) \rrbracket \vartheta \cdot n_{\Gamma} .
\end{aligned} \quad (3.32)$$

Similarly, (3.31) implies

$$J_2 = \llbracket (\alpha \vartheta \cdot \nabla u^*) (\nabla u \cdot n_{\Gamma}) \rrbracket = \llbracket \alpha (\nabla u^* \cdot n_{\Gamma}) (\nabla u \cdot n_{\Gamma}) \rrbracket \vartheta \cdot n_{\Gamma} . \quad (3.33)$$

Further we have by definition of the source ($f_2 = 0$) and $\llbracket u^* \rrbracket = 0$

$$\llbracket f u^* \rrbracket = \llbracket f \rrbracket u^* = f_1 u^* . \quad (3.34)$$

Inserting the last three identities (3.32), (3.33), (3.34) yields

$$dJ(\Omega)[\vartheta] = \oint_{\Gamma} (f_1 u^* + 2 \llbracket \alpha (\nabla u \cdot n_{\Gamma}) (\nabla u^* \cdot n_{\Gamma}) \rrbracket - \llbracket \alpha \nabla u \cdot \nabla u^* \rrbracket) \vartheta \cdot n_{\Gamma} .$$

□

Remarks on the Material Derivative

We consider a sufficiently smooth function $u = u(t, x)$ and the space-time dependent velocity field $T(t, x) = x + t\vartheta$ as defined in the first chapter. The material derivative of u with respect to the velocity T , well known from fluid dynamics is then defined as

$$\begin{aligned}\dot{u}(t, x) &:= \frac{d}{dt}u(t, T(t, x)) = \partial_t u(t, T(t, x)) + \frac{d}{dt}T(t, x) \cdot \nabla u(t, T(t, x)) \\ &= \partial_t u(t, T(t, x)) + \vartheta(x) \cdot \nabla u(t, T(t, x)) .\end{aligned}$$

Evaluated at $t = 0$ we obtain due to $T(0, x) = x$

$$\dot{u}(x) := \dot{u}(0, x) = \partial_t u(0, x) + \vartheta(x) \cdot \nabla u(0, x) =: \partial_t u + \vartheta \cdot \nabla u . \quad (3.35)$$

In the shape optimization context we investigated only differentiability properties of $u^t(x) = u_t(T(t, x)) := u(t, T(t, x))$ so far. Having (3.35) in mind, it is natural to ask as well for differentiability properties of $u_t(x) = u(t, x)$ and especially for the existence of the limit

$$u' = \lim_{t \searrow 0} \frac{u_t - u}{t} .$$

This is the analogue quantity to the partial derivative $\partial_t u$ in shape optimization and is called *local shape derivative*. Usually the local shape derivative is defined by means of the material derivative [SZ92, p. 111]

$$u' := \dot{u} - \vartheta \cdot \nabla u .$$

This definition recovers the usual connection between partial and material derivative.

Similar to the *Reynolds transport theorem* from fluid dynamics, it is possible to formulate a transport theorem that enables us to directly differentiate perturbed integrals [DZ11, Theorem 4.2]

$$\frac{d}{dt} \left(\int_{T_t(\Omega)} \Psi(t) \right) \Big|_{t=0} = \int_{\Omega} \Psi'(0) + \operatorname{div}(\Psi(0)\vartheta) .$$

The local shape derivative together with the transport theorem allows for an alternative derivation of boundary/interface expressions of the shape derivative (see [Stu15]). This derivation includes a proof of

$$\lim_{t \searrow 0} \frac{u_t - u}{t} = \dot{u} - \vartheta \cdot \nabla u \quad \text{in } H^1(\Omega),$$

which is needed in order to apply the transport theorem.

3.2 One-phase Poisson Problem

The next model problem is well studied in the literature (cf. [Stu15]), therefore we will only reference the proofs for the derivation of the shape derivative. The main purpose of this problem will be a comparison of the volume and boundary expression of the shape derivative with respect to their approximation quality in a numerical context.

We consider a bounded domain $\Omega \subset \Omega_0 \subset \mathbb{R}^d$ where $\partial\Omega_0$ is piecewise smooth. The state $u \in H_0^1(\Omega)$ solves the homogeneous Dirichlet problem

$$-\Delta u = f \quad \text{in } \Omega, \quad (3.36)$$

$$u = 0 \quad \text{on } \partial\Omega, \quad (3.37)$$

with $f \in H^1(\Omega_0)$. The shape function is chosen as

$$J(\Omega) = \int_{\Omega} (u - u_c)^2 \quad (3.38)$$

where $u_c \in C^1(\Omega_0)$. Similarly to the two-phase problem we define the adjoint state as the weak solution $u^* \in H_0^1(\Omega)$ of the problem

$$-\Delta u^* = 2(u - u_c) \quad \text{in } \Omega, \quad (3.39)$$

$$u^* = 0 \quad \text{on } \partial\Omega. \quad (3.40)$$

We will only present the shape derivative for this problem without a detailed derivation.

3.8. LEMMA [shape derivatives for model problem II]

The volume expression of the shape derivative of (3.38) is given by

$$\begin{aligned} dJ(\Omega)[\vartheta] &= \int_{\Omega} \operatorname{div}(\vartheta) \left((u - u_c)^2 + u^* \right) - \int_{\Omega} 2(\nabla u_c \cdot \vartheta) (u - u_c) \\ &\quad + \int_{\Omega} \left((D\vartheta + D\vartheta^T)\nabla u \right) \cdot \nabla u^* - \int_{\Omega} \operatorname{div}(\vartheta)\nabla u \cdot \nabla u^* + \int_{\Omega} (\nabla f \cdot \vartheta) u^*. \end{aligned} \quad (3.41)$$

If further $\partial\Omega \in C^1$ and $u, u^* \in H_0^1(\Omega) \cap H^2(\Omega)$, the boundary expression of (3.41) is well defined and given by

$$dJ(\Omega)[\vartheta] = \int_{\partial\Omega} g(\vartheta \cdot n), \quad (3.42)$$

where n is the outer unit normal of $\partial\Omega$ and

$$g = (u - u_c)^2 + (\nabla u \cdot n)(\nabla u^* \cdot n). \quad (3.43)$$

Proof. A proof of both statements can be found in [Stu15]. \square

Remark: We will take a closer look at the interface expression of the shape derivative for the two-phase problem (3.24) compared to the boundary expression for the one-phase problem (3.42). The "control function" \bar{u} does not occur in the interface expression whereas the boundary expression depends on u_c . This difference is connected to the fact that $\bar{u} \in C^1(\Omega)$ and thus $[[\bar{u}]] = 0$ on the interface Γ . For the one-phase case we did not assume $u_c = 0$ on $\partial\Omega$. The second difference, we observe is that the source term f occurs in the interface expression but in the boundary expression it does not. For the interface problem we assumed f to be discontinuous over the interface, i.e. $[[f]] \neq 0$ on Γ . For the boundary expression instead, all boundary integrals including the source f vanish, since f is always multiplied with a function $w \in H_0^1(\Omega)$ and thus $fw = 0$ on $\partial\Omega$.

Chapter 4

Level Set Representation of the Geometry

In this chapter we will present how the geometries i.e. the subdomains and the interface/boundary can be represented by a level set function. The first section introduces the main ideas of level set methods on the analytical level, especially the level set transport equation. In the second section we discuss an appropriate discretization of the level set function and the transport equation.

4.1 Continuous Level Set Functions

Continuous Geometry Representation

We consider the geometrical setting of the two-phase model problem from Section 3.1. The subdomains Ω_1, Ω_2 and the interface Γ are represented by a continuous level set function $\phi_0 \in C(\Omega)$ with the following properties:

$$\begin{aligned}x \in \Gamma &\Leftrightarrow \phi_0(x) = 0, \\x \in \Omega_1 &\Leftrightarrow \phi_0(x) < 0, \\x \in \Omega_2 &\Leftrightarrow \phi_0(x) > 0.\end{aligned}$$

Remark: For the case of a one-phase problem on a domain $\Omega \subset \Omega_0$, we consider the same strategy as above and replace Ω by Ω_0 , Ω_1 by Ω and Γ by $\partial\Omega$.

The level set function ϕ_0 is called a *signed distance function* if additionally holds

$$|\phi_0(x)| = \text{dist}(x, \Gamma).$$

Example: A signed distance function that represents an ellipse is given by

$$\phi_0(x, y) = \sqrt{\frac{(x - x_c)^2}{x_s} + \frac{(y - y_c)^2}{y_s}} - r$$

with $x_c, y_c \in \mathbb{R}$ and $x_s, y_s, r > 0$. We will often use such functions for the domain initialization in numerical experiments (see Figure 4.1 for a sketch).

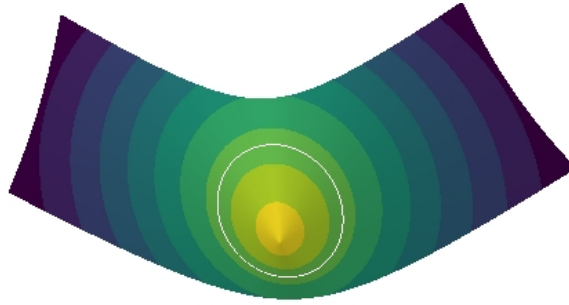


Figure 4.1: Signed distance function with an ellipse as zero level (white).

Level Set Transport Equation

In the shape optimization context we want to move the level set function along a descent direction β for a certain time T . Therefore we need to define the time dependent level set function $\phi = \phi(t, x)$. To move ϕ we need to solve a transport equation which is a first order hyperbolic equation. For those PDE's it is only meaningful to enforce boundary conditions on the inflow boundary

$$\partial\Omega_- := \{x \in \partial\Omega : \beta \cdot n_{\partial\Omega} < 0\}.$$

Given initial data $\phi_0 : \Omega \rightarrow \mathbb{R}$ and boundary data $\phi_D : [0, T] \times \Omega \rightarrow \mathbb{R}$, the level set transport equation reads as

find $\phi : [0, T] \times \Omega \rightarrow \mathbb{R}$ such that

$$\partial_t \phi + \beta \cdot \nabla \phi = 0 \quad \text{in } [0, T] \times \Omega, \quad (4.1)$$

$$\phi(x, 0) = \phi_0(x) \quad \text{in } \Omega, \quad (4.2)$$

$$\phi(x, t) = \phi_D(x, t) \quad \text{on } [0, T] \times \partial\Omega_- . \quad (4.3)$$

4.2 FE Discretization of the Level Set Function and the Level Set Transport

Discrete Geometry Representation

As in Section 3.1, we consider a bounded domain $\Omega \subset \mathbb{R}^2$ consisting of two subdomains Ω_1, Ω_2 that are separated by the interface $\Gamma = \overline{\Omega}_1 \cap \overline{\Omega}_2$. To define discrete quantities on Ω we need a mesh that subdivides Ω into simplices. We claim the following assumption on the mesh to hold for the rest of this thesis unless noted otherwise.

4.1. Definition/Assumption [mesh properties]

Let $\{\mathcal{T}_h\}$ be a family of simplicial triangulations of Ω . For $T \in \mathcal{T}_h$, h_T is defined as the diameter of the smallest ball that contains T and ρ_T as the diameter of the largest ball contained in T . The meshsize h is defined as $h = \max\{h_T : T \in \mathcal{T}_h\}$.

Shape regularity: A family of triangulations is called shape regular if $\exists K > 0$ such that $\rho_T \geq \frac{h_T}{K}$.

Quasi-uniformity: \mathcal{T}_h is called quasi-uniform if it is shape regular and $\exists c > 0$ such that $\forall T \in \mathcal{T}_h$ holds $ch \leq h_T$.

Assumption: We assume that \mathcal{T}_h is shape regular in the following.

We will approximate the continuous level set function ϕ by discrete counterparts defined on Finite Element spaces corresponding to the triangulation \mathcal{T}_h . Whereas the geometry should be represented by a continuous Finite Element function, for the level set transport it is beneficial to consider discontinuous Finite Element spaces. Therefore we need two different representatives, namely a continuous and a discontinuous one defined by

$$\phi_h^{cont} \in V_h := \{v_h \in H^1(\Omega) : v_h|_T \in \mathbb{P}_1(T), \text{ for } T \in \mathcal{T}_h\} \quad (4.4)$$

$$\phi_{h,0} \in W_h := \{w_h \in L^2(\Omega) : w_h|_T \in \mathbb{P}_1(T), \text{ for } T \in \mathcal{T}_h\}. \quad (4.5)$$

The continuous representative is used to define the discrete interface/domains

$$\begin{aligned} \Gamma_h &:= \{x \in \Omega : \phi_h^{cont}(x) = 0\} \\ \Omega_{1,h} &:= \{x \in \Omega : \phi_h^{cont}(x) < 0\} \\ \Omega_{2,h} &:= \{x \in \Omega : \phi_h^{cont}(x) > 0\}. \end{aligned}$$

Remark: For a piecewise linear geometry approximation holds $dist(\Gamma_h, \Gamma) \sim h^2$ for a sufficiently accurate approximation ϕ_h of ϕ . This will not deteriorate any error estimates if linear Finite Elements are applied (cf. [LR17, Lemma 3.7]).

To establish accurate definitions we need some more notation. Let $T \in \mathcal{T}_h$ then

$$T_i := T \cap \Omega_{i,h}, \quad i \in \{1, 2\}, \quad (4.6)$$

$$\Gamma_T := T \cap \Gamma_h, \quad (4.7)$$

$$\mathcal{T}_h^\Gamma := \{T : \text{meas}_{d-1}(T \cap \Gamma_h) > 0\}, \quad (\text{set of cut elements}), \quad (4.8)$$

$$\Omega^\Gamma := \{x \in T : T \in \mathcal{T}_h^\Gamma\}, \quad (\text{domain of cut elements}). \quad (4.9)$$

Interpolation Operators

It is desirable to map between W_h and V_h as well as between $C(\Omega)$ and V_h . Therefore we will define two suitable interpolation operators.

To map discontinuous Finite Element functions on continuous ones, we employ the *Oswald interpolation* (cf. [LR17], [Osw93]). Let \mathcal{X} denote the set of mesh nodes, then we define for any $x_i \in \mathcal{X}$ the set of elements that contain x_i

$$\omega(x_i) := \{T \in \mathcal{T}_h : x_i \in \bar{T}\} .$$

For any $w_h \in W_h$, $x_i \in \mathcal{X}$ we define the local average as

$$A_{x_i}(w_h) := \frac{1}{|\omega(x_i)|} \sum_{T \in \omega(x_i)} w_h|_T(x_i) .$$

The interpolation operator between W_h and V_h is then defined as

$$I_h^{\phi,dc}(w_h)(x_i) := A_{x_i}(w_h) , \quad (4.10)$$

which defines an unique element $I_h^{\phi,dc}(w_h) \in V_h$.

The interpolation operator between $C(\Omega)$ and V_h is defined by standard nodal interpolation (cf. [LR13, Definition 5.2])

$$I_h^{\phi,cont} : C(\Omega) \rightarrow V_h, \quad I_h^{\phi,cont}(\psi)(x_i) = \psi(x_i) \quad \forall x_i \in \mathcal{X} . \quad (4.11)$$

Note that this interpolation problem defines an unique element in V_h , since we consider linear Finite Elements.

DG Level Set Transport

In order to discretize (4.1)-(4.3) we consider the discontinuous level set function $\phi_{h,0} \in W_h$. A popular method to solve transport equations numerically, is the upwind-DG formulation which we will also use here. To present an accurate definition of this method, we need some more notation

$$\mathcal{F}_h^i := \{F = \partial T_1 \cap \partial T_2 : T_1, T_2 \in \mathcal{T}_h, T_1 \neq T_2\} \quad (\text{set of inner facets}) .$$

For each $F \in \mathcal{F}_h^i$ we consider a master element T_1 , the second element will be denoted by T_2 . The unique facet normal n_F is then defined as the outer unit normal of ∂T_1 . For $w_h \in W_h$ we further define on $F \in \mathcal{F}_h^i$

$$\begin{aligned} \llbracket w_h \rrbracket &:= w_h|_{T_1} - w_h|_{T_2} && (\text{facet jump}), \\ \{\!\!\{ w_h \}\!\!\} &:= \frac{1}{2} (w_h|_{T_1} + w_h|_{T_2}) && (\text{facet average}) . \end{aligned}$$

Given a discrete descent direction $\beta_h \in \mathbf{X}_h := \{\psi_h \in [H_0^1(\Omega)]^d : \psi_h|_T \in [\mathbb{P}_1(T)]^d, T \in \mathcal{T}_h\}$ the upwind bilinear form is defined by (cf. [DPE11])

$$\begin{aligned} c_h^{upw}(w_h, v_h) &:= \int_{\Omega} (\beta_h \cdot \nabla w_h) v_h + \oint_{\partial\Omega} (\beta_h \cdot n_{\partial\Omega})^{\ominus} w_h v_h \\ &\quad - \sum_{F \in \mathcal{F}_h^i} \oint_F (\beta_h \cdot n_F) \llbracket w_h \rrbracket \{\!\!\{ v_h \}\!\!\} \\ &\quad + \sum_{F \in \mathcal{F}_h^i} \oint_F \frac{1}{2} |\beta_h \cdot n_F| \llbracket w_h \rrbracket \llbracket v_h \rrbracket , \end{aligned} \quad (4.12)$$

where $x^\ominus = \frac{1}{2}(|x| - x)$ is the negative part. Given a discrete boundary condition $\phi_{h,D}$ the corresponding linear form is defined as

$$F_h^c(v_h) := \oint_{\partial\Omega} (\beta_h \cdot n_{\partial\Omega})^\ominus \phi_{h,D} v_h .$$

As boundary condition we will choose $\phi_{h,D} = \phi_{h,0}$.

Remark: For a derivation that also motivates the name "upwind-DG" and more details on the method we refer to [Leh10].

Before we are going to define the semidiscrete and fully discrete version of the level set transport we will have a closer look at the upwind bilinear form $c_h^{upw}(\cdot, \cdot)$. For $v_h \in W_h$ and $F \in \mathcal{F}_h^i$ we define on F

$$v_h^{down} := \begin{cases} v_h|_{T_1} & \beta_h \cdot n_F < 0, \\ v_h|_{T_2} & \beta_h \cdot n_F > 0, \end{cases}$$

so v_h^{down} always "chooses" the value on the downwind side of the facet F (see Figure 4.2).

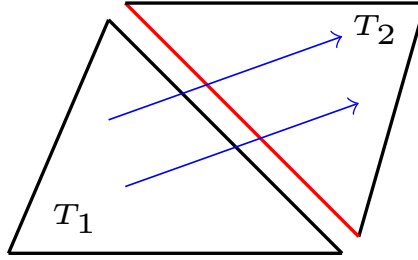


Figure 4.2: Two neighboring elements with the velocity field β_h (blue) and the downwind facet (red)

We would like to rewrite the two sums over the inner facets in (4.12). Therefore we have to distinct two cases.

Case 1: $\beta_h \cdot n_F < 0$ and thus $v_h^{down} = v_h|_{T_1}$

$$\begin{aligned} \frac{1}{2} |\beta_h \cdot n_F| \llbracket w_h \rrbracket \llbracket v_h \rrbracket - (\beta_h \cdot n_F) \llbracket w_h \rrbracket \{ \{ v_h \} \} &= -(\beta_h \cdot n_F) \llbracket w_h \rrbracket \left(\frac{1}{2} \llbracket v_h \rrbracket + \{ \{ v_h \} \} \right) \\ &= -(\beta_h \cdot n_F) \llbracket w_h \rrbracket \left(\frac{1}{2} (v_h|_{T_1} - v_h|_{T_2}) \right. \\ &\quad \left. + \frac{1}{2} (v_h|_{T_1} + v_h|_{T_2}) \right) \\ &= -(\beta_h \cdot n_F) \llbracket w_h \rrbracket v_h|_{T_1} \\ &= -(\beta_h \cdot n_F) \llbracket w_h \rrbracket v_h^{down} . \end{aligned}$$

Case 2: $\beta_h \cdot n_F > 0$ and thus $v_h^{down} = v_h|_{T_2}$. Here we conclude similarly

$$\frac{1}{2} |\beta_h \cdot n_F| \llbracket w_h \rrbracket \llbracket v_h \rrbracket - (\beta_h \cdot n_F) \llbracket w_h \rrbracket \{v_h\} = -(\beta_h \cdot n_F) \llbracket w_h \rrbracket v_h^{down} .$$

This investigation shows that we have an equivalent formulation of the upwind-DG bilinear form by

$$c_h^{upw}(w_h, v_h) := \int_{\Omega} (\beta_h \cdot \nabla w_h) v_h + \oint_{\partial\Omega} (\beta_h \cdot n_{\partial\Omega})^{\ominus} w_h v_h - \sum_{F \in \mathcal{F}_h^i} \oint_F (\beta_h \cdot n_F) \llbracket w_h \rrbracket v_h^{down} .$$

The semidiscrete variational formulation of (4.1)-(4.3) reads as

$$\begin{aligned} \text{find } \phi_h : [0, T] &\rightarrow W_h \text{ such that } \forall w_h \in W_h \\ \int_{\Omega} \partial_t \phi_h(t) w_h + c_h^{upw}(\phi_h(t), w_h) &= F_h^c(w_h) \\ \phi_h(0) &= \phi_{h,0} . \end{aligned} \quad (4.13)$$

This is a finite dimensional system of ordinary differential equations which can be fully discretized by an appropriate explicit or implicit time stepping scheme. We will choose an implicit Euler scheme. Let $N \in \mathbb{N}$ denote the number of time steps and $\Delta t := \frac{T}{N}$ the time step size. Starting with the initial condition $\phi_h^0 = \phi_{h,0}$ the solution at time instance $t^n = n\Delta t$ for $n \in \{1, \dots, N\}$ is then approximated by $\phi_h^n \approx \phi_h(t^n)$. The approximations are defined by the following scheme

$$\begin{aligned} \text{for } n = 1, \dots, N \text{ find } \phi_h^n \text{ such that } \forall w_h \in W_h \\ \int_{\Omega} \frac{1}{\Delta t} (\phi_h^n - \phi_h^{n-1}) w_h + c_h^{upw}(\phi_h^n, w_h) &= F_h^c(w_h) . \end{aligned} \quad (4.14)$$

Let $\dim(W_h) = L$ and $\{\omega_j : j = 1, \dots, L\} \subset W_h$ a basis of W_h . Then we can represent ϕ_h^n with respect to this basis $\phi_h^n = \sum_{j=1}^L c_j^n \omega_j$ with coefficients $c_j^n \in \mathbb{R}$. We obtain the following quantities

$$\begin{aligned} \mathbb{R}^L \ni \hat{\phi}^n &= (c_j^n)_{j=1}^L \\ \mathbb{R}^L \ni \hat{F} &= (F_h^c(\omega_j))_{j=1}^L \\ \mathbb{R}^{L \times L} \ni M &= \left((\omega_j, \omega_i)_{L^2(\Omega)} \right)_{i,j=1}^L \\ \mathbb{R}^{L \times L} \ni \hat{A} &= (c_h^{upw}(\omega_j, \omega_i))_{i,j=1}^L . \end{aligned}$$

Now we can rewrite (4.14) as the linear system

$$(M + \Delta t \hat{A}) \hat{\phi}^n = M \Delta \hat{\phi}^{n-1} + \Delta t \hat{F} . \quad (4.15)$$

Re-initialization

Usually the discrete level set function is initialized by an approximate signed distance function. During the level set transport, this property gets lost. In order to regain the signed distance property, the current level set function ϕ_h can be replaced after a few time steps by an approximate signed distance function $\tilde{\phi}_h$ that has the same zero level as ϕ_h . This process is known as *re-initialization* in the literature. The *fast marching method* (first introduced by Sethian [Set96]) is one possibility to implement such a re-initialization. The only information that is needed from the "old" level set function ϕ_h is its zero level Γ_h . Based on geometrical ideas, the values of $\tilde{\phi}_h$ close to the interface are assigned and then successively extended to the entire domain. For more details and further references we refer to [LR13, Section 9.3.2] and [GR11, Section 7.4.1].

In this thesis we try to avoid the use of re-initialization techniques. The underlying idea of this approach is, to transport the level set function by a velocity field β_h that doesn't deteriorate the signed distance property too much.

Chapter 5

FE Approximation of the One-phase Problem

In the first part of this chapter we will present an unfitted Finite Element method which yields solutions of optimal order for the one-phase problem introduced in Chapter 3.2. In the second part we will illustrate why an approximation of the velocity field based on the volume expression is superior over an approximation based on the boundary expression. We will see that the former one yields better approximation properties in a Finite Element context.

5.1 Fictitious Domain Method

We will present a fictitious domain method to solve the one-phase model problem. As our mesh is not aligned to the domain boundary, the boundary conditions have to be imposed in a weak sense. The presented idea goes back to Nitsche [Nit71], therefore the method is also called Nitsche fictitious domain method. Since our presentation is based on [BH12], we will only point out the main ideas and refer to this paper for more details.

Let $\Omega \subset \mathbb{R}^d$ a bounded domain, then we recall the problem (3.36)

$$\begin{aligned} -\Delta u &= f \quad \text{in } \Omega, \\ u &= 0 \quad \text{on } \partial\Omega. \end{aligned}$$

Mesh: For simplicity we assume here that \mathcal{T}_h is a quasi-uniform family of triangulations of the holdall domain $\Omega_0 \supset \Omega$. Please note that the domain boundary $\partial\Omega$ is not necessarily aligned to the element boundaries.

Let F be an facet of \mathcal{T}_h i.e. $F = T_1 \cap T_2$ with $T_1, T_2 \in \mathcal{T}_h$, $T_1 \neq T_2$ and $meas_{d-1}(F) > 0$. For each facet we fix a master element T_1 and define the facet normal n_F as the outer unit normal of T_1 . Further we define the set of facets close to the boundary

$$F_{\partial\Omega} := \{F = T_1 \cap T_2 : F \cap \Omega \neq \emptyset, T_1, T_2 \in \mathcal{T}_h, T_1 \cap \partial\Omega \neq \emptyset \text{ or } T_2 \cap \partial\Omega \neq \emptyset\}$$

and the active mesh/domain

$$\mathcal{T}_h^\Omega = \{T \in \mathcal{T}_h : T \cap \Omega \neq \emptyset\}, \quad \Omega^\mathcal{T} = \{x \in T : T \in \mathcal{T}_h^\Omega\}.$$

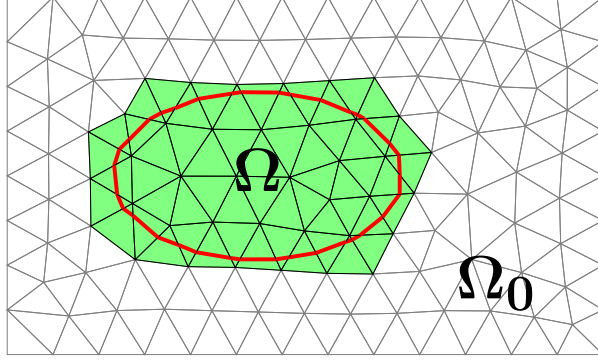


Figure 5.1: Background mesh with active mesh \mathcal{T}_h^Ω (green) and interface Γ (red)

The geometrical setting is sketched in Figure 5.1. We consider a standard Finite Element space on the active domain

$$V_h(\Omega^\mathcal{T}) = \{v_h \in H^1(\Omega^\mathcal{T}) : v_h|_T \in \mathbb{P}_1(T), T \in \mathcal{T}_h^\Omega\}.$$

For $v_h \in V_h(\Omega^\mathcal{T})$ the flux jump over a facet $F = T_1 \cap T_2$ is defined by

$$[[\nabla v_h \cdot n_F]] := (\nabla v_h|_{T_1} - \nabla v_h|_{T_2}) \cdot n_F.$$

Let n denote the outer unit normal of Ω and $\lambda \in \mathbb{R}$, then the Nitsche fictitious domain bilinear form $a_h^{fict}(\cdot, \cdot) : V_h(\Omega^\mathcal{T}) \times V_h(\Omega^\mathcal{T}) \rightarrow \mathbb{R}$ reads as

$$a_h^{fict}(u_h, v_h) := \int_\Omega \nabla u_h \cdot \nabla v_h - \oint_{\partial\Omega} \nabla u_h \cdot n v_h - \oint_{\partial\Omega} \nabla v_h \cdot n u_h + \oint_{\partial\Omega} \frac{\lambda}{h} u_h v_h.$$

Remark: For the sake of convenience, we assume that all integrals can be evaluated exactly.

To ensure stability in the case of small cuts ($|T \cap \Omega| \ll |T|$), an additional stabilization term is needed, the so called *ghost penalty*. For a facet $F = T_1 \cap T_2$ we define $h_F = \max\{\text{diam}(T_1), \text{diam}(T_2)\}$. Let $\mu \in \mathbb{R}$, then the *ghost penalty* bilinear form is defined by

$$j(u_h, v_h) := \sum_{F \in \mathcal{F}_{\partial\Omega}} \mu h_F \oint_F [[\nabla u_h \cdot n_F]] [[\nabla v_h \cdot n_F]].$$

This is all we need to formulate the fictitious domain variational problem for (3.36):

$$\begin{aligned} & \text{find } u_h \in V_h(\Omega^\mathcal{T}) \text{ such that } \forall v_h \in V_h(\Omega^\mathcal{T}) \\ B_h(u_h, v_h) & := a_h^{fict}(u_h, v_h) + j(u_h, v_h) = \int_\Omega f v_h. \end{aligned} \tag{5.1}$$

The properties of the solution to (5.1) are stated in the next lemma. The error bounds are given in the discrete energy norm defined by

$$\|v\|_h^2 := \sum_{T \in \mathcal{T}_h^\Omega} \int_T |\nabla v|^2 + h \oint_{\partial\Omega} (\nabla v \cdot n)^2 + \lambda h^{-1} \oint_{\partial\Omega} v^2 + j(v, v).$$

Remark: The discrete energy norm is defined on the active domain Ω^T that covers Ω . For a function $u \in H^2(\Omega)$ there exists a proper extension $E(u) \in H^2(\Omega^T)$ with $\|E(u)\|_{H^2(\Omega^T)} \leq C\|u\|_{H^2(\Omega)}$ (cf. [Ste70, Theorem 5, p.181]).

5.1. LEMMA [error bounds for u_h (one-phase)]

Let $u \in H^2(\Omega)$ be the solution to (3.36). The variational problem (5.1) admits a unique solution u_h for λ, μ sufficiently large, that fulfills

$$(i) \quad \|E(u) - u_h\|_h \leq Ch\|u\|_{H^2(\Omega)}$$

$$(ii) \quad \|u - u_h\|_{L^2(\Omega)} \leq Ch^2\|u\|_{H^2(\Omega)}.$$

Proof. See [BH12]. □

Similarly we can define the fictitious domain problem for the adjoint state (3.39) by

$$\begin{aligned} \text{find } u_h^* \in V_h(\Omega^T) \text{ such that } \forall v_h \in V_h(\Omega^T) \\ B_h(u_h^*, v_h) = \int_{\Omega} 2(u_h - u_c)v_h =: F_h^*(v_h). \end{aligned} \quad (5.2)$$

The same statement on the error bounds holds for the adjoint problem.

5.2. LEMMA [error bounds for u_h^* (one-phase)]

Let $u^* \in H^2(\Omega)$ be the solution to (3.36). The variational problem (5.2) admits a unique solution u_h^* for λ, μ sufficiently large, that fulfills

$$(i) \quad \|E(u^*) - u_h^*\|_h \leq Ch\|u^*\|_{H^2(\Omega)}$$

$$(ii) \quad \|u^* - u_h^*\|_{L^2(\Omega)} \leq Ch^2\|u^*\|_{H^2(\Omega)}.$$

Proof. The proof does not follow directly because the right hand side of the continuous and discrete adjoint problem differ. Therefore we define two auxiliary problems. The continuous problem with the perturbed source term

$$\begin{aligned} \text{find } w^* \in H_0^1(\Omega) \text{ such that } \forall v \in H_0^1(\Omega) \\ a(w^*, v) := \int_{\Omega} \nabla w^* \cdot \nabla v = \int_{\Omega} 2(u_h - u_c)v. \end{aligned}$$

And the discrete problem with the exact source term

$$\begin{aligned} \text{find } w_h^* \in V_h(\Omega^T) \text{ such that } \forall v_h \in V_h(\Omega^T) \\ B_h(w_h^*, v_h) = \int_{\Omega} 2(u - u_c)v_h. \end{aligned}$$

By the Poincaré inequality and Cauchy-Schwarz inequality we obtain

$$\begin{aligned}
\|w^* - u^*\|_{H^1(\Omega)}^2 &\leq Ca(w^* - u^*, w^* - u^*) \\
&= C \left(\int_{\Omega} 2(u_h - u_c)(w^* - u^*) - \int_{\Omega} 2(u - u_c)(w^* - u^*) \right) \\
&= 2C \int_{\Omega} (u - u_h)(w^* - u^*) \\
&\leq C \|w^* - u^*\|_{H^1(\Omega)} \|u - u_h\|_{L^2(\Omega)}.
\end{aligned}$$

Dividing by $\|w^* - u^*\|_{H^1(\Omega)}$ and application of Lemma 5.1 (ii) yields

$$\|w^* - u^*\|_{H^1(\Omega)} = \mathcal{O}(h^2).$$

An L^2 bound for $(w_h^* - u_h^*)$ can be found by the triangle inequality

$$\|w_h^* - u_h^*\|_{L^2(\Omega)} \leq \|w_h^* - u^*\|_{L^2(\Omega)} + \|u^* - w^*\|_{L^2(\Omega)} + \|w^* - u_h^*\|_{L^2(\Omega)} = \mathcal{O}(h^2).$$

The order of the second summand was shown above and the order for the first and third summand we can apply the standard error estimate as in Lemma 5.1 because w_h^*, u^* resp. u_h^*, w^* possess the same source term. Now we can apply the triangle inequality and conclude by using the error bounds above and discrete coercivity of $B_h(\cdot, \cdot)$ ([BH12, Lemma 6])

$$\begin{aligned}
\|E(u^*) - u_h^*\|_h^2 &\leq \|E(u^*) - w_h^*\|_h^2 + \|w_h^* - u_h^*\|_h^2 \\
&\leq C \left(h^2 + B_h(w_h^* - u_h^*, w_h^* - u_h^*) \right) \\
&= C \left(h^2 + \int_{\Omega} 2(u - u_h)(w_h^* - u_h^*) \right) \\
&\leq C \left(h^2 + \|u_h - u\|_{L^2(\Omega)} \|w_h^* - u_h^*\|_{L^2(\Omega)} \right) = \mathcal{O}(h^2) + \mathcal{O}(h^4).
\end{aligned}$$

Taking the square root yields the first claim. The second one is obtained directly by the triangle inequality

$$\begin{aligned}
\|u^* - u_h^*\|_{L^2(\Omega)} &\leq \|u^* - w^*\|_{L^2(\Omega)} + \|w^* - u_h^*\|_{L^2(\Omega)} \\
&\leq \|u^* - w^*\|_{H^1(\Omega)} + \|w^* - u_h^*\|_{L^2(\Omega)} = \mathcal{O}(h^2).
\end{aligned}$$

Where the order of the first summand was shown above and the order of the second one follows again by the standard estimate in Lemma 5.1. \square

5.2 Approximation of the Descent Direction

Continuous Descent Directions

To highlight the aspect of the choice of the descent direction, we consider the one-phase model problem from Section 3.2. Let the assumptions of Lemma 3.8 be valid and u, u^* be the solutions of problem (3.36) and (3.39). According to Lemma 3.8 we have two

expressions of the shape derivative that are equivalent on the analytical level. The volume expression

$$\begin{aligned} d^{VOL}[\vartheta] := & \int_{\Omega} \operatorname{div}(\vartheta) \left((u - u_c)^2 + u^* \right) - \int_{\Omega} 2(\nabla u_c \cdot \vartheta)(u - u_c) \\ & + \int_{\Omega} \left((D\vartheta + D\vartheta^T)\nabla u \right) \cdot \nabla u^* - \int_{\Omega} \operatorname{div}(\vartheta)\nabla u \cdot \nabla u^* + \int_{\Omega} (\nabla f \cdot \vartheta) u^* \end{aligned} \quad (5.3)$$

and the boundary expression

$$d^{BND}[\vartheta] := \int_{\partial\Omega} g(\vartheta \cdot n), \quad \text{with } g = (u - u_c)^2 + (\nabla u \cdot n)(\nabla u^* \cdot n) . \quad (5.4)$$

Remark: Since we claimed the assumptions of Lemma 3.8 to hold, we have that $g \in L^2(\partial\Omega)$. The Cauchy Schwarz inequality and the trace theorem imply further for $\vartheta \in \mathbf{X} = [H_0^1(\Omega_0)]^d$

$$d^{BND}[\vartheta] = \int_{\partial\Omega} g(\vartheta \cdot n) \leq \|g\|_{L^2(\partial\Omega)} \|\vartheta\|_{L^2(\partial\Omega)} \leq C \|g\|_{L^2(\partial\Omega)} \|\vartheta\|_{\mathbf{X}} .$$

Thus $d^{BND}[\cdot]$ is a linear and continuous functional on \mathbf{X} . Because both expressions are equal (on the analytical level), the same statement holds for $d^{VOL}[\cdot]$. Hence we obtain that the extension assumption (\mathbb{B}) from the first chapter is valid. Under weaker assumptions $d^{BND}[\cdot]$ may not be well defined at all and $d^{VOL}[\cdot]$ is only a linear and continuous functional on $W^{1,\infty}(\Omega)$.

To reduce the value of the shape function $J(\Omega) = \int_{\Omega} (u - u_c)^2$, we want to find a descent direction $\beta \in \mathbf{X}$. Let $b(\cdot, \cdot)$ be the inner product on \mathbf{X} and β' the Riesz representative of $-d^{VOL}[\cdot]$ i.e.

$$b(\beta', \psi) = -d^{VOL}[\psi], \quad \forall \psi \in \mathbf{X} .$$

Lemma 2.10 indicates that we have considerable freedom in the choice of β . We will investigate two possibilities namely

- $\beta^{VOL} = \beta'$
- β^{BND} with $\beta^{BND} \cdot n = -g$ on $\partial\Omega$,

where n is the outer unit normal of $\partial\Omega$.

Remark: For our purpose it is not enough to have a descent direction that is only defined on $\partial\Omega$ (such as g), since the level set transport equation requires a velocity field that is defined in the entire holdall domain Ω_0 . Therefore such descent directions require a Finite Element extension on Ω_0 before they can be used for the level set transport.

Discrete Descent Directions

To conclude this section we will now present an explanation why a volume based approximation of the descent direction should be preferred over a boundary based approximation. The main proposition of this section, which supports this statement, makes assumptions on error bounds of several discrete quantities. We want to emphasize that these assumptions need not necessarily to hold but are realistic very often (cf. [BEH⁺17]).

We consider a shape regular family of simplicial triangulations $\{\mathcal{T}_h\}$ of Ω_0 . The discrete counterparts for β^{VOL} and β^{BND} belong to the Finite Element space

$$\mathbf{X}_h = \{\psi_h \in [H_0^1(\Omega_0)]^d : \tau_h|_T \in [\mathbb{P}_1(T)]^d, T \in \mathcal{T}_h\}.$$

According to Corollary 2.6 for $\vartheta \in \mathbf{X}$, only the values of the normal component on $\partial\Omega$ influence the value of the shape derivative. So let $\beta \in \mathbf{X}$ be a descent direction and $\beta_h \in \mathbf{X}_h$ the corresponding discrete approximation, then we are interested in error bounds of the form

$$\|(\beta - \beta_h) \cdot n\|_{L^2(\partial\Omega)} \leq Ch^q \quad \text{for } q > 0.$$

The following result is a useful tool to bound L^p norms on the boundary for $p \geq 1$ and will be used later to bound the L^2 norm on the boundary.

5.3. LEMMA [trace inequality]

Let $\Omega \subset \mathbb{R}^d$ be a bounded domain with Lipschitz boundary. Then for $1 \leq p \leq \infty$, $\exists C > 0$ such that

$$\|v\|_{L^p(\partial\Omega)} \leq C \|v\|_{L^p(\Omega)}^{1-1/p} \|v\|_{W^{1,p}(\Omega)}^{1/p}, \quad \forall v \in W^{1,p}(\Omega).$$

Proof. See [BS07, Theorem 1.6.6]. □

Let $u_h, u_h^* \in V_h$ the solutions to (5.1), (5.2). The discrete version of the shape derivative (volume expression) is then defined by

$$\begin{aligned} d_h^{VOL}[\vartheta] := & \int_{\Omega} \operatorname{div}(\vartheta) \left((u_h - u_c)^2 + u_h^* \right) - \int_{\Omega} 2 (\nabla u_c \cdot \vartheta) (u_h - u_c) \\ & + \int_{\Omega} \left((D\vartheta + D\vartheta^T) \nabla u_h \right) \cdot \nabla u_h^* - \int_{\Omega} \operatorname{div}(\vartheta) \nabla u_h \cdot \nabla u_h^* + \int_{\Omega} (\nabla f \cdot \vartheta) u_h^*. \end{aligned} \quad (5.5)$$

The discrete Riesz representative is then defined as the unique $\beta'_h \in \mathbf{X}_h$ such that

$$b(\beta'_h, \psi_h) = -d_h^{VOL}[\psi_h], \quad \forall \psi_h \in \mathbf{X}_h. \quad (5.6)$$

According to Lemma 2.11 $\beta' \in [H_0^1(\Omega_0)]^d \cap [H^2(\Omega_0 \setminus \Omega)]^d \cap [H^2(\Omega)]^d$. We assumed further that $u, u^* \in H^2(\Omega)$. That motivates the following assumption on the corresponding error bounds.

5.4. Assumption [*optimal error bounds*]

$$\|\beta' - \beta'_h\|_{\mathbf{X}} = \mathcal{O}(h^{1/2}), \quad (5.7)$$

$$\|\beta' - \beta'_h\|_{[L^2(\Omega_0)]^d} = \mathcal{O}(h), \quad (5.8)$$

$$\|\nabla(u - u_h) \cdot n\|_{L^2(\partial\Omega)} = \mathcal{O}(h^{1/2}), \quad (5.9)$$

$$\|\nabla(u^* - u_h^*) \cdot n\|_{L^2(\partial\Omega)} = \mathcal{O}(h^{1/2}). \quad (5.10)$$

Remark: In order to proof the first two assumptions, one has to investigate the consistency error

$$\sup_{\psi_h \in \mathbf{X}_h} \frac{|d_h^{VOL}[\psi_h] - d^{VOL}[\psi_h]|}{\|\psi_h\|_{\mathbf{X}}}.$$

If the error bounds from Lemma 5.1 hold, the bounds (5.9)-(5.10) are relatively easy obtained by the use of the trace inequalities and interpolation errors on the boundary. Finally we want to emphasized, that these bounds are realistic and have been proven for a similar problem in [BEH⁺17].

For the discrete counterparts of β^{BND} and β^{VOL} we have

$$\beta_h^{BND} \cdot n = (u_h - u_c)^2 + (\nabla u_h \cdot n)(\nabla u_h^* \cdot n) =: g_h \quad \text{on } \partial\Omega \quad (5.11)$$

$$\beta_h^{VOL} = \beta'_h \quad \text{in } \Omega. \quad (5.12)$$

It is intuitive that the dominating error in $e_h(g) := \|g - g_h\|_{L^2(\partial\Omega)}$ will be

$$\|(\nabla u \cdot n)(\nabla u^* \cdot n) - (\nabla u_h \cdot n)(\nabla u_h^* \cdot n)\|_{L^2(\partial\Omega)}, \quad (5.13)$$

since in Finite Element methods the gradient of a function is less accurately approximated than the function itself. The following assumption is much stronger than Assumption 5.4 and claims that $e_h(g)$ can be controlled by the L^2 -error of the normal derivatives on the boundary.

5.5. ASSUMPTION [*error bound for the boundary representative*]

$$\|g - g_h\|_{L^2(\partial\Omega)} \leq C \left(\|\nabla(u - u_h) \cdot n\|_{L^2(\partial\Omega)} + \|\nabla(u^* - u_h^*) \cdot n\|_{L^2(\partial\Omega)} \right) \quad (5.14)$$

Now we can state the main result of this section.

5.6. PROPOSITION [*error bounds for discrete descent directions*]

Consider the discrete descent directions $\beta_h^{BND}, \beta_h^{VOL}$ as in (5.11), (5.12). If Assumptions 5.4 and 5.5 hold, then

$$\|(\beta^{BND} - \beta_h^{BND}) \cdot n\|_{L^2(\partial\Omega)} = \mathcal{O}(h^{1/2}),$$

$$\|(\beta^{VOL} - \beta_h^{VOL}) \cdot n\|_{L^2(\partial\Omega)} = \mathcal{O}(h^{3/4}).$$

Proof. For the first statement we obtain by Assumption 5.5 and Assumption 5.4 (5.9)/(5.10)

$$\begin{aligned} \|(\beta^{BND} - \beta_h^{BND}) \cdot n\|_{L^2(\partial\Omega)}^2 &\leq \|g - g_h\|_{L^2(\partial\Omega)} \\ &\leq C \left(\|\nabla(u - u_h) \cdot n\|_{L^2(\partial\Omega)} + \|\nabla(u^* - u_h^*) \cdot n\|_{L^2(\partial\Omega)} \right) = \mathcal{O}(h^{1/2}), \end{aligned}$$

which yields the first claim. For the second statement on β_h^{VOL} we obtain, using the trace inequality Lemma 5.3 and Young's inequality for $r \in \mathbb{R}$ arbitrary

$$\begin{aligned} \|(\beta^{VOL} - \beta_h^{VOL}) \cdot n\|_{L^2(\partial\Omega)} &= \|(\beta' - \beta'_h) \cdot n\|_{L^2(\partial\Omega)} \leq \|\beta' - \beta'_h\|_{[L^2(\partial\Omega)]^d} \\ &\stackrel{5.3}{\leq} C \left(\|\beta' - \beta'_h\|_{[L^2(\Omega)]^d}^{1/2} \|\beta' - \beta'_h\|_{\mathbf{X}}^{1/2} \right) \\ &\leq C \left(h^{-r} \|\beta' - \beta'_h\|_{[L^2(\Omega)]^d} + h^r \|\beta' - \beta'_h\|_{\mathbf{X}} \right) \\ &\leq C \left(h^{1-r} + h^{1/2+r} \right), \end{aligned}$$

where we used (5.7)/(5.8) in the last step. The choice $r = 1/4$ yields the error bound $\mathcal{O}(h^{3/4})$. \square

The above reasoning should motivate, why we will prefer the descent direction β_h^{VOL} stemming from the volume expression of the shape derivative. Although we privileged the boundary expression by the strong assumption on the error bound (Assumption 5.5), the volume expression yielded a more accurate descent direction. Numerical examples in accordance to the conjectured error bounds will be shown in Chapter 7.

Related Work

Another aspect that can be considered in this context is to compare the functionals $d_h^{VOL}[\cdot]$ and $d_h^{BND}[\cdot]$, where

$$d_h^{BND}[\vartheta] := \int_{\Omega} g_h(\vartheta \cdot n).$$

On the analytical level $d^{VOL}[\cdot]$ and $d^{BND}[\cdot]$ are equivalent, which does not hold for their discrete approximations. In [HPS15] it is investigated, how the corresponding approximation errors

$$\sup_{\|\beta\|_{\mathbf{X}}=1} \left| d_h^{VOL}[\beta] - d[\beta] \right| \tag{5.15}$$

$$\sup_{\|\beta\|_{\mathbf{X}}=1} \left| d_h^{BND}[\beta] - d[\beta] \right| \tag{5.16}$$

behave. To estimate (5.15) and (5.16), \mathbf{X} is replaced by a finite dimensional subspace $\mathbf{Y} \subset C^1(\Omega)$. For smooth domains, one can observe an experimental order of $\mathcal{O}(h^2)$ for the error of the volume functional and only $\mathcal{O}(h)$ for the error of the boundary functional. For more details, the reader is referred to [HPS15].

Chapter 6

FE Approximation of the Optimal Interface Problem

This chapter introduces all numerical methods which are needed to discretize the shape optimization problem introduced in Section 3.1. In the first section we will present the appropriate Finite Element spaces for unfitted interface problems. The second section of this chapter presents the discrete formulation of all sub problems of the full optimization procedure. The chapter is concluded by an optimization algorithm for problem (3.1) that also summarizes the former substeps.

6.1 The unfitted Finite Element Method (XFEM and CutFEM)

Since we work with a level set geometry representation (that moves in every optimization step) and a fixed mesh \mathcal{T}_h , the mesh elements are not aligned to the interface Γ . This leads to the fact, that we lose approximation accuracy. To maintain an optimal approximation order, the standard Finite Element spaces need to be modified.

Approximation Orders

We consider functions that are domain-wise smooth but can have a strong or weak discontinuity over the interface i.e. $u \in H^l(\Omega_1) \cap H^l(\Omega_2)$ or $u \in H^l(\Omega_1) \cap H^l(\Omega_2) \cap H^1(\Omega)$ for $l \geq 1$. We consider the standard Finite Element spaces

$$V_h^c := \{v \in H^1(\Omega) : v|_T \in \mathbb{P}_1(T), T \in \mathcal{T}_h\}, \quad V_h^{dc} := \{v \in L^2(\Omega) : v|_T \in \mathbb{P}_1(T), T \in \mathcal{T}_h\}.$$

For the selected spaces, the following approximation result holds

6.1. LEMMA [approximation order of standard FE spaces]

There exist shape regular families of triangulations $\{\mathcal{T}_h\}$, interfaces $\Gamma \in C^1$ and $w \in H^l(\Omega_1) \cap H^l(\Omega_2)$, $u \in H^l(\Omega_1) \cap H^l(\Omega_2) \cap H^1(\Omega)$ with $l \geq 2$ such that

$$(i) \quad \inf_{v_h \in V_h} \|w - v_h\|_{L^2(\Omega)} \geq Ch^{1/2}, \quad V_h \in \{V_h^c, V_h^{dc}\}.$$

$$(ii) \quad \inf_{v_h \in V_h} \|u - v_h\|_{L^2(\Omega)} \geq Ch^{3/2}, \quad V_h \in \{V_h^c, V_h^{dc}\}.$$

Proof. For (i) see [GR11, Section 7.9.1], for (ii) see Appendix (Proposition A.3). \square

Remark: The approximation orders in the last lemma do not improve, if the polynomial degree is increased to $k > 1$.

This lack of accuracy needs to be fixed, thus we will introduce FE-spaces that recover the domain-wise optimal approximation order globally. To do so we need more degrees of freedom in the region of the interface Γ . We define the restriction operator $\mathcal{R}_i : L^2(\Omega) \rightarrow L^2(\Omega)$ by

$$\mathcal{R}_i v = \begin{cases} v|_{\Omega_i} & \text{in } \Omega_i \\ 0 & \text{in } \Omega \setminus \Omega_i . \end{cases}$$

Now we can apply the restriction operator on the standard Finite Element space $V_h = \{v_h \in H^1(\Omega) : v_h|_T \in \mathbb{P}_1(T), T \in \mathcal{T}_h\}$, which defines the unfitted Finite Element space

$$V_h^\Gamma := \mathcal{R}_1 V_h \oplus \mathcal{R}_2 V_h .$$

The above definition describes V_h^Γ as the direct sum of two restricted/cut Finite Element spaces. Therefore, using this this description is referred to as CutFEM.

For V_h^Γ we obtain now an optimal approximation order again.

6.2. LEMMA [approximation order of V_h^Γ]

Let $u \in H^2(\Omega_1) \cap H^2(\Omega_2)$, then

$$\inf_{v_h \in V_h^\Gamma} \|u - v_h\|_{L^2(\Omega)} \leq Ch^2 \left(\|u\|_{H^2(\Omega_1)} + \|u\|_{H^2(\Omega_2)} \right) .$$

Proof. A proof can be found in [GR11, Theorem 7.9.3, p.254] . □

Remark: The approximation result of the last lemma remains valid for higher polynomial degrees $k > 1$ and yields an error bound h^{k+1} for $u \in H^{k+1}(\Omega_1) \cap H^{k+1}(\Omega_2)$. Since we only consider low order Finite Elements, the error bound for $k = 1$ will be sufficient in this thesis.

XFEM Characterization

The abstract space V_h^Γ can be characterized by an enrichment of the standard FE space V_h . This approach is referred to as XFEM. We follow [GR11, Section 7.9.2] to construct such enrichment basis functions.

Let $n = \dim(V_h)$, $\mathcal{J} = \{1, \dots, n\}$ and $\{\varphi_j : j \in \mathcal{J}\}$ a nodal basis of V_h i.e. for the i -th node x_i holds $\varphi_j(x_i) = \delta_{ij}$. We define the index set of nodes belonging to a basis function close to the interface

$$\mathcal{J}_\Gamma = \{j \in \mathcal{J} : \Gamma \cap \text{supp}(\varphi_j) \neq \emptyset\} .$$

For a basis function φ_i with $i \in \mathcal{J}_\Gamma$ and the corresponding node x_i we define

$$\Omega(x_i) = \begin{cases} \Omega_1 & \text{if } x_i \in \Omega_1 \\ \Omega_2 & \text{if } x_i \in \Omega_2 . \end{cases}$$

For every $i \in \mathcal{J}_\Gamma$ we add an enrichment function φ_i^Γ defined as

$$\varphi_i^\Gamma(x) = \begin{cases} 0 & \text{if } x \in \Omega(x_i) \\ \varphi_i(x) & \text{if } x \notin \Omega(x_i) . \end{cases}$$

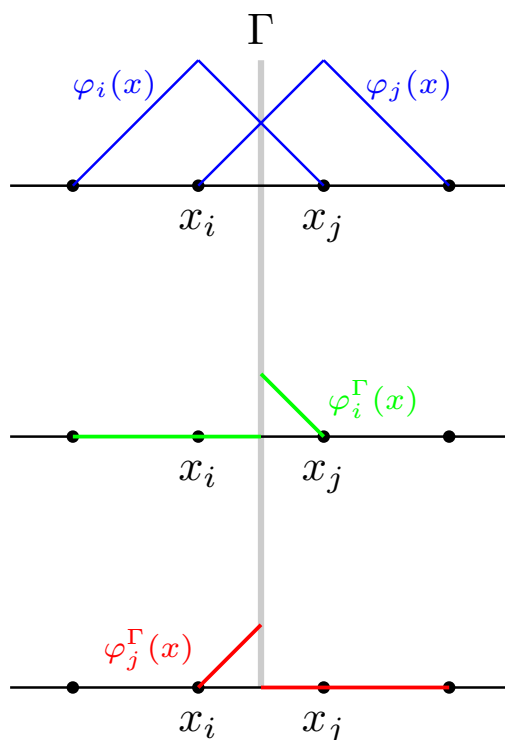


Figure 6.1: Two standard basis functions in 1D (upper) and the two corresponding enrichment functions (middle and lower).

The unfitted Finite Element space can now be represented as the direct sum of the standard and enrichment space i.e. $V_h^\Gamma = V_h \oplus \text{span}\{\varphi_j^\Gamma : j \in \mathcal{J}_\Gamma\} =: V_h \oplus V_h^x$. By construction we have two useful properties of $\varphi_j^\Gamma \in V_h^x$:

- $\text{supp}(\varphi_j^\Gamma) \subset \Omega^\Gamma$, $\forall j \in \mathcal{J}_\Gamma$ (nonzero only on cut elements)
- $\varphi_j^\Gamma(x_i) = 0$, $\forall j \in \mathcal{J}_\Gamma, i \in \mathcal{J}$ (enrichment function vanishes at all nodes) .

6.2 Shape Optimization Procedure for an Interface Problem

In this section we will derive an optimization algorithm for the two-phase problem from Section 3.1. Therefore we will give detailed descriptions of all discrete sub problems which need to be solved in each optimization step. This includes a unfitted Nitsche formulation for the state and adjoint state equation and the construction of a descent direction for the level set transport equation.

6.2.1 An unfitted Nitsche Method for the State and Adjoint State

We recall problem (3.2)-(3.5) from the last chapter. With a bounded domain $\Omega \subset \mathbb{R}^2$ that can be decomposed into two subdomains Ω_1 and Ω_2 , separated by the interface $\Gamma := \bar{\Omega}_1 \cap \bar{\Omega}_2$. Further it is assumed that Ω_1 is fully surrounded by Ω_2 .

$$-\operatorname{div}(\alpha \nabla u) = f \quad \text{in } \Omega \quad (6.1)$$

$$[[u]] = 0 \quad \text{on } \Gamma \quad (6.2)$$

$$[-\alpha \nabla u \cdot n_\Gamma] = 0 \quad \text{on } \Gamma \quad (6.3)$$

$$\nabla u \cdot n + \gamma u = 0 \quad \text{on } \partial\Omega \quad (6.4)$$

The weak formulation of this problem reads as

$$\begin{aligned} & \text{find } u \in H^1(\Omega) \text{ such that } \forall v \in H^1(\Omega) \\ & \sum_{i=1}^2 \alpha_i \int_{\Omega_i} \nabla u \cdot \nabla v + \int_{\partial\Omega} \gamma u v = \int_{\Omega} f v . \end{aligned} \quad (6.5)$$

To approximate u by a Finite Element solution we choose the unfitted Finite Element space introduced in the first section of this chapter

$$V_h^\Gamma = V_h|_{\Omega_1} \oplus V_h|_{\Omega_2} .$$

Remark: Note that we consider the unfitted Finite Element space with respect to the subdomains Ω_i . In fact, the Finite Element spaces are defined with respect to the discrete subdomains $\Omega_{i,h}$ but we assume for simplicity that the geometry can be approximated exactly. A deeper investigation shows that the geometry error does not deteriorate the subsequent error bounds (cf. [LR17]).

Since $V_h^\Gamma \not\subset C^0(\Omega)$, a discrete function $v_h \in V_h^\Gamma$ is in general not single valued on the interface Γ . Let n_Γ be the unit normal of Γ pointing outwards Ω_1 , $s \in \mathbb{R}$ and $x \in \Gamma$, then for any function w we define the two corresponding values of w by

$$w^-(x) := \lim_{s \searrow 0} w(x - sn_\Gamma) , \quad w^+(x) := \lim_{s \searrow 0} w(x + sn_\Gamma) .$$

Let $\kappa_1, \kappa_2 \geq 0$ with $\kappa_1 + \kappa_2 = 1$, then we define the jump and average operator (well known from discontinuous Galerkin methods) on the interface by

$$\begin{aligned} [[w(x)]] &= w^-(x) - w^+(x) , & x \in \Gamma \\ \{\{w(x)\}\} &= \kappa_1 w^-(x) + \kappa_2 w^+(x) , & x \in \Gamma . \end{aligned}$$

We define the discrete bilinear form $a_h : V_h^\Gamma \times V_h^\Gamma \rightarrow \mathbb{R}$ by

$$\begin{aligned} a_h(u_h, v_h) := & \sum_{i=1}^2 \alpha_i \int_{\Omega_i} \nabla u_h \cdot \nabla v_h + \oint_{\partial\Omega} \gamma u_h v_h \\ & - \oint_{\Gamma} \llbracket u_h \rrbracket \{ \alpha \nabla v_h \cdot n_\Gamma \} - \oint_{\Gamma} \llbracket v_h \rrbracket \{ \alpha \nabla u_h \cdot n_\Gamma \} + \oint_{\Gamma} \lambda \llbracket u_h \rrbracket \llbracket v_h \rrbracket , \end{aligned}$$

where $\lambda \geq 0$. The method corresponding to the bilinear form $a_h(\cdot, \cdot)$ is often called *Nitsche* method in the literature. The corresponding linear form $F_h : V_h^\Gamma \rightarrow \mathbb{R}$ is defined by

$$F(v_h) := \int_{\Omega} f v_h .$$

Thus the discrete variational problem reads:

$$\begin{aligned} \text{find } u_h \in V_h^\Gamma \text{ such that } \forall v_h \in V_h^\Gamma \\ a_h(u_h, v_h) = F(v_h) . \end{aligned} \tag{6.6}$$

For the error analysis of this discrete variational problem we will refer to the results in [LR17], where optimal error bounds are proven for a scalar interface problem with homogeneous Dirichlet boundary conditions. The paper is focussed on higher order methods but the analysis includes $k = 1$ as a special case. The only difference in the variational formulation is that we consider a Robin problem. However, since the outer boundary $\partial\Omega$ is fitted to the mesh, the generalization to this case is straightforward.

The coefficient of the average operator will be element wise defined by

$$\kappa_i = \frac{|T_i|}{|T|}, \quad \text{where } |T| = \text{meas}_d(T) ,$$

this particular choice has been first introduced by *Hansbo* and *Hansbo* (cf. [HH02]). To analyze the bilinear form $a_h(\cdot, \cdot)$, further norms are needed. The mesh dependent norms on the interface

$$\|v\|_{1/2, h, \Gamma}^2 := \sum_{T \in \mathcal{T}_h^\Gamma} \frac{(\alpha_1 + \alpha_2)}{2h_T} \int_{\Gamma_T} v^2, \quad \|v\|_{-1/2, h, \Gamma}^2 := \sum_{T \in \mathcal{T}_h^\Gamma} \frac{2h_T}{(\alpha_1 + \alpha_2)} \int_{\Gamma_T} v^2$$

and the full norm

$$\|v\|_h^2 := \sum_{i=1}^2 \int_{\Omega_{i, h}} \nabla v \cdot \nabla v + \oint_{\partial\Omega_R} v^2 + \|\{ \alpha \nabla v \cdot n_{\Gamma_h} \}\|_{-1/2, h, \Gamma}^2 + \|\llbracket v \rrbracket\|_{1/2, h, \Gamma}^2 .$$

We quote the following two results.

6.3. LEMMA [*properties of $a_h(\cdot, \cdot)$*]

Let $V_{reg} := H^1(\Omega) \cap H^2(\Omega_1) \cap H^2(\Omega_2)$, then for λ sufficiently large the bilinear form $a_h(\cdot, \cdot)$ has the following properties:

(i) *Continuity*

$$a_h(u, v) \leq \|u\|_h \|v\|_h \quad \forall u, v \in V_{reg} + V_h^\Gamma .$$

(ii) *Discrete coercivity*

$$a_h(v_h, v_h) \geq \|v_h\|_h^2 \quad \forall v_h \in V_h^\Gamma .$$

Proof. The proof is analogue to [Lemma 5.2][LR17]. \square

6.4. LEMMA [*interpolation error*]

There exists an interpolation operator $I_h^\Gamma : H^1(\Omega) \rightarrow V_h^\Gamma$ such that

$$\|v - I_h^\Gamma\|_h \leq Ch \left(\|v\|_{H^2(\Omega_1)} + \|v\|_{H^2(\Omega_2)} \right) \quad \forall v \in V_{reg} .$$

Proof. The proof is analogue to [Lemma 5.7][LR17]. \square

Those results yield the existence of a unique solution u_h of (6.6). The discrete solution fulfills the following optimal error bounds.

6.5. LEMMA [*error bounds for u_h (two-phase)*]

Let u be the solution of (6.5), then

$$(i) \quad \|u - u_h\|_h \leq Ch \left(\|u\|_{H^2(\Omega_1)} + \|u\|_{H^2(\Omega_2)} \right)$$

$$(ii) \quad \|u - u_h\|_{L^2(\Omega)} \leq Ch^2 \left(\|u\|_{H^2(\Omega_1)} + \|u\|_{H^2(\Omega_2)} \right)$$

Proof. The proof of the first statement is analogue to [Theorem 5.8][LR17]. A proof analogue to the second statement can be found in [Theorem 6.5][LR18]. \square

Similar to the discretized state equation (6.6) we discretize the adjoint equation (3.22). Therefore we define the discrete linear form

$$F_h^*(v_h) := \int_{\Omega} 2(u_h - \bar{u})v_h .$$

Thus the discrete adjoint problem reads

$$\begin{aligned} \text{find } u_h^* \in V_h^\Gamma \text{ such that } \forall v_h \in V_h^\Gamma \\ a_h(u_h^*, v_h) = F_h^*(v_h) . \end{aligned} \tag{6.7}$$

Similarly to the state problem, the discrete adjoint problem has a unique solution $u_h^* \in V_h^\Gamma$ that fulfills the same error bounds than u_h . To proof this statement, we need an additional lemma.

6.6. LEMMA [*consistency of the adjoint problem*]

Let u, u^* be the solutions of (6.5) and (3.22) with $u^* \in H^2(\Omega_1) \cap H^2(\Omega_2)$, then

$$a_h(u^*, v_h) = \int_{\Omega} 2(u - \bar{u})v_h, \quad \forall v_h \in V_h^{\Gamma}.$$

Proof. Since u^* is the exact solution of the adjoint problem $[[u^*]] = 0$ on Γ and thus

$$a_h(u^*, v_h) = \sum_{i=1}^2 \alpha_i \int_{\Omega_i} \nabla u^* \cdot \nabla v_h + \oint_{\partial\Omega} \gamma u^* v_h - \oint_{\Gamma} [[v_h]] \{ \alpha \nabla u^* \cdot n_{\Gamma} \}. \quad (6.8)$$

To treat the interface integral we note that for the exact solution u^* holds $\{ \alpha \nabla u^* \cdot n_{\Gamma} \} = \alpha_1 \nabla u^* \cdot n_{\Gamma} = \alpha_2 \nabla u^* \cdot n_{\Gamma}$ on Γ and $\alpha_2 \nabla u^* \cdot n = \gamma u^*$ on $\partial\Omega$. Further on the subdomains Ω_i holds $-\alpha_i \Delta u^* = 2(u - \bar{u})$. Integration by parts (Green's formula) yields

$$\begin{aligned} \oint_{\Gamma} [[v_h]] \{ \alpha \nabla u^* \cdot n_{\Gamma} \} &= \oint_{\partial\Omega_1} v_h^- \alpha_1 \nabla u^* \cdot n_{\Gamma} + \oint_{\partial\Omega_2} v_h^+ \alpha_2 \nabla u^* \cdot n_{\partial\Omega_2} + \oint_{\partial\Omega} v_h \alpha_2 \nabla u^* \cdot n \\ &= \sum_{i=1}^2 \alpha_i \int_{\Omega_i} \nabla u^* \cdot \nabla v_h + \sum_{i=1}^2 \int_{\Omega_i} (\alpha_i \Delta u^*) v_h + \oint_{\partial\Omega} \gamma u^* v_h \\ &= \sum_{i=1}^2 \alpha_i \int_{\Omega_i} \nabla u^* \cdot \nabla v_h + \oint_{\partial\Omega} \gamma u^* v_h - \int_{\Omega} 2(u - \bar{u})v_h. \end{aligned}$$

Inserting this identity into (6.8) yields the claim. \square

Finally we can state a lemma that ensures also optimal error bounds for u_h^* .

6.7. LEMMA [*error bounds for u_h^* (two-phase)*]

Let u^* be the solution of (3.22), then

$$(i) \quad \|u^* - u_h^*\|_h \leq Ch \left(\|u^*\|_{H^2(\Omega_1)} + \|u^*\|_{H^2(\Omega_2)} \right)$$

$$(ii) \quad \|u^* - u_h^*\|_{L^2(\Omega)} \leq Ch^2 \left(\|u^*\|_{H^2(\Omega_1)} + \|u^*\|_{H^2(\Omega_2)} \right)$$

Proof. Similarly as in Lemma 5.2, we have to take into account the perturbation on the right hand side. Let $F^*(\cdot)$ denote the source term corresponding to the exact solution i.e.

$$F^*(v) = \int_{\Omega} 2(u - \bar{u})v.$$

Due to the triangle inequality it is sufficient to consider the approximation error, since

$$\|u^* - u_h^*\|_h \leq \|u^* - I_h^{\Gamma}(u^*)\|_h + \|I_h^{\Gamma}(u^*) - u_h^*\|_h$$

and the interpolation error can be estimated by Lemma 6.4. For the approximation error we obtain using coercivity (Lemma 6.3) and consistency (Lemma 6.6)

$$\begin{aligned}
\|I_h^\Gamma(u^*) - u_h^*\|_h^2 &= a_h(I_h^\Gamma(u^*) - u_h^*, I_h^\Gamma(u^*) - u_h^*) \\
&= a_h(I_h^\Gamma(u^*) - u^*, I_h^\Gamma(u^*) - u_h^*) + a_h(u^* - u_h^*, I_h^\Gamma(u^*) - u_h^*) \\
&= a_h(I_h^\Gamma(u^*) - u^*, I_h^\Gamma(u^*) - u_h^*) + F_h^*(I_h^\Gamma(u^*) - u_h^*) - F_h^*(I_h^\Gamma(u^*) - u_h^*) \\
&\leq C \|I_h^\Gamma(u^*) - u_h^*\|_h \left(\|I_h^\Gamma(u^*) - u^*\|_h + \|u - u_h\|_{L^2(\Omega)} \right).
\end{aligned}$$

Dividing by $\|I_h^\Gamma(u^*) - u_h^*\|_h$ and application of Lemma 6.4, Lemma 6.5 on the quantities on the right hand side yields the first claim.

The second statement can be now obtained by a standard duality argument which will be skipped here. \square

6.2.2 Construction of a Descent Direction

So far we did not specify, which discrete velocity field β_h should be used in the level set transport equation. We will motivate our particular choice of β_h by a variational problem on the domain of cut elements which allows also for an analysis of the approximation error. The final variational problem will follow the same idea but will be formulated on whole Ω . This has the purpose to simplify the algorithm and it should be emphasized that a globally defined descent direction, for which the error analysis also applies, can be easily constructed.

In Section 5.2 we already indicated that for the one-phase problem, the volume expression of the shape derivative yields better approximation properties than the boundary expression. Therefore we will also for the two-phase problem prefer a descent direction that is based on the volume expression of the shape derivative. The discrete volume expression is given by

$$\begin{aligned}
d_h[\vartheta] &:= \int_{\Omega} \operatorname{div}(\vartheta) \left((u_h - \bar{u})^2 + f u_h^* \right) - \int_{\Omega} 2(\nabla \bar{u} \cdot \vartheta)(u_h - \bar{u}) \\
&\quad - \sum_{i=1}^2 \alpha_i \int_{\Omega_i} \operatorname{div}(\vartheta) \nabla u_h \cdot \nabla u_h^* + \sum_{i=1}^2 \alpha_i \int_{\Omega_i} \left((D\vartheta + D\vartheta^T) \nabla u_h \right) \cdot \nabla u_h^*,
\end{aligned} \tag{6.9}$$

where u_h, u_h^* are the solutions of (6.6) and (6.7). Let β'_h be the discrete Riesz representative of $-d_h[\cdot]$ i.e the unique $\beta'_h \in \mathbf{X}_h$ with

$$b(\beta'_h, \psi_h) = -d_h[\psi_h], \quad \forall \psi_h \in \mathbf{X}_h, \tag{6.10}$$

with the inner product $b(\beta, \psi) = \int_{\Omega} \beta \cdot \psi + \int_{\Omega} \nabla \beta : \nabla \psi$. According to Lemma 2.10 we won't violate the descent property if we change the values of β'_h in $\Omega \setminus \Gamma$. Therefore we will design a velocity field that that approximates β'_h on Γ and is extended to $\Omega \setminus \Gamma$ in such a way that the signed distance property around the interface is (approximately) preserved.

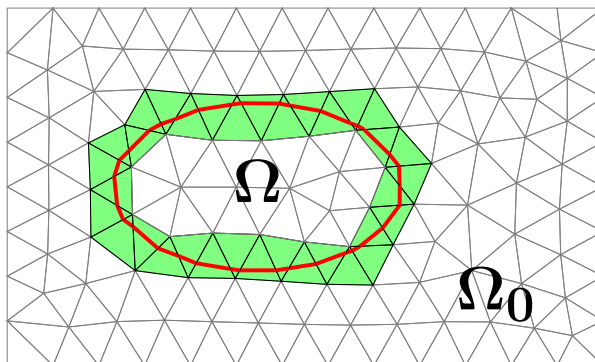


Figure 6.2: Background mesh with domain of cut elements Ω^Γ (green) and interface Γ (red)

Extension Close to the Interface

Assume we have a discrete level set function $\phi_{h,0} \in W_h$ that fulfills the approximate signed distance property on the domain of cut elements Ω^Γ (4.9), i.e. $|\phi_{h,0}(x)| \approx \text{dist}(x, \Gamma)$. In order to preserve the signed distance property approximately during the level set transport (4.14), the velocity field β_h should only have small alterations in the normal direction of the interface Γ because this would preserve the distance between two level sets. In [ZCMO96] the authors show that a signed distance function ϕ remains a signed distance function during the level set transport if

$$\beta \cdot \nabla \phi = 0 .$$

Since β_h is assumed to be not time dependent, the best we can do is to claim this approximate property for the initial geometry represented by ϕ_h^{cont} . Before we are going to define an extension on the whole domain Ω , we construct an extension on the domain of cut elements Ω^Γ (see Figure 6.2). A standard Finite Element space on this domain is defined by

$$V_h(\Omega^\Gamma) := \{v_h \in H^1(\Omega^\Gamma) : v_h|_T \in \mathbb{P}_1(T), T \in \mathcal{T}_h^\Gamma\} .$$

The outer unit normal of the interface is given by the normalized gradient of the continuous level set function $n_h^\phi(x) := \|\nabla \phi_h^{\text{cont}}(x)\|_2^{-1} \nabla \phi_h^{\text{cont}}(x)$. The corresponding extension problem is defined by

$$\begin{aligned} & \text{find } \beta_{h,j}^\Gamma \in V_h(\Omega^\Gamma), j \in \{1, 2\} \text{ such that } \forall v_h \in V_h \\ & \int_{\Omega^\Gamma} (\nabla \beta_{h,j}^\Gamma \cdot n_h^\phi) (\nabla v_h \cdot n_h^\phi) + h^{-1} \int_\Gamma \beta_{h,j}^\Gamma v_h = h^{-1} \int_\Gamma \beta_j' v_h . \end{aligned} \quad (6.11)$$

Remark: The volume integral in (6.11) corresponds to an anisotropic diffusion operator in direction of n_h^ϕ . By the boundary integrals, we want to approximate the descent direction β_j' on the interface Γ .

We define the tubular neighborhood of the interface by

$$U_\delta(\Gamma) := \{x \in \Omega : \text{dist}(x, \Gamma) \leq \delta\}, \quad \delta \in \mathbb{R}.$$

In order to show an approximation result on the interface, we need the following auxiliary lemma.

6.8. LEMMA [*estimate on U_δ*]

Let $w \in H^1(\Omega_1) \cap H^1(\Omega_2)$, then

$$\|w\|_{L^2(U_\delta)} \leq C\delta^{1/2} \left(\|w\|_{H^1(\Omega_1)} + \|w\|_{H^1(\Omega_2)} \right).$$

Proof. See [ER13, Lemma 4.10]. \square

From Lemma 2.11 we obtain that for the H^1 Riesz representative holds $\beta' \in [H^2(\Omega_1)]^d \cap [H^2(\Omega_2)]^d := [H^2(\Omega_{1,2})]^d$. As discussed in Section 5.2, we want to achieve an accurate approximation of β' at the interface Γ . By considering a discrete representative β'_h we introduce the errors

$$\|\beta' - \beta'_h\|_{\mathbf{x}} \tag{6.12}$$

$$\|\beta' - \beta'_h\|_{[L^2(\Gamma)]^d}. \tag{6.13}$$

The extension β_h^Γ introduces an additional approximation error

$$\|\beta_h^\Gamma - \beta'\|_{[L^2(\Gamma)]^d}. \tag{6.14}$$

The next lemma shows that we can bound (6.14) by means of (6.12) and (6.13).

6.9. LEMMA [*approximation error of β_h^Γ*]

The following error bound on the velocity field β_h^Γ holds:

$$\|\beta_h^\Gamma - \beta'\|_{[L^2(\Gamma)]^d} \leq C \left(\|\beta' - \beta'_h\|_{[L^2(\Gamma)]^d} + h \|\beta'\|_{[H^2(\Omega_{1,2})]^d} + h^{1/2} \|\beta' - \beta'_h\|_{\mathbf{x}} \right),$$

where $\|\cdot\|_{[H^2(\Omega_{1,2})]^d}^2 := \|\cdot\|_{[H^2(\Omega_1)]^d}^2 + \|\cdot\|_{[H^2(\Omega_2)]^d}^2$.

Proof. At first we note, that by the triangle inequality holds

$$\|\beta_h^\Gamma - \beta'\|_{[L^2(\Gamma)]^d} \leq \|\beta_h^\Gamma - \beta'_h\|_{[L^2(\Gamma)]^d} + \|\beta'_h - \beta'\|_{[L^2(\Gamma)]^d}. \tag{6.15}$$

We will further derive an estimate for the first summand. For the components of β_h holds that $\beta_{h,j} \in V_h$ and thus $\beta_{h,j}|_{\Omega^\Gamma} \in V_h(\Omega^\Gamma)$ is a valid test function for the variational problem (6.11). Taking advantage of that fact, we can use the variational formulation (6.11) and Young's inequality to obtain

$$\begin{aligned} & \int_{\Omega^\Gamma} \left(\nabla(\beta_{h,j}^\Gamma - \beta'_{h,j}) \cdot n_h^\phi \right)^2 + h^{-1} \oint_{\Gamma} (\beta_{h,j}^\Gamma - \beta'_{h,j})^2 \\ &= h^{-1} \oint_{\Gamma} \beta'_{h,j} (\beta_{h,j}^\Gamma - \beta'_{h,j}) - \int_{\Omega^\Gamma} \left(\nabla \beta'_{h,j} \cdot n_h^\phi \right) \left(\nabla(\beta_{h,j}^\Gamma - \beta'_{h,j}) \cdot n_h^\phi \right) - h^{-1} \oint_{\Gamma} \beta'_{h,j} (\beta_{h,j}^\Gamma - \beta'_{h,j}) \\ &\leq \frac{1}{4} \int_{\Omega^\Gamma} \left(\nabla \beta'_{h,j} \cdot n_h^\phi \right)^2 + \int_{\Omega^\Gamma} \left(\nabla(\beta_{h,j}^\Gamma - \beta'_{h,j}) \cdot n_h^\phi \right)^2. \end{aligned}$$

Subtracting the second summand on the right hand side, multiplying by h and taking the square root yields

$$\|\beta_h^\Gamma - \beta'_h\|_{[L^2(\Gamma)]^d} \leq \frac{1}{2}h^{1/2} \sqrt{\int_{\Omega^\Gamma} (\nabla \beta'_{h,j} \cdot n_h^\phi)^2} \leq h^{1/2} \|\nabla \beta'_{h,j}\|_{[L^2(U_h(\Gamma))]^d},$$

where we used $\Omega^\Gamma \subset U_h(\Gamma)$ in the last estimate. We obtain further by the triangle inequality and Lemma 6.8

$$\begin{aligned} h^{1/2} \|\nabla \beta'_{h,j}\|_{[L^2(U_h(\Gamma))]^d} &\leq h^{1/2} \|\beta' - \beta'_h\|_{\mathbf{X}} + h^{1/2} \|\nabla \beta'\|_{[L^2(U_h(\Gamma))]^d} \\ &\leq h^{1/2} \|\beta' - \beta'_h\|_{\mathbf{X}} + Ch \|\beta'_j\|_{H^2(\Omega_{1,2})}. \end{aligned}$$

All in all we have proven

$$\|\beta_h^\Gamma - \beta'_h\|_{[L^2(\Gamma)]^d} \leq C \left(h \|\beta'\|_{[H^2(\Omega_{1,2})]^d} + h^{1/2} \|\beta' - \beta'_h\|_{\mathbf{X}} \right).$$

Inserting this identity into (6.15) yields the claim. \square

Remark: If we assume error bounds similar to Assumption 5.4, the previous lemma shows that the approximation error of β_h^Γ can be bounded by the approximation error of the discrete Riesz representative β'_h and a term of order $\mathcal{O}(h)$. Hence, the approximation error of β_h^Γ won't be worse than the error introduced by β'_h .

Global Extension

A velocity field that is only defined on the band of cut elements Ω^Γ is not suitable for the level set transport, since we need a velocity field that is defined on whole Ω . Motivated by the former lemma we define the global variant of (6.11) by replacing Ω^Γ with Ω . To obtain a descent direction with a moderate scaling, β'_h is normalized before it is extended.

$$\begin{aligned} &\text{find } \beta_{h,j}^e \in V_h, j \in \{1, 2\} \text{ such that } \forall v_h \in V_h \\ &\int_{\Omega} (\nabla \beta_{h,j}^e \cdot n_h^\phi) (\nabla v_h \cdot n_h^\phi) + h^{-1} \oint_{\Gamma} \beta_{h,j}^e v_h = h^{-1} \|\beta'_h\|_{\mathbf{X}}^{-1} \oint_{\Gamma} \beta'_{h,j} v_h. \end{aligned} \quad (6.16)$$

The resulting velocity field $\beta_h^e \in [V_h]^2$ will be used in the level set transport equation (4.14) to move the level set function $\phi_{h,0}$.

Remark: The presented error analysis does not apply for the globally defined descent direction β_h^e . However, if we would extend the locally defined descent direction β_h^Γ to $\Omega \setminus \Omega^\Gamma$ with the same strategy, we would obtain a global velocity field that fulfills the error bounds of Lemma 6.9. In this thesis we chose a direct extension to Ω in order to keep the optimization algorithm simpler.

6.2.3 Optimization Algorithm

All the previously introduced discrete subproblems can be summarized by an optimization algorithm that solves problem (3.1). We give a rough summary what happens in one optimization step:

- Compute the discrete state and adjoint state u_h, u_h^* , (6.6), (6.7).
- Set up the discrete shape derivative $d_h[\cdot]$, (6.9).
- Compute the descent direction β_h^e , (6.16).
- Move the discontinuous level set function along β_h^e (6.16) by means of (4.14) and obtain ϕ_h^N at the final time instance.
- Update the geometry by means of the interpolation operator (4.10),
 $\phi_h^{cont} = I_h^{\phi, dc}(\phi_h^N)$.
- Compute the new state u_h on the updated geometry.
- Check if the value of the shape function is reduced.

The complete procedure corresponding to this workflow is presented in Algorithm 1, which is also the final result of this chapter.

Algorithm 1: optimization algorithm for problem (3.1)

Data: TOL (tolerance), $\phi \in C(\Omega)$ (exact initial level set function), T_{max} (maximum time step), T_{min} (minimum time step), $T_{old} = T_{new}$ (initial time step), i_{max} (maximum number of iterations), $p_1 > 1$ (increasing factor), $p_2 \in (0, 1)$ (decreasing factor)

$\phi_h^{cont} = I_h^{\phi, cont}(\phi)$ // initialize CG level set function by interpolation (4.11)
 $\phi_{h,0} = \phi_h^{cont}$ // initialize DG level set function
 $i = 0$ // initialize iteration counter
 Compute u_h // solve for the state (6.6)
 $Res = J(u_h)$ // set initial residual
 $Res_{old} = Res$ // store residual of last iteration

while ($Res > TOL$) **do**

$i += 1$ // increase iteration counter
 $rejected = True$ // set boolean for time step adaption
 Compute u_h^* // solve for the adjoint state (6.7)
 Set up $d_h[\cdot]$ // discrete shape derivative according to (6.9)
 Compute β_h' // solve for the discrete Riesz representative (6.10)
 Compute β_h^e // construct the descent direction according to (6.16)
 $T_{new} = \min(p_1 \cdot T_{old}, T_{max})$ // set new time step size

while ($rejected = True$) **do**

Compute ϕ_h^N // level set transport with $\beta_h = \beta_h^e$, $T = T_{new}$ (4.14)
 $\phi_h^{cont} = I_h^{\phi, dc}(\phi_h^N)$ // set CG level set function by interpolation (4.10)
 Compute u_h // solve for the new state (6.6) on the update geometry
 $Res = J(u_h)$ // set residual

if ($Res < Res_{old}$) **then**

$rejected = False$ // accept time step
 $\phi_{h,0} = \phi_h^N$ // update initial discontinuous level set function

else

$T_{new} = p_2 \cdot T_{new}$ // reject time step and decrease step size
if ($T_{new} < T_{min}$) **then**
 \mathbf{stop} // time step too small
 $\phi_h^{cont} = I_h^{\phi, dc}(\phi_{h,0})$ // set CG level set function back to old domain

$Res_{old} = Res$ // update old residual

if ($i > i_{max}$) **then**

\mathbf{stop} // maximum number of iterations exceeded

Result: Optimal shape represented by ϕ_h^{cont}

Remark: The stopping criteria ($Res \leq TOL$) may require a priori knowledge on the behavior of the optimization problem. Alternatively we could stop if the residual does not significantly improve anymore i.e. if $Res_{old} - Res < \epsilon$, where $\epsilon > 0$ and $i > 0$.

Chapter 7

Numerical Results

In this chapter we will present numerical experiments to highlight the following aspects

- Section 7.1: Accuracy of descent directions for the one-phase model problem of Section 3.2 with focus on the comparison between volume and boundary expression.
- Section 7.2: Accuracy of descent directions for the two-phase model problem of Section 3.1 with focus on the choice of the approximation space.
- Section 7.3: Performance of the full optimization algorithm (Algorithm 1).
- Section 7.4: Comparison of the descent directions β'_h (Riesz representative) and β_h^e (anisotropic extension).
- Section 7.5: Behavior of geometry error and residual error.

All numerical methods and experiments have been implemented in the add-on library `ngsxfem` to the Finite Element software `NGSolve` [Sch14].

7.1 Comparison of Volume and Boundary Expression

We recall the setting of Section 5.2. As a model problem we consider $\Omega_0 = [-1, -1] \times [1, 1]$ for the holdall domain and the Dirichlet problem

$$-\Delta u = f \quad \text{in } \Omega \tag{7.1}$$

$$u = 0 \quad \text{on } \partial\Omega, \tag{7.2}$$

with $f = 8(0.25 - 2(x^2 + y^2))$ and the shape function

$$J(\Omega) = \int_{\Omega} (u - u_c)^2 .$$

We choose $u_c = (x^2 + y^2 - 0.25)^2$, which is the exact solution to (7.1), where Ω is a circle with radius 0.5 and center (0,0). As initial domain we choose an ellipse corresponding to the signed distance function

$$\phi(x, y) = \sqrt{\frac{x^2}{1.6} + \frac{y^2}{0.4}} - 0.5 .$$

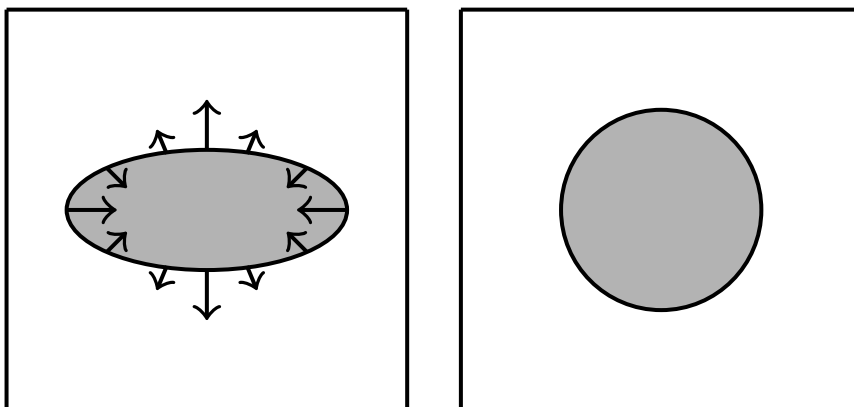


Figure 7.1: Initial domain (left) with expected velocity field and optimal domain (right)

The domains are sketched in Figure 7.1. To get approximations of the two descent directions we compute u_h, u_h^* with the fictitious domain method (5.1), (5.2). We further compute the discrete Riesz representative β'_h according to (5.6) and the discrete boundary representative g_h according to (5.11). The computations are done on a uniformly refined mesh with meshsizes $h_n := \frac{\sqrt{2}}{2^n}$, where $n \in \{0, \dots, 7\}$. To get comparable results we scale both quantities by the L^2 -norm on the boundary. As a reference solution we choose the finest approximation i.e $g_{ref} := g_{h_7}$ and $\beta'_{ref} := \beta'_{h_7}$. This yields the two error estimators

$$\begin{aligned} e_h^V &= \left(\|\beta'_h\|_{L^2(\partial\Omega)} \right)^{-1} \beta'_h - \left(\|\beta'_{ref}\|_{L^2(\partial\Omega)} \right)^{-1} \beta'_{ref} \quad \text{defined on } \Omega \\ e_h^B &= \left(\|g_h\|_{L^2(\partial\Omega)} \right)^{-1} g_h - \left(\|g_{ref}\|_{L^2(\partial\Omega)} \right)^{-1} g_{ref} \quad \text{defined on } \partial\Omega . \end{aligned}$$

The results for $\|e_h^V\|_{L^2(\partial\Omega)}$ and $\|e_h^B\|_{L^2(\partial\Omega)}$ are shown in Figure 7.2. The results are in accordance with the error bounds conjectured in Section 5.2. Moreover we see that the approximation based on the boundary expression does just show the predicted convergence order of $\mathcal{O}(h^{1/2})$. On the other hand, the approximation based on the volume expression shows a better behavior than the predicted $\mathcal{O}(h^{3/4})$. We can observe an experimental order of $\mathcal{O}(h^{3/2})$.

Since e_h^V is defined on the entire holdall Ω_0 we can also check the predicted convergence properties with respect to the $L^2(\Omega_0)$, and $H^1(\Omega_0)$ norm, the results are shown in Figure 7.3. In the $H^1(\Omega_0)$ norm, we can observe slightly better rates than the predicted order of $\mathcal{O}(h^{1/2})$. In the $L^2(\Omega_0)$ norm we see an experimental order of $\mathcal{O}(h^{3/2})$, which is better than the order $\mathcal{O}(h)$ that was assumed in Section 5.2.

A descent direction based on the boundary expression of the shape derivative can be extended from the interface Γ into the whole domain Ω with a strategy similar to Section 6.2.2. That enables us to employ this velocity field for the level set transport step

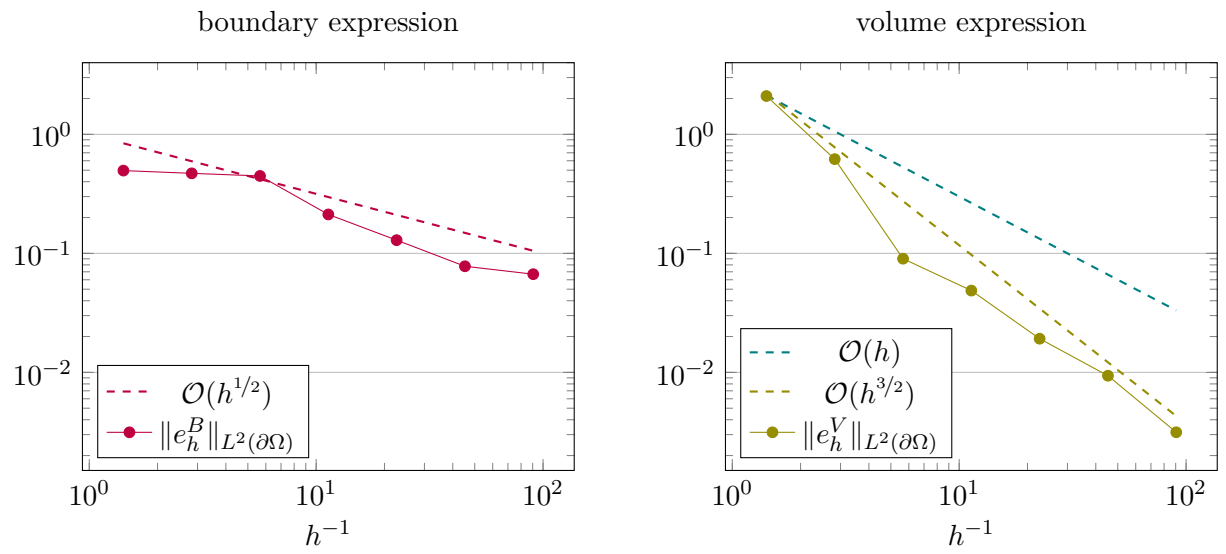


Figure 7.2: Errors estimators at the boundary

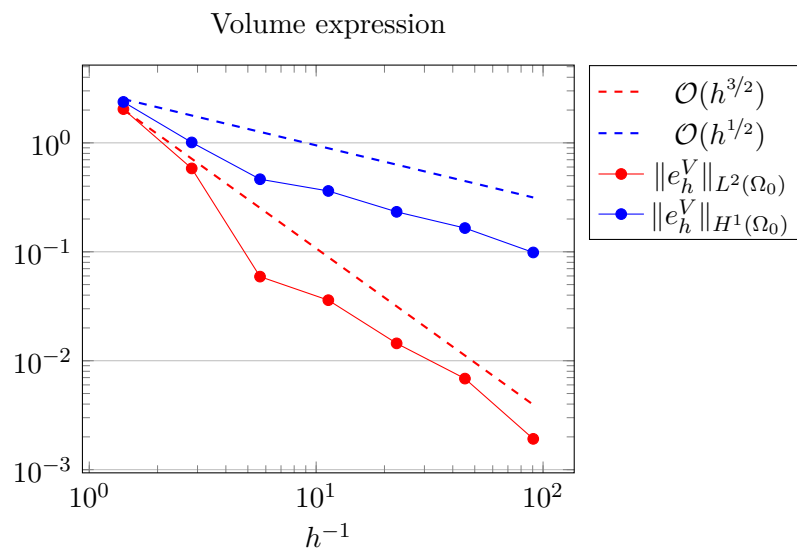


Figure 7.3: Errors estimators in the volume

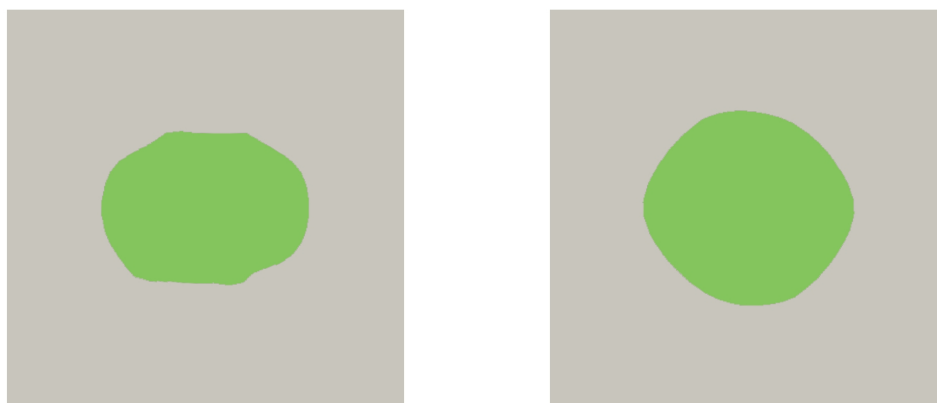


Figure 7.4: Final shapes using a boundary based descent direction (left) and a volume based descent direction (right)

in Algorithm 1. We can compare the performance of both directions (volume based, boundary based) in the full optimization procedure. We consider the same example as before and observe that the algorithm using the boundary based descent direction stops much earlier with a residual of $3.36 \cdot 10^{-3}$. Using the volume based descent direction β_h^e yields a lower final residual of $1.34 \cdot 10^{-3}$ and also the final domain looks much better. The final shapes of both runs are shown in Figure 7.4.

7.2 Approximation Spaces for the Descent Direction

For the remaining part of this chapter we consider the two-phase model problem introduced in Section 3.1. So far we considered an XFEM-approximation only for the discrete state and adjoint state equation with corresponding solutions u_h, u_h^* . However, for the discrete Riesz representative β_h' we still used a conforming approach. In this section we will investigate if an extended approximation of β_h' yields better convergence results. We recall the conforming, vector-valued Finite Element space

$$\mathbf{X}_h := \{\tau_h \in [H_0^1(\Omega_0)]^d : \tau_h|_T \in [\mathbb{P}_1(T)]^d, T \in \mathcal{T}_h\}.$$

The corresponding unfitted Finite Element space is defined similarly to Section 6.1 by

$$\mathbf{X}_h^\Gamma := \mathbf{X}_h|_{\Omega_1} \oplus \mathbf{X}_h|_{\Omega_2}.$$

To obtain a variational formulation we define the bilinear form $b^\Gamma(\cdot, \cdot) : \mathbf{X}_h^\Gamma \times \mathbf{X}_h^\Gamma \rightarrow \mathbb{R}$ by

$$b^\Gamma(\beta_h, \psi_h) := b(\beta_h, \psi_h) - \oint_\Gamma \{\!\!\{ \nabla \beta_h n_\Gamma \}\!\!\} \cdot \llbracket \psi_h \rrbracket - \oint_\Gamma \{\!\!\{ \nabla \psi_h n_\Gamma \}\!\!\} \cdot \llbracket \beta_h \rrbracket + \oint_\Gamma \frac{\lambda}{h} \llbracket \beta_h \rrbracket \cdot \llbracket \psi_h \rrbracket,$$

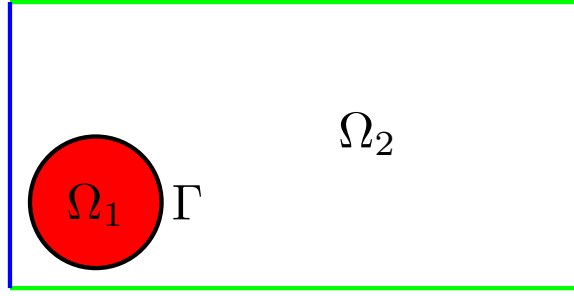


Figure 7.5: Robin boundary (green) and Neumann boundary (blue)

with $\lambda = 40$. Let $d_h[\cdot]$ be the discrete shape derivative defined in (6.9), then the XFEM variational formulation reads as

$$\begin{aligned} \text{find } \beta_h^{cut'} \in \mathbf{X}_h^\Gamma \text{ such that } \forall \psi_h \in \mathbf{X}_h^\Gamma \\ b^\Gamma(\beta_h^{cut'}, \psi_h) = -d_h[\psi_h] . \end{aligned} \quad (7.3)$$

We consider the holdall domain $\Omega = [0, 2] \times [0, 1]$ where the subdomain Ω_1 is a circle with center $(0.3, 0.3)$ and radius 0.23 . For the Neumann boundary we take $\partial\Omega_N = \{0\} \times [0, 1]$ and thus $\partial\Omega_R = \partial\Omega \setminus \partial\Omega_N$. The geometry is sketched in Figure 7.5.

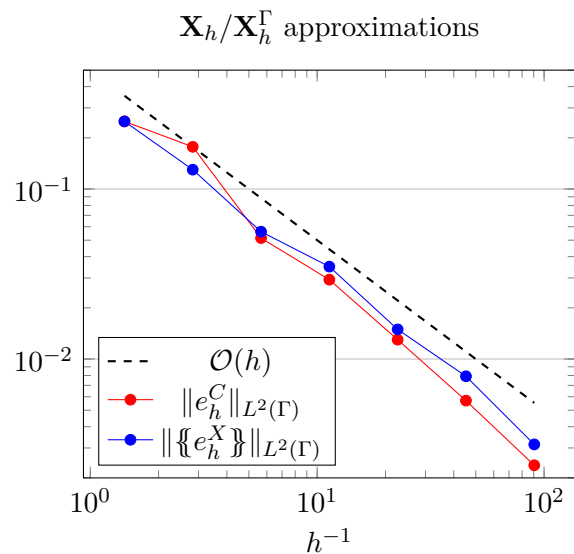
Further we choose the following data

$$\alpha_1 = 2, \quad \alpha_2 = 1, \quad f_1 = 10, \quad \bar{u} = 0.4, \quad \gamma_0 = 1 .$$

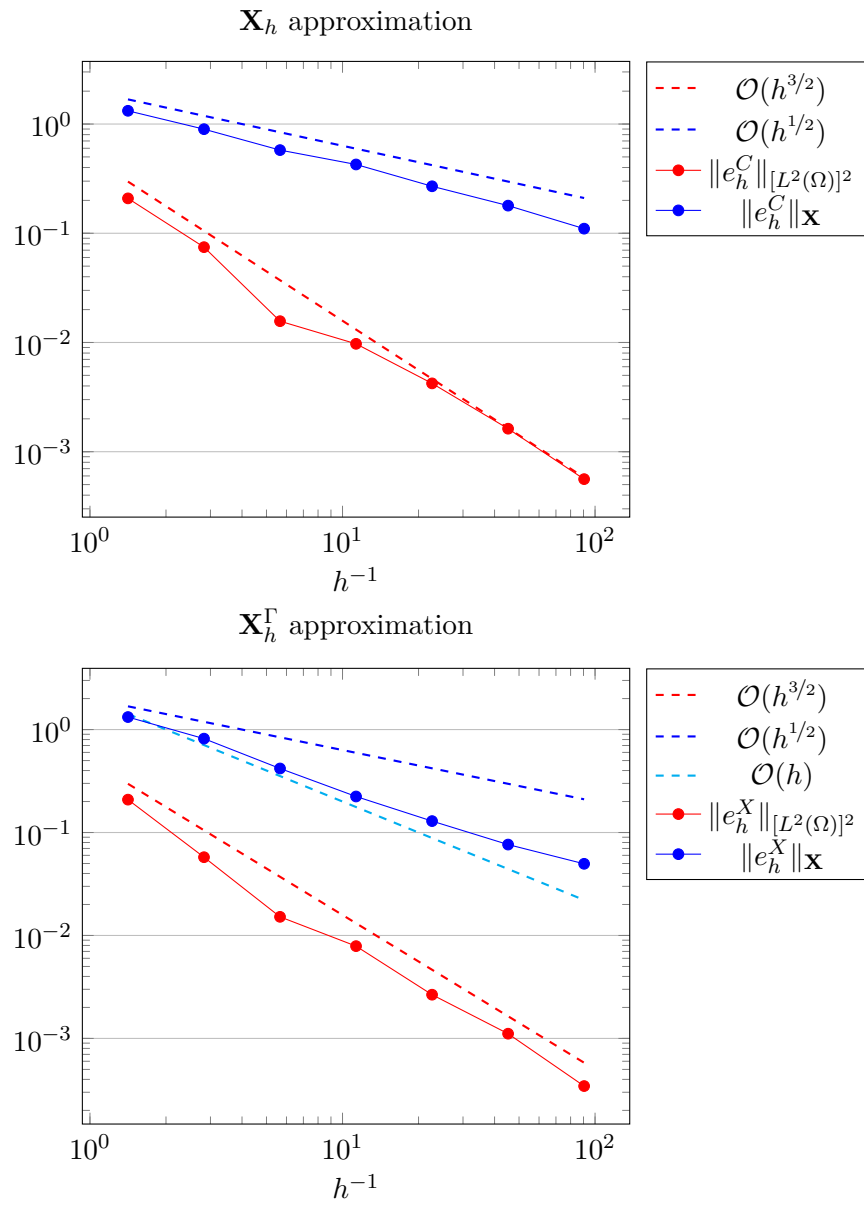
Let β'_h be defined by (6.10) and $\beta_h^{cut'}$ by (7.3). Similarly to the previous section we consider a sequence of meshsizes $h_n := \frac{\sqrt{2}}{2^n}$, $n \in \{1, \dots, 8\}$. The reference solutions are taken from the finest grid i.e. $\beta'_{ref} := \beta'_{h_8}$ and $\beta_{ref}^{cut'} := \beta_{h_8}^{cut'}$. The error estimators are defined by

$$\begin{aligned} e_h^C &= (\|\beta'_h\|_{\mathbf{X}})^{-1} \beta'_h - (\|\beta'_{ref}\|_{\mathbf{X}})^{-1} \beta'_{ref} && \text{defined on } \Omega \\ e_h^X &= (\|\beta_h^{cut'}\|_{\mathbf{X}})^{-1} \beta_h^{cut'} - (\|\beta_{ref}^{cut'}\|_{\mathbf{X}})^{-1} \beta_{ref}^{cut'} && \text{defined on } \Omega \\ \{e_h^X\} &= \frac{1}{2} (\|\beta_h^{cut'}\|_{\mathbf{X}})^{-1} (\beta_h^{cut'}|_{\Omega_1} + \beta_h^{cut'}|_{\Omega_2}) && \text{defined on } \Gamma . \end{aligned}$$

The average is necessary because $\beta_h^{cut'}$ is not single valued on Γ . The results with respect to the $L^2(\Gamma)$ norm are shown in Figure 7.6. We observe that both approximations show the same experimental order of $\mathcal{O}(h)$, we do not obtain a higher convergence order by applying an unfitted approach on the descent direction. Further it should be noted that the order $\mathcal{O}(h)$ for the $L^2(\Gamma)$ norm is less than the corresponding order for the $L^2(\partial\Omega)$ norm in case of the one-phase problem. There we observed $\|e_h^V\|_{L^2(\partial\Omega)} = \mathcal{O}(h^{3/2})$ on the boundary.

Figure 7.6: Convergence rates on the interface Γ

We do also investigate the behavior of e_h^C , e_h^V with respect to the volume norms $\|\cdot\|_{\mathbf{X}}$ and $\|\cdot\|_{[L^2(\Omega)]^2}$. The results are shown in Figure 7.7. The experimental order of the unfitted approximation with respect to the \mathbf{X} -norm is slightly better and we reach almost order $\mathcal{O}(h)$ whereas the conforming approximation shows only order $\mathcal{O}(h^{1/2})$. In the L^2 norm we observe the same order $\mathcal{O}(h^{3/2})$ for both approximations. The experimental convergence orders with respect to the volume norms coincide with those obtained for the one-phase problem.

Figure 7.7: Convergence rates in the volume Ω

7.3 Full Geometry Optimization

In this section we will present two examples that show the full optimization algorithm (Algorithm 1) in action.

Example 1

We will start with an easy reconstruction example to ensure that we obtain reasonable results. As the holdall domain we consider the unit square $\Omega = [0, 1]^2$ with Robin boundary conditions everywhere i.e. $\partial\Omega_R = \partial\Omega$. Further we choose the following data

$$\alpha_1 = 2, \alpha_2 = 1, f_1 = 1, \gamma_0 = 1 .$$

The reference domain Ω_1^{ref} is chosen a circle with center $(0.7, 0.7)$ and radius 0.2, thus the corresponding interface is defined by $\Gamma^{ref} := \partial\Omega_1^{ref}$. The reference distribution \bar{u} is approximated by the Finite Element solution of the variational problem

$$\begin{aligned} \text{find } \bar{u}_h \in V_h^{\Gamma^{ref}} \text{ such that } \forall v_h \in V_h^{\Gamma^{ref}} \\ a_h(\bar{u}_h, v_h) := F_h(v_h) . \end{aligned}$$

We start with an initial inner domain Ω_1 that is a circle with center $(0.4, 0.4)$, radius 0.3 and we seek to reconstruct Γ^{ref} . The computations are done on a uniform triangular mesh with meshsize $h = \frac{\sqrt{2}}{25} \approx 0.044$. The results are shown in Figure 7.9. We observe that the circle is first shrunk to a smaller circle and afterwards transported to the expected position. The algorithm stops, because the residual does not decrease anymore and the minimum time step size is reached. A graph that shows how the residual decreases is shown in Figure 7.8.

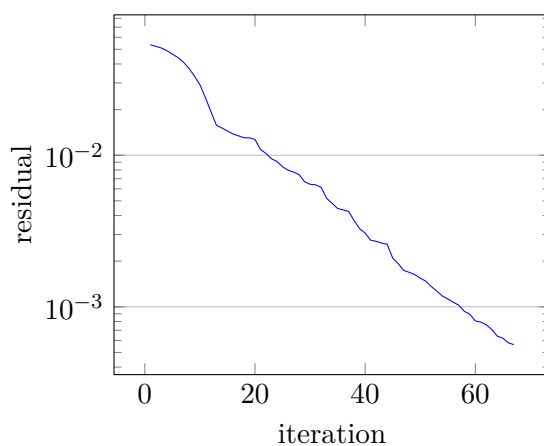


Figure 7.8: Residuals for the reconstruction example

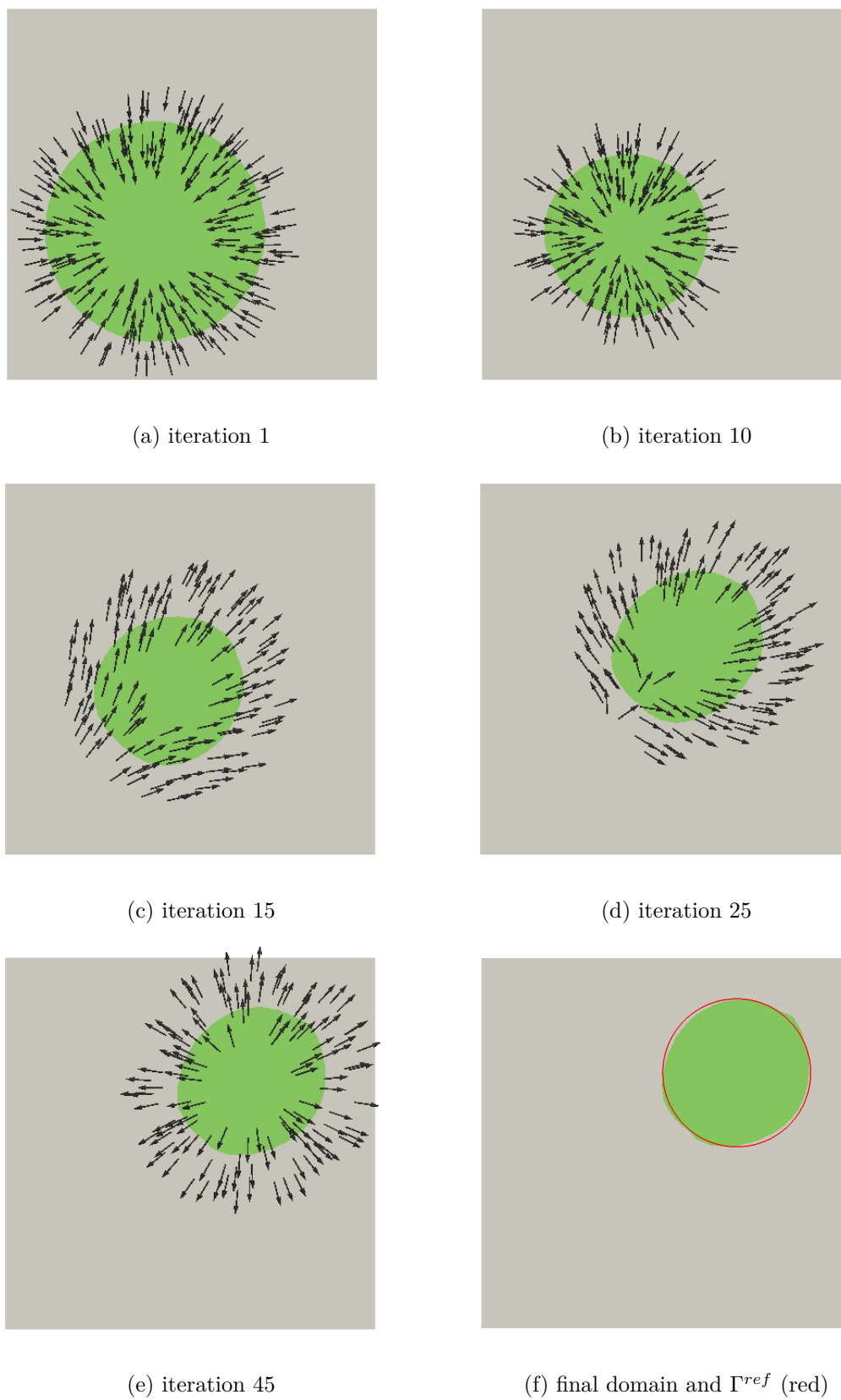


Figure 7.9: Current domain and descent direction around the interface (reconstruction example)

In this case, a final residual of zero would be possible. However, a zero residual is not achieved due to several discretization errors that perturb the accuracy.

- Discretization of the shape derivative $d[\cdot] \rightarrow d_h[\cdot]$ by replacing the primal and dual solutions u, u^* by their discrete approximations u_h, u_h^* . Thus the exact Riesz representative β' is only approximated by the discrete one β'_h .
- Since we do not consider a re-initialization step during the level set transport, the signed distance property of the discrete level set function is perturbed. For a deeper investigation of this effect we refer to the next section.

Example 2

For the next example we design a more interesting scenario. We consider a room that has doors and windows which are modeled by a Robin boundary. The corresponding geometry is sketched in Figure 7.10.

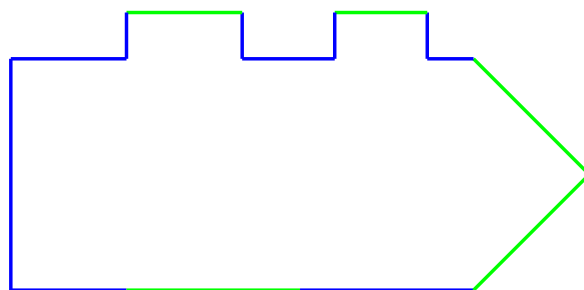


Figure 7.10: Room geometry with doors/windows (green) and isolated walls (blue)

Further we choose the following data

$$\alpha_1 = 10, \alpha_2 = 1, f_1 = 180, \gamma_0 = 1, \bar{u}(x, y) = 25 - (x - 1)^2 + 2y .$$

The initial inner domain Ω_1 (location of the heat source) for the first attempt is chosen according to the levelset function

$$\phi(x, y) = \sqrt{\frac{(x - 0.4)^2}{0.6} + \frac{(y - 0.5)^2}{1.4}} - 0.25 .$$

The results are shown in Figure 7.13. We will check the robustness of the algorithm with respect to the multiple transport steps by choosing an initial inner domain that is closer to the optimal domain of the first attempt, therefore we set the initial level set function to

$$\phi(x, y) = \sqrt{\frac{(x - 1.6)^2}{1.9} + \frac{(y - 0.7)^2}{0.1}} - 0.4 .$$

We hope that the final domain for the second attempt does not yield a significantly smaller residual. The results for the second attempt are shown in Figure 7.12. Although the final shape looks a bit different now, we obtain almost the same residual. The second attempt needs much less iterations to terminate, which is also intuitive. The residuals for both runs are shown in Figure 7.11. In the setting of the second example we don't have any knowledge on existence and/or uniqueness of optimal solutions. Therefore it is not surprising that the algorithm terminates at different final shapes for different initial values.

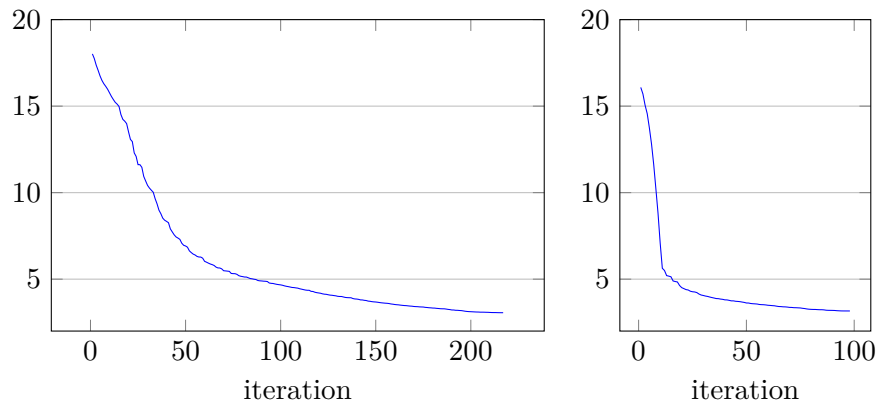


Figure 7.11: Residual for first (left) and second attempt (right)

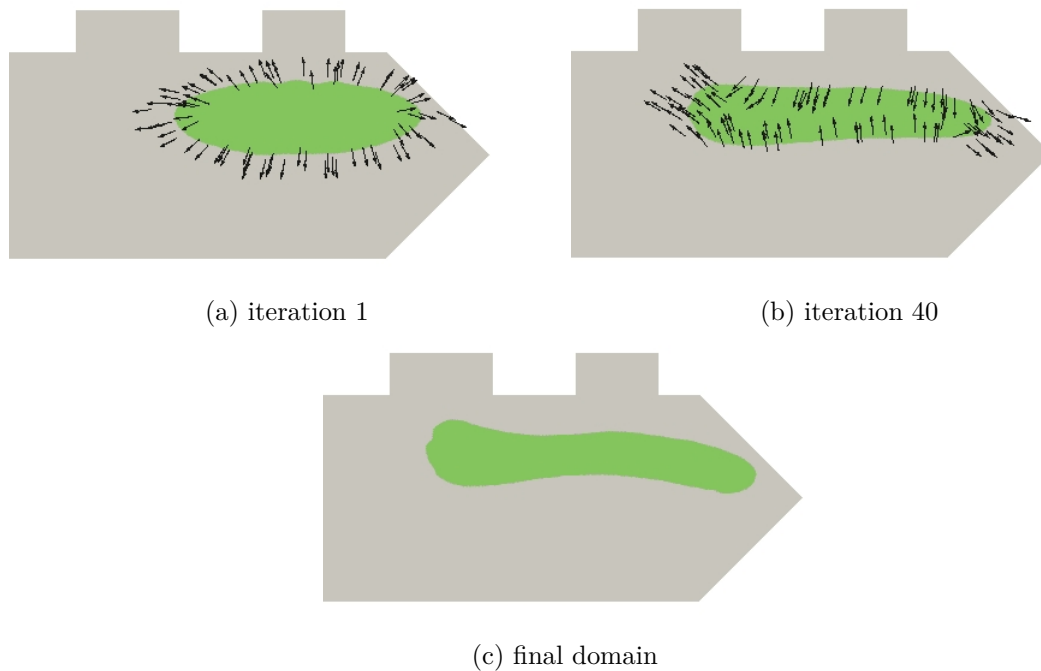
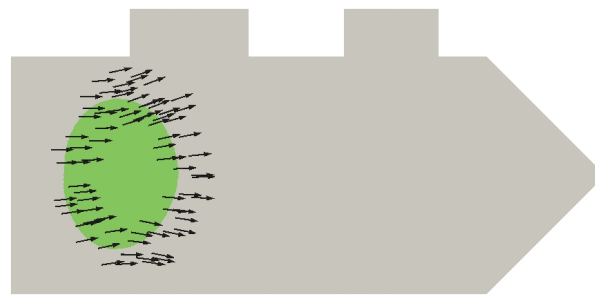
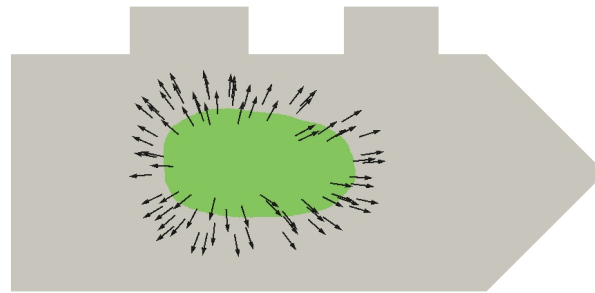


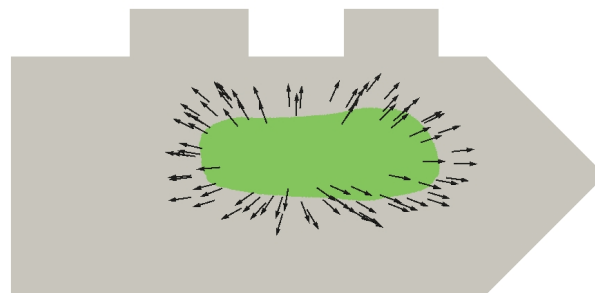
Figure 7.12: Room heating example second attempt



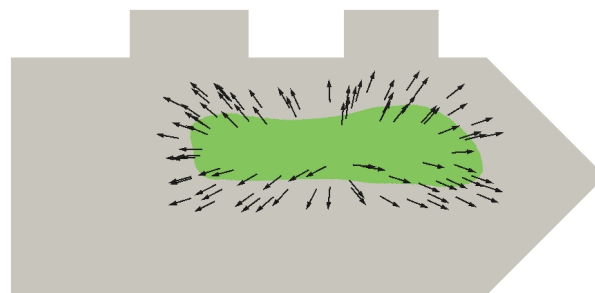
(a) iteration 1



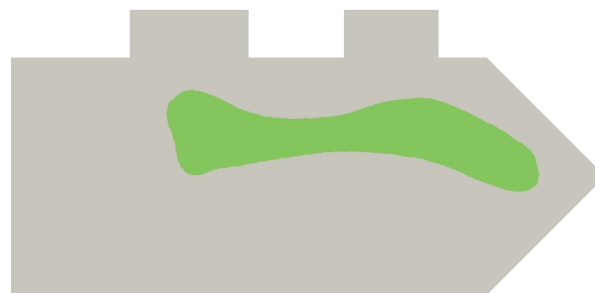
(b) iteration 40



(c) iteration 80



(d) iteration 120



(e) final domain

Figure 7.13: Room heating example first attempt

7.4 Velocity Extension

In this section we will give numerical evidence that the construction of the descent direction according to section 6.2.2 helps to preserve the distance between the isolines of the level set function. We consider a model problem on the rectangle $[0, 2] \times [0, 1] = \Omega$ with data

$$\alpha_1 = 2, \alpha_2 = 1, f_1 = 10, \gamma_0 = 0.5, \bar{u} = 0.9 .$$

Again we take the left boundary as Neumann boundary $\partial\Omega_N = \{0\} \times [0, 1]$ and thus $\partial\Omega_R = \partial\Omega \setminus \partial\Omega_N$. The initial domain is an ellipse close to the left boundary and yields an initial residual of 0.488. The optimization is done twice, where we change the descent direction in Algorithm 1 to the normalized discrete Riesz representative $\|\beta'_h\|_{\mathbf{X}}^{-1} \beta'_h$ (6.10) for the second run. Please note that this is also a descent direction according to Lemma 2.10. The results are shown in Figure 7.14 and 7.15. The algorithm stops when the residual does not decrease anymore and the minimum time step size is reached. This happens in the first run after 271 iterations with a residual of 0.155 and in the second run after 136 iterations with a residual of 0.196. Inspecting the level set function, we can clearly see that β_h^e preserves the signed distance property at least approximately. In case of the modified descent direction, artefacts close to the interface can be observed. Further the signed distance property is not at all preserved since the isolines on the right hand side of the interface are extremely close whereas on the left hand side they are far apart.

Remark: This example shows that the quality of the discrete level set function can have a huge impact on the optimization result. Of course, also the descent direction $\|\beta'_h\|_{\mathbf{X}}^{-1} \beta'_h$ could be used but then it should be combined with a re-initialization method (cf. Section 4.2).

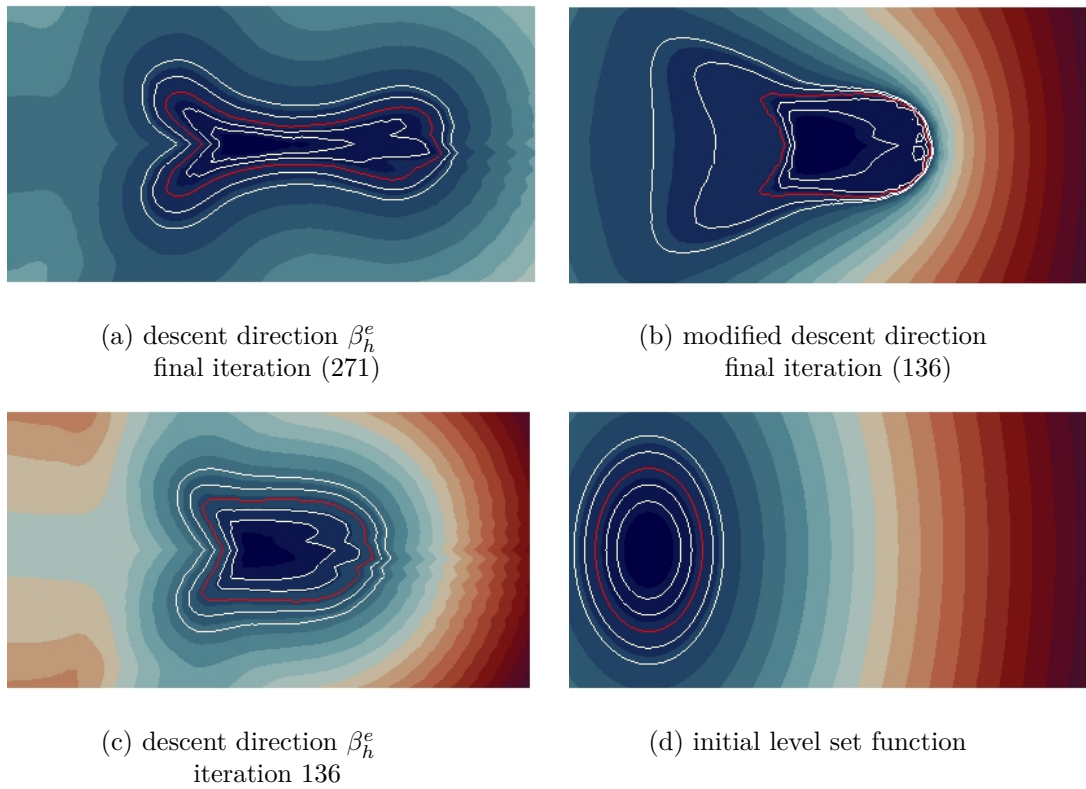


Figure 7.14: Isolines ± 0.1 , ± 0.05 (white) and 0 (red)

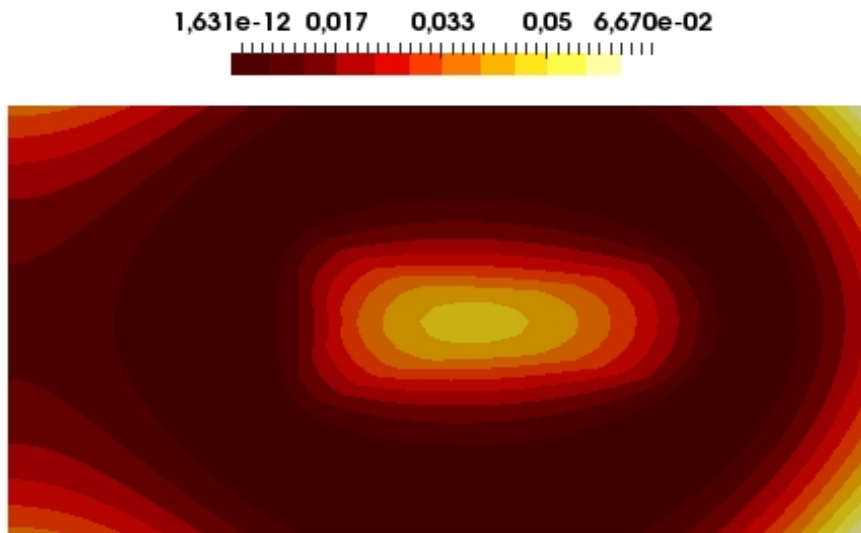


Figure 7.15: $(u_h - \bar{u})^2$ after final iteration using the descent direction β_h^e

7.5 Geometry and Residual Error

In this section we will consider an interface problem where the optimal solution is known a priori. That enables us to investigate how the final residual and the final geometry error decreases under mesh refinements. The holdall domain Ω is the unit circle and the optimal inner domain Ω_1^{opt} is a circle with center (0,0) and radius $\frac{1}{2}$. As Robin boundary we choose the entire boundary $\partial\Omega_R = \partial\Omega$. For the data $f_1 = 1$, $\alpha_1 = 2$, $\alpha_2 = 1$, $\gamma_0 = 1$, the solution of the interface problem (3.2)-(3.5) with $\Omega_1 = \Omega_1^{opt}$ is given by

$$\bar{u}(r) = \begin{cases} \frac{5+4\log 2}{32} - \frac{1}{8}r^2 & \text{in } \Omega_1^{opt}, \\ -\frac{1}{8}\log r + \frac{1}{8} & \text{in } \Omega \setminus \Omega_1^{opt}, \end{cases}$$

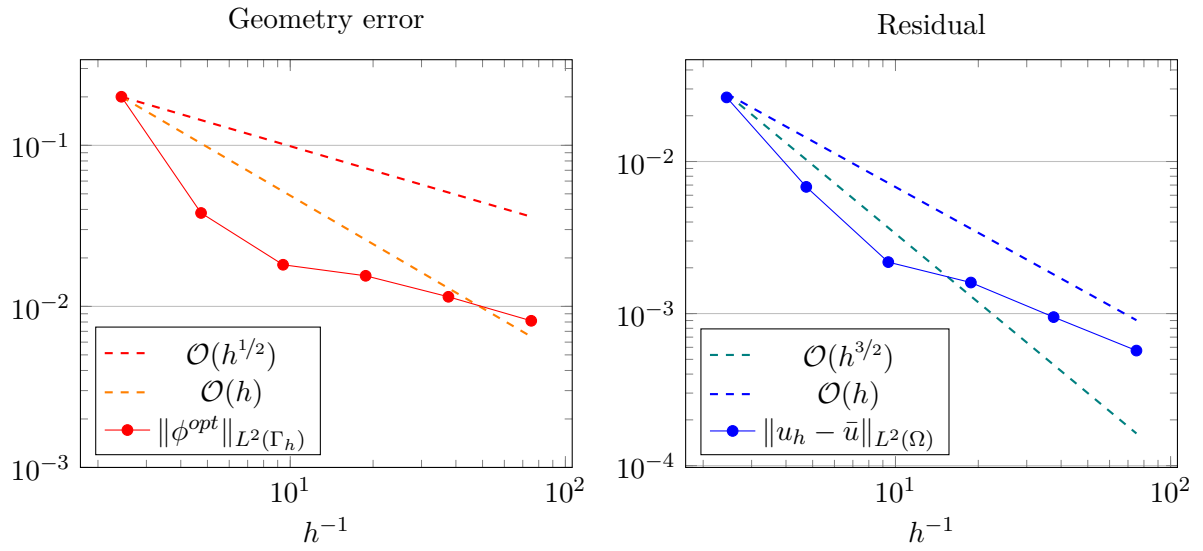
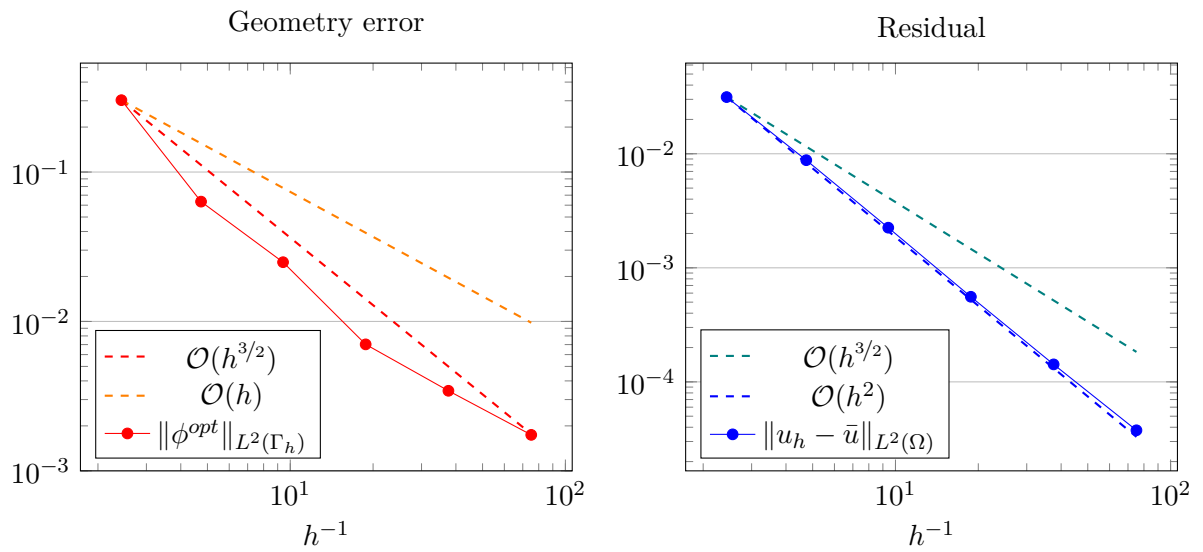
where $r = \sqrt{x^2 + y^2}$. For the initial geometry we choose the inner domain Ω_1 as a circle with center (0.2, 0.2) and radius 0.3. For a fixed mesh size h let u_h be the final discrete state and Γ_h the final discrete interface (by final we mean the results of Algorithm 1). The quantities of interest are the square root of the final residual i.e. $\|u_h - \bar{u}\|_{L^2(\Omega)}$ and the geometry error, which both ideally converge to zero. The latter one can be estimated by means of the signed distance function corresponding to the optimal domain $\phi^{opt}(x, y) = \sqrt{x^2 + y^2} - 0.5$, evaluated on the discrete interface Γ_h . We measure the distance between the final interface and the optimal interface by $\|\phi^{opt}\|_{L^2(\Gamma_h)}$. The results for the sequence of mesh sizes $h_n = \frac{1}{2^n}$, $n \in \{1, \dots, 6\}$ are shown in Figure 7.16. We observe that the geometry error decays with a rate of at least $\mathcal{O}(h^{1/2})$ and the residual with $\mathcal{O}(h)$.

As a second example we will consider the same problem with a modified source function f . Instead of a domain wise constant f , we choose $f = 1$ in the entire holdall domain Ω . This modification does not exactly fit into the setting which was introduced in Section 3.1, nevertheless it will be included here because it yields some interesting results. The corresponding exact solution is now given by

$$\bar{u}(r) = \begin{cases} -\frac{1}{8}r^2 + \frac{23}{32} & \text{in } \Omega_1^{opt}, \\ -\frac{1}{4}r^2 + \frac{3}{4} & \text{in } \Omega \setminus \Omega_1^{opt}. \end{cases}$$

We employ the same convergence studies as in the first case. The results are shown in Figure 7.17. For the geometry error we gain half of an order which results in a decay of $\mathcal{O}(h^{3/2})$. Concerning $\|u_h - \bar{u}\|_{L^2(\Omega)}$, the result is even better. We can really see a decay of order $\mathcal{O}(h^2)$. This is remarkable since that rate is of optimal order. The decay of the residual for all iterations and both source terms is shown in Figure 7.18.

Increasing the regularity of the source term from $L^2(\Omega)$ to $H^1(\Omega)$ seems to affect the decay of the residual as well as the geometry error. However, since $\alpha_1 \neq \alpha_2$, the regularity of u, u^* does not increase. Further numerical experiments show that we loose the optimal order rate of $\mathcal{O}(h^2)$ for the residual if α_1 is increased.

Figure 7.16: Geometry error and residual (discontinuous source f)Figure 7.17: Geometry error and residual (continuous source f)

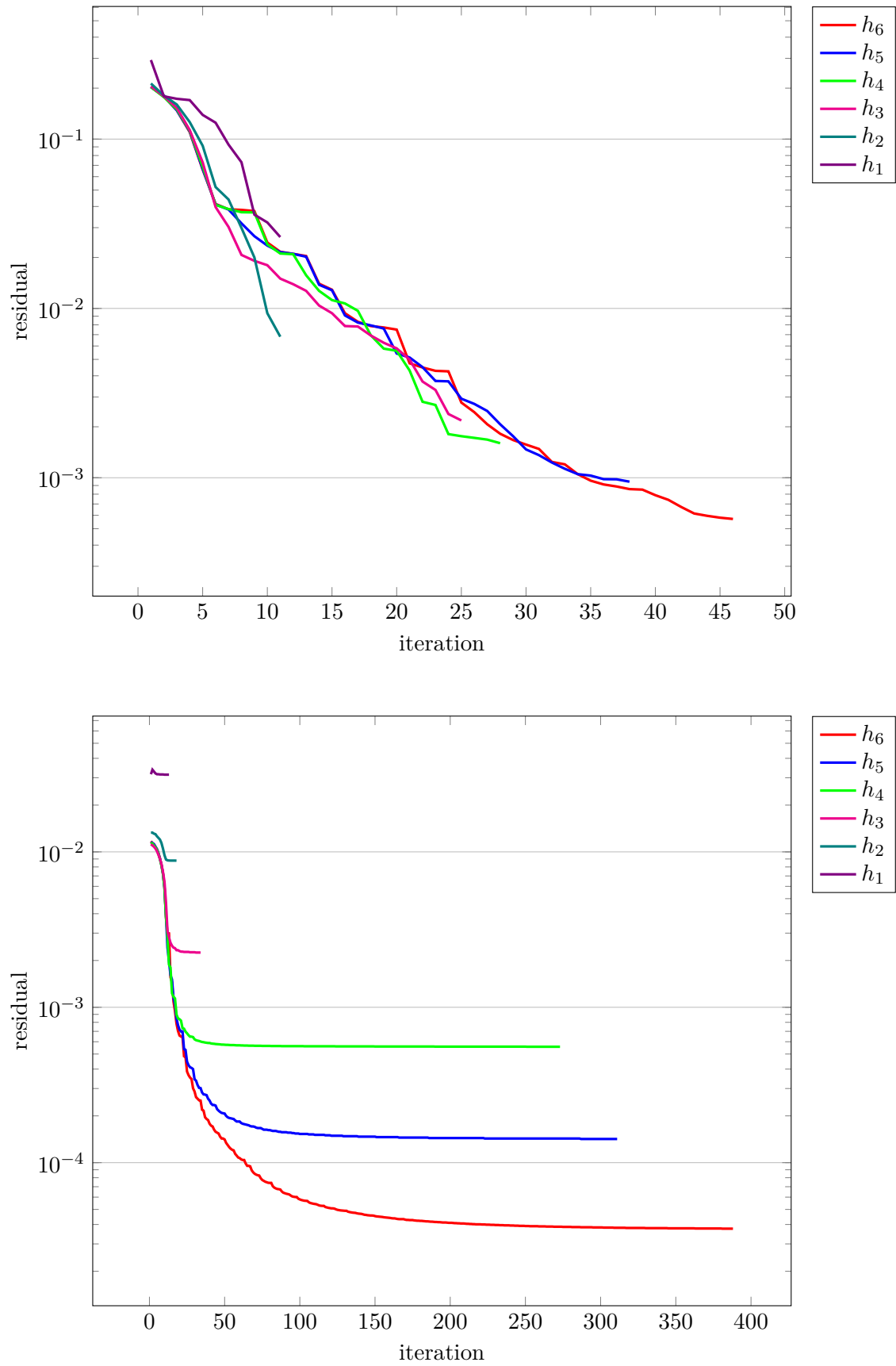


Figure 7.18: Residuals of all iterations for the discontinuous source f (upper) and the continuous source f (lower)

Chapter 8

Conclusion and Outlook

We presented a shape optimization method for a shape function constrained by a scalar interface problem. In this chapter we summarize the most important aspects of this thesis and point out open problems.

8.1 Summary

Analytical shape derivative

Based on standard techniques from the theory of shape optimization, we derived the volume expression of the shape derivative for an interface problem with a domain wise constant source term and Robin-Neumann boundary conditions in Section 3.1. The corresponding interface expression was also derived solely by elementary tools from vector calculus.

Discrete volume and boundary expression

In Section 5.2 we considered the one-phase model problem and compared two descent directions $(\beta_h^{VOL}, \beta_h^{BND})$ based on the volume expression resp. boundary expression. Under reasonable assumptions on discretization errors, we showed that the volume based descent direction is more accurate (cf. Lemma 5.6). In Section 7.1 we presented numerical experiments in accordance with the bounds shown in Section 5.2.

Velocity extension

We have seen in Section 2.1 and 3.1 that under sufficient regularity assumptions, the shape derivative depends only on normal components on the interface. Hence, there is considerable freedom in the choice of the descent direction. In Section 6.2.2 we constructed a descent direction that helps to preserve the approximate signed distance property of the discrete level set function during the level set transport. We also presented a proof of an estimate that bounds the approximation error on the interface (cf. Lemma 6.9).

8.2 Open Problems

Error analysis and $W^{k,p}$ estimates

A major aspect of the error analysis of the presented shape optimization method would

be an error bound on the velocity approximation i.e.

$$\|\beta' - \beta'_h\|_{\mathbf{X}} \leq Ch^q, \quad q \in \mathbb{R}.$$

In the following, we will outline the essential ingredients to derive such an estimate. The presented ideas are based on the error analysis in [BEH⁺17]. We assume exact geometry approximation and recall the definition of the exact shape derivative $d[\cdot]$ (3.23) and the discrete shape derivative $d_h[\cdot]$ (6.9). For the exact/discrete Riesz representatives β' , β'_h holds

$$b(\beta', \psi) = -d[\psi], \quad \forall \psi \in \mathbf{X}, \quad (8.1)$$

$$b(\beta'_h, \psi_h) = -d_h[\psi_h], \quad \forall \psi_h \in \mathbf{X}_h, \quad (8.2)$$

with the inner product $b(\cdot, \cdot)$ on $\mathbf{X} = [H_0^1(\Omega)]^d$. For any $\psi_h \in \mathbf{X}_h$ we obtain by (8.1)/(8.2)

$$\begin{aligned} \|\beta'_h - \psi_h\|_{\mathbf{X}}^2 &= b(\beta'_h - \psi_h, \beta'_h - \psi_h) \\ &= b(\beta'_h - \beta', \beta'_h - \psi_h) + b(\beta' - \psi_h, \beta'_h - \psi_h) \\ &\leq \left| d[\beta'_h - \psi_h] - d_h[\beta'_h - \psi_h] \right| + \|\beta' - \psi_h\|_{\mathbf{X}} \|\beta'_h - \psi_h\|_{\mathbf{X}} \end{aligned}$$

Dividing by $\|\beta'_h - \psi_h\|_{\mathbf{X}}$ yields further

$$\begin{aligned} \|\beta'_h - \psi_h\|_{\mathbf{X}} &\leq \frac{\left| d[\beta'_h - \psi_h] - d_h[\beta'_h - \psi_h] \right|}{\|\beta'_h - \psi_h\|_{\mathbf{X}}} + \|\beta' - \psi_h\|_{\mathbf{X}} \\ &\leq \sup_{\vartheta_h \in \mathbf{X}_h} \frac{\left| d[\vartheta_h] - d_h[\vartheta_h] \right|}{\|\vartheta_h\|_{\mathbf{X}}} + \|\beta' - \psi_h\|_{\mathbf{X}} \end{aligned}$$

Finally we use the fact that ψ_h was arbitrary and the triangle inequality to conclude

$$\|\beta' - \beta'_h\|_{\mathbf{X}} \leq 2 \inf_{\psi_h \in \mathbf{X}_h} \|\beta' - \psi_h\|_{\mathbf{X}} + \sup_{\vartheta_h \in \mathbf{X}_h} \frac{\left| d[\vartheta_h] - d_h[\vartheta_h] \right|}{\|\vartheta_h\|_{\mathbf{X}}}.$$

Thus it remains to bound the consistency error, introduced by the discretization of the shape derivative. This requires an additional regularity assumption on the solutions u, u^* of the state/adjoint problem (3.11)/(3.22), namely

$$u, u^* \in W^{1,\infty}(\Omega_i), \quad i = 1, 2. \quad (8.3)$$

Remark: For the case $d \leq 3$ (8.3) holds for $u, u^* \in W^{2,4}(\Omega_i)$ by the Sobolev embedding theorem (cf. [Alt12, Satz 8.8, p.342]).

We take a closer look at the nominator of the consistency error

$$\begin{aligned}
|d[\vartheta_h] - d_h[\vartheta_h]| &\leq \left| \int_{\Omega} \operatorname{div}(\vartheta_h) \left((u - \bar{u})^2 - (u_h - \bar{u})^2 \right) \right| \\
&\quad + \left| \int_{\Omega} \operatorname{div}(\vartheta_h) f(u^* - u_h^*) \right| \\
&\quad + \left| \int_{\Omega} 2(\nabla \bar{u} \cdot v_h) (u - u_h) \right| \\
&\quad + \left| \sum_{i=1}^2 \alpha_i \int_{\Omega_i} \operatorname{div}(\vartheta_h) [(\nabla u \cdot \nabla u^*) - (\nabla u_h \cdot \nabla u_h^*)] \right| \\
&\quad + \left| \sum_{i=1}^2 \alpha_i \int_{\Omega_i} \left[((D\vartheta_h + D\vartheta_h^T)\nabla u) \cdot \nabla u^* - ((D\vartheta_h + D\vartheta_h^T)\nabla u_h) \cdot \nabla u_h^* \right] \right| \\
&=: Q_1 + Q_2 + Q_3 + Q_4 + Q_5 .
\end{aligned}$$

We will present the further treatment of the right hand side in detail for the summand Q_4 . Let $i \in \{1, 2\}$, then Hölder's inequality yields

$$\begin{aligned}
&\left| \int_{\Omega_i} \operatorname{div}(\vartheta_h) [(\nabla u \cdot \nabla u^*) - (\nabla u_h \cdot \nabla u_h^*)] \right| \\
&\leq \left| \int_{\Omega_i} \operatorname{div}(\vartheta_h) [\nabla(u - u_h) \cdot \nabla u^*] \right| \\
&\quad + \left| \int_{\Omega_i} \operatorname{div}(\vartheta_h) [\nabla u \cdot \nabla(u^* - u_h^*)] \right| \\
&\quad + \left| \int_{\Omega_i} \operatorname{div}(\vartheta_h) [\nabla(u - u_h) \cdot \nabla(u^* - u_h^*)] \right| \\
&\leq C \|\vartheta_h\|_{\mathbf{X}} \|u - u_h\|_{W^{1,2}(\Omega_i)} \|u^*\|_{W^{1,\infty}(\Omega_i)} \\
&\quad + C \|\vartheta_h\|_{\mathbf{X}} \|u^* - u_h^*\|_{W^{1,2}(\Omega_i)} \|u\|_{W^{1,\infty}(\Omega_i)} \\
&\quad + C \|\vartheta_h\|_{\mathbf{X}} \|u - u_h\|_{W^{1,4}(\Omega_i)} \|u^* - u_h^*\|_{W^{1,4}(\Omega_i)}
\end{aligned}$$

and thus we conclude

$$Q_4 \leq C \|\vartheta_h\|_{\mathbf{X}} \left(\|u - u_h\|_{W^{1,2}(\Omega_i)} + \|u^* - u_h^*\|_{W^{1,2}(\Omega)} + \|u - u_h\|_{W^{1,4}(\Omega)} \|u^* - u_h^*\|_{W^{1,4}(\Omega)} \right) .$$

By similar techniques, one derives

$$Q_1 \leq C \|\vartheta_h\|_{\mathbf{X}} \|u - u_h\|_{L^4(\Omega)} ,$$

$$Q_2 \leq C \|\vartheta_h\|_{\mathbf{X}} \|u^* - u_h^*\|_{L^2(\Omega)} ,$$

$$Q_3 \leq C \|\vartheta_h\|_{\mathbf{X}} \|u - u_h\|_{L^2(\Omega)} ,$$

$$Q_5 \leq C \|\vartheta_h\|_{\mathbf{X}} \left(\|u - u_h\|_{W^{1,2}(\Omega_i)} + \|u^* - u_h^*\|_{W^{1,2}(\Omega)} + \|u - u_h\|_{W^{1,4}(\Omega)} \|u^* - u_h^*\|_{W^{1,4}(\Omega)} \right) .$$

We define the overall error bound

$$\begin{aligned}
B(u, u_h, u^*, u_h^*) &:= \|u - u_h\|_{W^{1,2}(\Omega_i)} + \|u^* - u_h^*\|_{W^{1,2}(\Omega)} + \|u - u_h\|_{W^{1,4}(\Omega)} \|u^* - u_h^*\|_{W^{1,4}(\Omega)} \\
&\quad + \|u - u_h\|_{L^4(\Omega)} .
\end{aligned} \tag{8.4}$$

Now we are able to bound the consistency error by means of (8.4)

$$\sup_{\vartheta_h \in \mathbf{X}_h} \frac{|d[\vartheta_h] - d_h[\vartheta_h]|}{\|\vartheta_h\|_{\mathbf{X}}} \leq \sup_{\vartheta_h \in \mathbf{X}_h} \frac{C B(u, u_h, u^*, u_h^*) \|\vartheta_h\|_{\mathbf{X}}}{\|\vartheta_h\|_{\mathbf{X}}} = C B(u, u_h, u^*, u_h^*).$$

Unfortunately $B(u, u_h, u^*, u_h^*)$ contains $W^{k,p}$ estimates for $k \in \{0, 1\}$ and $p = 4$. Optimal order $W^{k,p}$ error estimates for piecewise standard linear Finite Elements are known in the literature (cf. [RS82]). However, it is not clear if such estimates can also be derived for piecewise linear unfitted Finite Element spaces. This is an interesting question for future research, also isolated from the shape optimization context.

Unfitted approximation of the descent direction

The Riesz representative of the shape derivative possesses only limited global regularity due to a kink at the interface (cf. Lemma 2.11). For such functions, the best approximation of the standard Finite Element space \mathbf{X}_h is limited and can be improved by considering the corresponding unfitted Finite Element space \mathbf{X}_h^Γ (cf. Section 6.1). However, we have seen in numerical experiments that an unfitted Finite Element discretization of the descent direction does not significantly improve its approximation properties (cf. Section 7.2). It needs to be investigated why the error bounds do not improve and if this issue can be fixed by a modification of the variational formulation (7.3).

Higher order methods

Clearly, a natural extension of the presented method is the application of higher order Finite Element spaces. Increasing the polynomial degree of the approximation spaces (W_h, V_h, \mathbf{X}_h) pays off if all components of the approximation process $(u, u^*, \Gamma_h, \beta_h')$ reach higher order accuracy. For the primal/dual solution and the discrete interface, this is possible. In [LR17] the authors present an unfitted higher order method that offers optimal order bounds for the Finite Element and geometry approximation. It remains to clarify if also the discrete Riesz representative of the shape derivative β_h' benefits from higher order. In order to achieve higher order bounds for β_h' it is necessary to improve the error bounds for the unfitted low order approximation discussed in the previous paragraph.

Re-initialization and topology changes

For a geometry optimization problem, where the topology of an optimal solution is completely unknown, the approach of topology optimization may be better suited. Nevertheless, it would be desirable that also the shape optimization approach with a level set geometry representation allows for topology changes on a basic level, for instance merging of two domains. In [BEH⁺17] the authors present a method that employs re-initialization (cf. Section 4.2) and is able to perform basic topology changes in numerical experiments. It would be interesting to investigate if the method presented in this thesis allows basic topology changes if re-initialization is included in the level set transport.

Appendix A

Auxiliary Proofs

A.1. PROPOSITION [vector identity]

Let $\Omega \subset \mathbb{R}^d$ a bounded domain and $u, v \in H^2(\Omega)$, $\vartheta \in [H^1(\Omega)]^d$ then the following vector identity holds

$$\vartheta \cdot \nabla(\nabla u \cdot \nabla v) + \left((D\vartheta + D\vartheta^T)\nabla u \right) \cdot \nabla v = \nabla(\vartheta \cdot \nabla u) \cdot \nabla v + \nabla(\vartheta \cdot \nabla v) \cdot \nabla u .$$

Proof. The proof follows by direct calculation and the fact that $\frac{\partial^2 u}{\partial x_i \partial x_j} = \frac{\partial^2 u}{\partial x_j \partial x_i}$ for $i, j \in \{1, \dots, d\}$.

$$\begin{aligned} & \vartheta \cdot \nabla(\nabla u \cdot \nabla v) + \left((D\vartheta + D\vartheta^T)\nabla u \right) \cdot \nabla v \\ &= \sum_{i=1}^d \vartheta_i \left(\frac{\partial}{\partial x_i} \left(\sum_{j=1}^d \frac{\partial u}{\partial x_j} \frac{\partial v}{\partial x_j} \right) \right) + \sum_{i=1}^d \frac{\partial v}{\partial x_i} \left(\sum_{j=1}^d \left(\frac{\partial \vartheta_i}{\partial x_j} + \frac{\partial \vartheta_j}{\partial x_i} \right) \frac{\partial u}{\partial x_j} \right) \\ &= \sum_{i,j=1}^d \vartheta_i \frac{\partial v}{\partial x_j} \frac{\partial^2 u}{\partial x_j \partial x_i} + \sum_{i,j=1}^d \vartheta_i \frac{\partial^2 v}{\partial x_j \partial x_i} \frac{\partial u}{\partial x_j} \\ & \quad \sum_{i,j=1}^d \frac{\partial \vartheta_i}{\partial x_j} \frac{\partial u}{\partial x_j} \frac{\partial v}{\partial x_i} + \sum_{i,j=1}^d \frac{\partial \vartheta_j}{\partial x_i} \frac{\partial u}{\partial x_j} \frac{\partial v}{\partial x_i} \\ &= \nabla(\vartheta \cdot \nabla u) \cdot \nabla v + \nabla(\vartheta \cdot \nabla v) \cdot \nabla u . \end{aligned}$$

□

Notation/Definition: We give a few definitions that are valid for the subsequent statements:

Let Ω be a bounded domain in \mathbb{R}^d and $\Omega_1 \subset \Omega$ with a C^1 boundary $\Gamma := \partial\Omega_1$ and outer unit normal n_Γ . Further $\Omega_2 := \Omega \setminus \Omega_1$.

A.2. PROPOSITION [tangential gradient continuity]

Let $u \in H^1(\Omega) \cap H^2(\Omega_1) \cap H^2(\Omega_2)$ with $[[u]] = 0$ on Γ .

$$[[\nabla_\Gamma u]] = (P\nabla u)|_{\Omega_1} - (P\nabla u)|_{\Omega_2} = 0 \quad \text{in } L^2(\Gamma) . \quad (\text{A.1})$$

With the tangential projection $P = I - n_\Gamma n_\Gamma^T$.

Proof. Denote by $u_i := u|_{\Omega_i}$, the restrictions of u to the subdomains. Since $\Gamma \in C^1$ we can find functions $v_i \in C^\infty(\overline{\Omega_i})$ smooth up to the interface with $\|u_i - v_i\|_{H^2(\Omega_i)} < \epsilon$ (see [Eva10, Theorem 3 p.266]).

To prove the statement we follow the ideas of [Stu15, Remark 3.3]. Let $x \in \Gamma$ arbitrary but fixed. Further we consider a C^1 parametrization of the boundary $\gamma : [0, T] \rightarrow \Gamma$, $T > 0$ with $\gamma(0) = x$ and $\gamma'(0) =: w$. We differentiate $\llbracket v \rrbracket := v_1 - v_2$ along the interface and obtain

$$\begin{aligned} 0 &= \frac{d}{dt} \llbracket v(\gamma(t)) \rrbracket = \nabla v_1 \cdot \gamma'(0) - \nabla v_2 \cdot \gamma'(0) \\ &= (P(\nabla v_1 - \nabla v_2)) \cdot w + (\nabla v_1 \cdot n_\Gamma - \nabla v_2 \cdot n_\Gamma) n_\Gamma \cdot w \\ &= (P(\nabla v_1 - \nabla v_2)) \cdot w =: \llbracket \nabla_\Gamma v \rrbracket \cdot w \end{aligned}$$

Since w was arbitrary but tangential we obtain that $\llbracket \nabla_\Gamma v \rrbracket$ is orthogonal to all tangential vectors on Γ . By construction $\llbracket \nabla_\Gamma v \rrbracket$ is also orthogonal to n_Γ and hence $\llbracket \nabla_\Gamma v \rrbracket = 0$. The trace theorem then implies

$$\begin{aligned} \oint_\Gamma \llbracket \nabla_\Gamma u \rrbracket^2 &\leq C \left(\oint_\Gamma (\nabla_\Gamma u_1 - \nabla_\Gamma v_1)^2 + \oint_\Gamma (\nabla_\Gamma v_1 - \nabla_\Gamma v_2)^2 + \oint_\Gamma (\nabla_\Gamma v_2 - \nabla_\Gamma u_1)^2 \right) \\ &\leq C \left(\|u_1 - v_1\|_{H^2(\Omega_1)} + \|u_2 - v_2\|_{H^2(\Omega_2)} \right) \leq C\epsilon . \end{aligned}$$

Since ϵ was arbitrary, this yields the claim. \square

A.3. PROPOSITION [approximation example]

There exist shape regular families of triangulations $\{\mathcal{T}_h\}$, interfaces $\Gamma \in C^1$ and $u \in H^l(\Omega_1) \cap H^l(\Omega_2) \cap H^1(\Omega)$ with $l \geq 2$ such that

$$\inf_{v_h \in V_h^{dc}} \|u - v_h\|_{L^2(\Omega)} \geq Ch^{3/2} ,$$

with the Finite Element space $V_h^{dc} := \{v_h \in L^2(\Omega) : v_h|_T \in \mathbb{P}_1(T), T \in \mathcal{T}_h\}$.

Proof. We construct an example for $d = 1$. The idea can be generalized to higher space dimensions. We choose the following data

$$\begin{aligned} \Omega &= [0, 1] \\ \Gamma &= \frac{1}{3} \\ \mathcal{T}_h^n &= \{[(j-1)2^{-n}, j2^{-n}]\}_{j=1, \dots, 2^n} \\ u(x) &= \begin{cases} 1 - 3x & x \leq 1/3 \\ 0 & x > 1/3 . \end{cases} \end{aligned}$$

Since u is a piecewise linear polynomial, the approximation error occurs only in the element T^Γ cut by the interface. Let l_{T^Γ} be the left endpoint of T^Γ then we can define

a mapping Φ_h that maps the reference element $\hat{T} = [0, 1]$ onto T^Γ by

$$\Phi_h(x) = l_{T^\Gamma} + hx .$$

Applying the transformation on u yields

$$(u \circ \Phi_h)(x) = \begin{cases} 1 - 3\Phi_h(x) & \Phi_h(x) \leq 1/3 \\ 0 & \Phi_h(x) > 1/3 . \end{cases}$$

The left endpoint of T^Γ can be rewritten with a real number $\theta \in (0, 1)$ to $l_{T^\Gamma} = 1/3 - \theta h$. In fact $\theta \in \{1/3, 2/3\}$ and *w.l.o.g.* we assume $\theta = 1/3$. Since $\Phi_h(x) \leq 1/3 \Leftrightarrow x \leq 1/3$ we obtain

$$(u \circ \Phi_h)(x) = \begin{cases} h(1 - 3x) & x \leq 1/3 \\ 0 & x > 1/3 . \end{cases} = hu(x)$$

For the best approximation error holds

$$\begin{aligned} \inf_{v_h \in V_h^{dc}} \|u - v_h\|_{L^2(\Omega)}^2 &= \inf_{v_h \in V_h^{dc}} \|u - v_h\|_{L^2(T^\Gamma)}^2 = \inf_{v_h \in V_h^{dc}} \int_{l_{T^\Gamma}}^{l_{T^\Gamma}+h} (u - v_h)^2 \\ &= \inf_{v_h \in V_h^{dc}} h \int_0^1 (u \circ \Phi_h - v_h \circ \Phi_h)^2 = \inf_{w_h \in \mathbb{P}_1(\Omega)} h \int_0^1 (u \circ \Phi_h - w_h)^2 . \end{aligned}$$

The best approximating element $w_h \in \mathbb{P}_1(\Omega)$ is uniquely defined due to the orthogonal projection in Hilbert spaces. We have $w_h(x) = ax + b$ and the coefficients can be easily identified by the two orthogonality relations

$$\begin{aligned} \int_0^1 (u \circ \Phi_h - ax - b) &= 0 \\ \int_0^1 (u \circ \Phi_h - ax - b)x &= 0 . \end{aligned}$$

Solving this linear system for the coefficients a, b yields

$$w_h(x) = h \left(-\frac{7}{9}x + \frac{5}{9} \right) =: hw(x) .$$

Inserting this identity into the best approximation error yields

$$\begin{aligned} \inf_{v_h \in V_h^{dc}} \|u - v_h\|_{L^2(\Omega)}^2 &= \inf_{w_h \in \mathbb{P}_1(\Omega)} h \int_0^1 (hu - w_h)^2 \\ &= h^3 \int_0^1 (u - w)^2 \end{aligned}$$

and taking the square root yields the claim for $C < \int_0^1 (u - w)^2$. □

Bibliography

- [ADK07] Lekbir Afraites, Marc Dambrine, and Djalil Kateb. Shape methods for the transmission problem with a single measurement. *Numerical functional analysis and optimization*, 28(5-6):519–551, 2007.
- [AE01] Herbert Amann and Joachim Escher. *Analysis II. Grundstudium Mathematik*. Birkhäuser Verlag, Basel, 2001.
- [Alt12] Hans Wilhelm Alt. *Lineare Funktionalanalysis: Eine anwendungsorientierte Einführung*. Springer-Verlag, 2012.
- [BEH⁺17] Erik Burman, Daniel Elfverson, Peter Hansbo, Mats G Larson, and Karl Larsson. A cut finite element method for the bernoulli free boundary value problem. *Computer Methods in Applied Mechanics and Engineering*, 317:598–618, 2017.
- [Ber10] Martin Berggren. A unified discrete–continuous sensitivity analysis method for shape optimization. In *Applied and numerical partial differential equations*, pages 25–39. Springer, 2010.
- [BH12] Erik Burman and Peter Hansbo. Fictitious domain finite element methods using cut elements: II. A stabilized Nitsche method. *Applied Numerical Mathematics*, 62(4):328–341, 2012.
- [Bor02] Liliana Borcea. Electrical impedance tomography. *Inverse Problems*, 18(6):R99, 2002.
- [Bre10] Haim Brezis. *Functional analysis, Sobolev spaces and partial differential equations*. Springer Science & Business Media, 2010.
- [BS95] Martin P Bendsøe and Ole Sigmund. *Optimization of structural topology, shape, and material*, volume 414. Springer, 1995.
- [BS07] Susanne Brenner and Ridgway Scott. *The mathematical theory of finite element methods*, volume 15. Springer Science & Business Media, 2007.
- [BS13] Martin Philip Bendsoe and Ole Sigmund. *Topology optimization: theory, methods, and applications*. Springer Science & Business Media, 2013.
- [Cal06] Alberto P Calderón. On an inverse boundary value problem. *Computational & Applied Mathematics*, 25(2-3):133–138, 2006.

- [CIN99] Margaret Cheney, David Isaacson, and Jonathan C Newell. Electrical impedance tomography. *SIAM review*, 41(1):85–101, 1999.
- [CZ98] Zhiming Chen and Jun Zou. Finite element methods and their convergence for elliptic and parabolic interface problems. *Numerische Mathematik*, 79(2):175–202, 1998.
- [DPE11] Daniele Antonio Di Pietro and Alexandre Ern. *Mathematical aspects of discontinuous Galerkin methods*, volume 69. Springer Science & Business Media, 2011.
- [Duh06] D Duhamel. Shape optimization of noise barriers using genetic algorithms. *Journal of sound and vibration*, 297(1-2):432–443, 2006.
- [DZ11] M. Delfour and J. Zolésio. *Shapes and Geometries*. Society for Industrial and Applied Mathematics, second edition, 2011.
- [EG13] Alexandre Ern and Jean-Luc Guermond. *Theory and practice of finite elements*, volume 159. Springer Science & Business Media, 2013.
- [ER13] Charles M Elliott and Thomas Ranner. Finite element analysis for a coupled bulk–surface partial differential equation. *IMA Journal of Numerical Analysis*, 33(2):377–402, 2013.
- [Eva10] Lawrence C. Evans. *Partial differential equations*, volume 19 of *Graduate Studies in Mathematics*. ams, Providence, Rhode Island, 2010.
- [GR11] Sven Gross and Arnold Reusken. *Numerical methods for two-phase incompressible flows*, volume 40. Springer Science & Business Media, 2011.
- [Had08] Jacques. Hadamard. Mémoire sur le problème d’analyse relatif à l’équilibre des plaques élastiques encastrées. *Mém. Sav. étrang. (2)* 33, Nr. 4, 128 S (1908)., 1908.
- [Her12] José Herskovits. *Advances in structural optimization*, volume 25. Springer Science & Business Media, 2012.
- [HH02] Anita Hansbo and Peter Hansbo. An unfitted finite element method, based on Nitsche’s method, for elliptic interface problems. *Computer methods in applied mechanics and engineering*, 191(47-48):5537–5552, 2002.
- [HPS15] Ralf Hiptmair, Alberto Paganini, and Sahar Sargheini. Comparison of approximate shape gradients. *BIT Numerical Mathematics*, 55(2):459–485, 2015.
- [Kor18] Benjamin S Koren. The grand hall of the Elbphilharmonie Hamburg: Development of parametric and digital fabrication tools in architectural and acoustical design. In *Humanizing Digital Reality*, pages 141–151. Springer, 2018.

- [Leh10] Christoph Lehrenfeld. Hybrid Discontinuous Galerkin Methods for Incompressible Flow Problems. Master's thesis, RWTH Aachen, May 2010.
- [LR13] Eva Loch and Arnold Reusken. *The level set method for capturing interfaces with applications in two-phase flow problems*. PhD thesis, Hochschulbibliothek der Rheinisch-Westfälischen Technischen Hochschule Aachen, 2013.
- [LR17] Christoph Lehrenfeld and Arnold Reusken. Analysis of a high order unfitted finite element method for an elliptic interface problem. *IMA J. Numer. Anal.*, 00:1–37, 2017. first online.
- [LR18] Christoph Lehrenfeld and Arnold Reusken. L^2 -estimates for a high order unfitted finite element method for elliptic interface problems. *Journal of Numerical Mathematics*, 00:–, 2018. first online.
- [LS13] A. Laurain and K. Sturm. *Domain Expression of the Shape Derivative and Application to Electrical Impedance Tomography*. Preprint: Weierstraß-Institut für Angewandte Analysis und Stochastik. WIAS, 2013.
- [Mar02] Steffen Marburg. Developments in structural-acoustic optimization for passive noise control. *Archives of computational methods in engineering*, 9(4):291–370, 2002.
- [Nit71] Joachim Nitsche. Über ein Variationsprinzip zur Lösung von Dirichlet-Problemen bei Verwendung von Teilräumen, die keinen Randbedingungen unterworfen sind. In *Abhandlungen aus dem mathematischen Seminar der Universität Hamburg*, volume 36, pages 9–15. Springer, 1971.
- [NS12] Antonio André Novotny and Jan Sokołowski. *Topological derivatives in shape optimization*. Springer Science & Business Media, 2012.
- [Osw93] P. Oswald. On a BPX-preconditioner for P1 elements. *Computing*, 51(2):125–133, 1993.
- [RS82] Rolf Rannacher and Ridgway Scott. Some optimal error estimates for piecewise linear finite element approximations. *Math. Comput.*, 38:437–445, 1982.
- [Sch14] Joachim Schöberl. C++11 implementation of finite elements in NGSolve. Technical Report ASC-2014-30, Institute for Analysis and Scientific Computing, September 2014.
- [Set96] James A Sethian. A fast marching level set method for monotonically advancing fronts. *Proceedings of the National Academy of Sciences*, 93(4):1591–1595, 1996.
- [Ste70] Elias M. Stein. Singular integrals and differentiability properties of functions. Princeton, N.J.: Princeton University Press. XIV, 287 p. (1970)., 1970.

-
- [Stu15] Kevin Sturm. *On shape optimization with non-linear partial differential equations*. PhD thesis, TU Berlin, 2015.
- [SZ92] Jan Sokolowski and Jean-Paul Zolesio. *Introduction to shape optimization: shape sensitivity analysis*. Springer-Verlag, 1992.
- [ZCMO96] Hong-Kai Zhao, T. Chan, B. Merriman, and S. Osher. A variational level set approach to multiphase motion. *J. Comput. Phys.*, 127(1):179–195, 1996.
- [Zie12] William P Ziemer. *Weakly differentiable functions: Sobolev spaces and functions of bounded variation*, volume 120. Springer Science & Business Media, 2012.
- [Zol79] Jean-Paul Zolesio. Identification de domaines par déformations. Université de Nice, 1979. Thèse de doctorat d'état.